KU Leuven

Biomedical Sciences Group

Department of Pharmaceutical and

Pharmacological Sciences

Laboratory for Molecular Biodiscovery

Evans blue as a diagnostic tool for non-muscle-invasive bladder cancer

A preclinical study

Sanne Elsen

Jury:
Promotor:
Prof. Dr. Peter A. M. de Witte
Co-promotor:
Prof. Dr. Hein Van Poppel
Chair:
Prof. Dr. Myriam Baes
Jury members:
Prof. Dr. Evelyne Lerut
Prof. Dr. Yicheng Ni
Prof. Dr. Dirk de Ridder
Prof. Dr. Juan Palou Redorta

Dissertation presented in partial fulfillment of the requirements for the degree of Doctor in Pharmaceutical Sciences

Leuven, 2016

Auditorium Wolfspoort

Huis Bethlehem

Schapenstraat 34

3000 Leuven, Belgium

25 February, 2016

Promotor: Professor Dr. Peter de Witte

Departement Farmaceutische en Farmacologische Wetenschappen

Laboratorium voor Moleculaire Bio-Ontdekking

Herestraat 49, O&N II, bus 824

3000 Leuven

Co-promotor: Professor Dr. Hein Van Poppel

Faculteit Geneeskunde, Afdeling Urologie

UZ Herestraat 49, bus 7003 41

3000 Leuven

DANKWOORD

'Every new beginning comes from some other beginning's end' (Semisonic – Closing time), deze zin geeft mooi het gevoel weer waarmee ik dit doctoraat afsluit. De voorbije 4,5 jaren heb ik voornamelijk gespendeerd aan dit onderzoek. Vandaag kan ik met een gerust hart deze periode afsluiten en tegelijk vooruitkijken naar de toekomst. Er zijn een hele hoop mensen die een bedankje verdienen voor de hulp en de mentale steun gedurende de voorbije jaren.

Allereerst zou ik graag mijn promoter, professor Peter de Witte, willen bedanken. Peter, bedankt om mij een plaatsje te geven bij jou in het labo om mijn doctoraat te kunnen verwezenlijken. Ik was een beetje de vreemde eend in de bijt tussen al het zebravisonderzoek, maar je hebt steeds je best gedaan om ook mijn project goed te begeleiden. Bedankt! Ik zou ook graag mijn co-promoter, professor Hein Van Poppel, willen bedanken om mij in te leiden in de wereld van de urologie. Bedankt om steeds tijd vrij te maken om aanwezig te zijn op mijn presentaties. Ook Drs Frank Van der Aa en Ben Van Cleynenbreugel mag ik niet vergeten: bedankt om mij steeds verder te helpen met urologie-gerelateerde kwesties en papers na te lezen.

I would also like to express my grattitude to the members of the jury: professors Myriam Baes, Evelyne Lerut, Yicheng Ni, Dirk de Ridder and Juan Palou. Thank you for taking the time to read my thesis manuscript and providing valuable suggestions and remarks.

Uiteraard zijn er ook de collega's van het labo voor Moleculaire Bio-Ontdekking die in de bloemetjes mogen gezet worden. Ik ben enorm blij dat ik de voorbije jaren in jullie goed gezelschap heb mogen doorbrengen. De sfeer in het labo was altijd opperbest en vormde een enorme stimulans voor het maken van mijn doctoraat. Hartelijk bedankt daarvoor, zowel de 'oude' generatie labogenoten – Thierry, Evelien, Ann-Sophie, Rik, Lorena, Adriana, Tatiana, Olivia, Angela, Mel, Wu, Ibrahim en de masterstudenten – als diegenen die hier nog een tijdje zullen blijven: Jan, Daniëlle, Bac, Hung, Yifan, Annelii, Ola, Monika, Chloë, Jo, Niels en Xin-Xin.

In het bijzonder zou ik volgende collega's willen bedanken:

Daniëlle, mijn allerliefste bureaugenootje, dank je om altijd – zelfs wanneer je zelf verdronk in het werk – voor mij klaar te staan. Ik apprecieer je steun en positieve instelling enorm en ik zal je heel hard missen op mijn volgende werkplek. Bedankt ook voor de leuke avondjes op restaurant en je bezoekjes bij mij thuis! *Jan*, bedankt voor alle bestellingen, hulp in noodgevallen wanneer een toestel het liet afweten en vooral voor je aangename gezelschap! *Chloë*, bedankt voor de vele babbels, zowel over werk als niet-werk gerelateerde zaken. Ik ben blij dat je uiteindelijk toch in ons labo bent kunnen blijven want zo heb ik een fantastisch persoon leren kennen! *Jo*, jij stond steeds klaar met een antwoord op farmacologische vragen en natuurlijk ook voor een gezellig babbeltje tijdens een thee-pauze. *Yifan*, thank you for your everlasting kindness. I wish you all the best at your wedding day in China. *Hung* and *Bac*, thank you for improving my knowledge about the Vietnamese culture and for the nice conversations we had. *Ola* and *Annelii*, thank you very much for the many questions during lab meetings and for your pleasant presence in the lab. *Niels*, ik wens je veel geluk met je doctoraat. Ik weet zeker dat je er een mooi werk van zal maken. Bedankt ook om mee de sfeer te creëren tijdens de labo-uitstapjes! *Evelien*, zowel de eerste jaren in het labo als de latere jaren buiten het labo hebben we mooie tijden beleefd. Dank je voor je luisterend oor! Ik ben er zeker van dat er nog vele leuke momenten zullen volgen samen ;).

Angela, thank you for the nice talks and moments we shared. I wish you all the best back in Hungary and I hope we will still see each other from time to time!

Ook een welgemeende dankjewel aan de 'mensen van het labo hiernaast'. Bedankt voor de babbeltjes in de gang of tijdens de middagpauzes!

Rita, An H en Chantal, bedankt voor al het logistieke en administratieve geregel!

Naast mijn collega's zijn er nog een heleboel vrienden die ik graag zou willen bedanken. *Kathleen*, wij kennen elkaar al sinds het middelbaar en ondanks het feit dat we eigenlijk maar 2 jaar bij elkaar in de klas hebben gezeten, ben je nog steeds een super-vriendin. Ik herinner me met plezier onze middelbare schooltijd, de kookavondjes als uniefstudent en de brunches, restaurantjes en films sinds we zijn afgestudeerd! Bedankt ook om af en toe op Izzie te babysitten. *Bastiaan*, ik heb je leren kennen tijdens ons 1e jaar Biologie. Ondertussen hebben we beiden een heel ander pad bewandeld, ik als doctoraatsstudente, jij als fotograaf. Ondanks het feit dat we elkaar ondertussen wat minder zien, ben ik steeds heel blij als ik je kan uithoren over je vele avonturen in binnen- en buitenland ;). Bedankt voor de vele, leuke, ontspannende babbels! *Lise*, wij hebben een groot deel van ons doctoraat samen mogen beleven, zij het in ander labo's. Jij wist als de beste hoe je me kon laten 'ontstressen'. We hebben samen dan ook vele leuke momenten meegemaakt, tijdens de spinning, coctail-avondjes, (bier)festivals of gewoon bij ons thuis. Super bedankt daarvoor, jij bent ook mijn 'schatje-van-patatje' ;). Ten slotte zou ik nog graag mijn 'biologie-vrienden' willen bedanken: *Inez, Sanne, Karen, Kim, An, Laurine, Michaël* en *Eveline*. Bedankt om onze studie Biologie zo plezant te maken! We hebben samen fantastische tijden beleefd op bios-td's, ecologische uitstappen naar Slapton en Dale of gewoon 'op An haar kot' (want dat was nu eenmaal het grootste ☺). Ook nu staan jullie nog steeds voor mij klaar, dankjewel daarvoor! Iedereen die nog bezig is met hun doctoraat wens ik veel succes toe! Jawel, er komt ooit een einde aan ;). *Inez*, jou zou ik nog speciaal willen bedanken voor de vele avonden die we samen doorbrachten tijdens onze studententijd. Op kot, op café of bij jou in Schelle, het was steeds de moeite!

Moeke en *vake*, jullie zijn fantastische ouders! Bedankt om me steeds te steunen en me de vrijheid te geven om mijn eigen keuzes te maken, maar vooral bedankt om steeds voor een warme thuis te zorgen. *Hilke* en *Siebe*, ik kan me geen betere, leukere en lievere zus en broer voorstellen dan jullie! Bedankt voor de vele mooie tijden die we samen beleefd hebben, zowel toen we nog allemaal thuis woonden als nu! Sara, ook jij maakt nu deel uit van de familie en ik ben blij dat ik je mijn schoonzusje mag noemen ☺. Ook *Anke, Saartje* , *Jeroen, Mia* en *Joost* wil ik bedanken: jullie zijn zoveel meer dan 'gewoon' familie. Bedankt voor de vele gezellige momenten die we samen hebben beleefd en zeker en vast nog zullen beleven! Liefste *André, Odrada, Nele, Hanne, Karolien, Wim* en *Katharina*. Hartelijk dank om mij vanaf de eerste moment met open armen te ontvangen in jullie familie. Bedankt voor alle support!

Tom en *Izzie*, jullie zijn ongetwijfeld de 2 allerbelangrijkste personen in mijn leven. *Tom*, ik had nooit gedacht dat een vakantie in Namibië zoveel voor mij in petto zou hebben ;). Ik ben supergelukkig dat ik mijn leven samen met jou mag delen. Ik wil je dan ook enorm bedanken voor de steun die jij me de voorbije jaren hebt gegeven, op wetenschappelijk maar vooral op niet-wetenschappelijk vlak. Jij kan telkens weer een glimlach op mijn gezicht toveren en dat maakt mij

de gelukkigste vrouw op aarde! *Izzie*, je bent een schat van een dochter! Jouw lach en prachtige oogjes doen telkens opnieuw mijn hart smelten. Je zal ongetwijfeld een fantastische 'grote zus' worden voor dat kleine wezentje in mijn buik ;)!

TABLE OF CONTENTS

LIST OF ABBREVIATIONS

5-ALA	5-aminolevulinic acid
AJ	adherens junction
BBN	*N*-butyl-*N*-(4-hydroxybutyl)nitrosamine
BC	bladder cancer
BCFI	Belgisch Centrum voor Farmacotherapeutische Informatie
BCG	bacillus Calmette-Guérin
CIS	carcinoma *in situ*
DiO	3,3'-dioctadexyloxacarbocyanine perchlorate
EAU	European Association of Urology
EB	Evans blue
EMT	epithelial-to-mesenchymal transition
FANT	*N*-[4-5-nitro-2-furyl-2-thiazolyl]-formamide
FCS	fetal calf serum
FDA	Food and Drug Administration
FDR	false discovery rate
GAG	glycosaminoglycan
GEM	genetically engineered mice
GSTM	glutathione S-transferase
H&E	hematoxylin and eosin
HAL	hexaminolevulinate
HPLC	high-performance liquid chromatography
IC	interstitial cystitis
IS	internal standard
IV	intravenous
ISUP	International Society of Urological Pathology

KEGG	Kyoto Encyclopedia of Genes and Genomes
LCM	laser-capture microdissection
MEM	minimal essential medium
MIBC	muscle-invasive bladder cancer
MNU	*N*-methyl-*N*-nitrosurea
NAT	N-acetyltransferase
NBB	naphtol blue black
NBI	narrow band imaging
NMIBC	non-muscle-invasive bladder cancer
NTP	National Toxicology Program
OCT	optical coherence tomography
PBS	painful bladder syndrome
PBS	phosphate buffered saline
PCA	principal component analysis
PDD	photodynamic diagnosis
PpIX	protoporhyrin IX
PUNLMP	papillary urothelial neoplasm of low malignant potential
PVP	polyvinylpyrrolidone
PW	pathway
SCC	squamous cell carcinoma
SNP	single nucleotide polymorphism
SPIES	Storz Professional Imaging System
SV40	simian virus 40
TCC	transitional cell carcinoma
TEM	transmission electron microscopy
TJ	tight junction
TNM	'Tumor, Node, Metastasis'

TUR(B)(T)	transurethral resection (of bladder) (tumors)
UCC	urothelial cell carcinoma
UICC	Union for International Cancer Control
UPKII	uroplakin 2
WHO	World Health Organization
WL(C)	white-light cystoscopy

SUMMARY

Bladder cancer is a major health problem, with an estimated 429,000 new cases accompanied with 165,000 deaths in 2012. In the world, bladder cancer is the 4th most common cancer in men and the 8th most common malignancy in women. The incidence and prevalence rises with age. At first diagnosis, the large majority of detected lesions (70-75 %) are classified as non-muscle-invasive bladder cancer (NMIBC) originating from the urothelium. The primary treatment for NMIBC is the removal of cancerous tissue from the bladder, called transurethral resection (TUR), used both as a diagnostic and therapeutic tool. After a first TUR, most patients (30-80%) experience a recurrence of the disease and a variable amount of superficial lesions will eventually progress to invasive cancer (1-45% within 5 years). The need to continuously monitor the patients together with the expensive treatments, make the cost per patient (from diagnosis to death) the highest among all cancers. Therefore, accurate and early diagnosis of NMIBC is essential to offer the patients the most appropriate treatment and the highest cure rate, but also to decrease the costs associated with this disease.

White-light (WL) cystoscopy is the gold standard for the visualization of suspicious lesions during TUR. In general, this technique works well in the detection of exophytic lesions, but small papillary lesions and flat lesions such as carcinoma *in situ* (CIS) are underdiagnosed. It is believed that between 10 and 20 % of tumors are missed with standard equipment. Hence, there is a need for better visualization. Recently, the use of fluorescence-guided diagnosis or photodynamic diagnosis (PDD) has been implemented in clinical practice. Different studies have indicated that PDD improves detection of bladder tumors and reduces recurrence rates up to 1 year. Unfortunately, the widespread use and implementation of this technique is hampered by the requirement of specific, expensive equipment. The use of a dye that specifically piles up in or between tumor cells would be an ideal solution: the advantages of PDD could then be combined with the cheaper WL cystoscopy protocol. Our group previously investigated different compounds with high absorption coefficients in the visible light spectrum. From this analysis, Evans blue (EB) was selected as the only dye showing the desired tumoritropic characteristics as revealed with spheroids composed of malignant urothelial cells. It was concluded that the compound is a possible promising tool as a clinical diagnostic for bladder cancer.

Evans blue, also named T-1824 or Direct blue 53, is a water-soluble poly-aromatic diazo dye that has a very intense blue color (molar absorption coefficient of 78,100 $M^{-1}cm^{-1}$ at 626 nm). In this study, the tumoritropic characteristics of EB were further investigated using a syngeneic, orthotopic AY-27 rat bladder urothelial cell carcinoma model. First, using the fluorescence properties of EB, the biodistribution of this compound in the different layers of the bladder wall (urothelium, submucosa and muscle) was investigated in healthy and tumor-bearing rat bladders. It was concluded that the accumulation of EB in malignant bladders was substantially higher compared with healthy bladders, especially in the outer layer of the bladder wall, the urothelium. In case of a 1 mM EB instillation for 2 hrs, the EB-associated fluorescence in malignant urothelium was 55 times higher as compared to the fluorescence found in normal urothelium. Instillations of EB also resulted in some accumulation of the compound in the inner layers of the bladder, i.e. the muscle layer. This was observed especially when applying longer instillation times (2 hrs). Since the future goal of this research is to apply EB in combination with WL cystoscopy without the need for fluorescence imaging, the level of staining of the inner bladder wall after EB

instillations was visually inspected. It was clear that tumor-inoculated bladders exhibited a more intense blue color as compared to the normal bladders. This observation was confirmed by quantitative analysis after a chemical extraction, with a 5.5-fold higher concentration of EB in tumor tissue after an instillation of 1 mM for 2 hrs. However, especially for the higher concentrations tested, healthy bladder walls also presented with some spots of blue staining, possibly due to inflammation or small injuries as a consequence of catheterization. In case of the tumor bladders, it was observed that the blue staining was not uniformly spread throughout the entire inner bladder wall. This observation could be explained by a non-uniform proliferation of the AY-27 tumor cells in the bladder wall or by the local regeneration of normal urothelium at the spots with less blue staining. This model-related issue requires further investigation in the future.

To investigate local adverse effects of intravesically instilled EB, this compound was instilled daily in healthy rat bladders for up to 7 consecutive days. Histological analysis showed that the urothelium was completely intact after exposure to low (1 mM) and high (5 mM) concentrations of EB. In some of the rats, slight inflammation and oedema was noticed in the underlying layers, e.g. in the lamina propria and muscularis. Since this kind of inflammation was also noticed in the control rat bladders in the same extent, we hypothesize that the inflammation was due to the repeated instillation procedure and not to adverse effects induced by EB itself.

Next, to determine the amount of EB that evades from the bladder into the circulatory system, EB was extracted from rat plasma. After intravesical instillations, approximately 5 % of the amount of EB was able to reach the blood circulation. This observation could raise some safety concerns. However, since EB has been frequently used as a dye marker to determine blood volume in humans without any adverse reactions, the safety risk for patients after an intravesical instillation is considered to be very low.

Finally, to investigate the mechanisms behind the specific accumulation of EB in tumor tissue, cell adhesion between urothelial cells was investigated in different ways. First, transmission electron microscopy (TEM) pointed to ultrastructural differences between healthy and malignant urothelium. Cells of the healthy urothelium were very tightly interconnected and were characterized by the presence of normal cell adhesion junctions, e.g. tight junctions (TJs), adherens junctions (AJs) and desmosomes. Conversely, in tumor samples, cells were loosely attached to each other and a decreased number of cell junctions were observed. Secondly, immunohistochemistry showed that desmoglein-1, an important component of desmosomes, was expressed at a lower level in malignant compared with healthy urothelium. E-cadherin, one of the building blocks of AJs, was not differentially expressed. Thirdly, transcriptomics of normal and malignant urothelium demonstrated that many genes related to cell adhesion were differentially expressed, particularly genes coding for proteins involved in TJ formation and regulation. Of interest, pathway (PW) analysis of our data set also demonstrated the importance of cell adhesion, since the categories ‘tight junction pathway’ and ‘adherens junction pathway’ were significantly enriched.

SAMENVATTING

Blaaskanker is een belangrijk gezondheidsprobleem, met jaarlijks een geschatte 429.000 nieuwe gevallen en 165.000 overlijdens ten gevolge van deze ziekte (cijfers gebaseerd op het jaar 2012). Globaal gezien is blaaskanker de vierde en achtst meest voorkomende soort kanker in de mannelijke en vrouwelijke populatie, respectievelijk. De kans op blaaskanker neemt toe met de leeftijd. Bij de initiële diagnose wordt de meerderheid van gedetecteerde letsels (70-75 %) geclassificeerd als 'niet-spier-invasieve' tumors, beperkt tot de dikte van het blaasslijmvlies. Initiële therapie voor dit soort tumor is het operatief verwijderen van het maligne weefsel in de blaas, een 'transurethrale resectie' (TUR). Deze operatieve techniek dient zowel voor diagnose als voor therapie. Na een eerste TUR ervaren een groot aantal patiënten (30-80 %) een herval. Bovendien zullen een aantal lesies uiteindelijk spier-invasief worden (1-45 % binnen de 5 jaar). Doordat patiënten frequent moeten worden opgevolgd en de behandelingen duur zijn, zijn de kosten geassocieerd met deze ziekte zeer hoog. Meer nog, de kosten van patiënten met blaaskanker (van diagnose tot sterfte) worden tot de hoogste gerekend van alle soorten kankers. Een correcte en tijdige diagnose van niet-spier-invasieve blaastumors is dus van essentieel belang om patiënten de beste behandelingsmogelijkheden en de grootste kans op genezing te bieden, maar ook om de kosten van deze ziekte te drukken.

De dag van vandaag is cystoscopie met wit licht (WL) de algemene standaard voor de visualizatie van verdachte lesies tijdens een TUR. In het algemeen is deze aanpak voldoende voor de detectie van grote letsels, maar de detectie van kleine papillaire letsels en 'carcinoma *in situ*' is dikwijls onvoldoende. Met deze standaard techniek worden ongeveer 10 tot 20 % tumors gemist. Deze cijfers beklemtonen de noodzaak voor een betere visualizatie tijdens TUR procedures. Recent werd het gebruik van fluorescentie cystoscopie of fotodynamische diagnose ingevoerd in de klinische praktijk. Verschillende studies hebben aangetoond dat fotodynamische diagnose de detectie van blaastumors verbeterd en het aantal recidieven verminderd tot 1 jaar na de ingreep. Jammer genoeg is het algemene gebruik van deze techniek beperkt doordat specifiek, duur materiaal moet aangekocht worden. Het gebruik van een kleurstof die zich specifiek opstapelt in of tussen tumorcellen zou een ideale oplossing zijn: de voordelen van fotodynamische diagnose zouden op deze manier gecombineerd kunnen worden met het goedkopere protocol van wit licht cystoscopie. In het verleden heeft onze onderzoeksgroep verschillende componenten onderzocht met hoge absorptiewaarden in het zichtbare licht spectrum. Door gebruik te maken van sferoïden samengesteld uit maligne urotheelcellen, werd aangetoond dat Evans blauw (EB) de enige kleurstof was met de juiste tumor-opstapelende eigenschappen. Bijgevolg is deze kleurstof een veelbelovend klinisch diagnostich middel voor blaaskanker detectie.

Evans blauw, ook wel T-1824 of Direct blauw 53 genaamd, is een water-oplosbare poly-aromatische diazo kleurstof met een zeer intense blauwe kleur (molaire absorptie coëfficiënt van 78.000 $M^{-1}cm^{-1}$ bij 626 nm). In dit project werden de tumor-opstapelende eigenschappen van EB onderzocht door gebruik te maken van een syngeneïsch, orthotopisch AY-27 rat blaaskanker model. Tijdens een eerste experiment werd gebruik gemaakt van de fluorescerende eigenschappen van EB om de verdeling in de verschillende lagen van de blaaswand (urotheel, blaasslijmvlies en spierlaag) na te gaan in rattenblazen met en zonder blaastumors. Dit experiment toonde aan dat de opstapeling van EB in de tumorblazen duidelijk hoger lag vergeleken met gezonde blazen, voornamelijk in de buitenste laag van de blaaswand, het urotheel. Een 2 uur-

durende instillatie van 1 mM EB leidde tot een 55-keer hogere fluorescentiewaarde van EB in maligne urotheel in vergelijking met gezond urotheel. Instillaties van EB resulteerden eveneens in opstapeling van deze kleurstof in de diepere lagen, d.w.z. in de spierlagen. Dit werd voornamelijk gezien in het geval van langere instillatietijden (2 uur). Aangezien het uiteindelijk doel van dit onderzoek erin bestaat om EB toe te dienen in combinatie met WL cystoscopie zonder fluorescentie-visualizatie, werd de graad van kleuring van de binnenste blaaswand visueel onderzocht na EB instillaties. Hieruit bleek dat blazen met tumors een intensere blauwe kleur vertoonden dan de normale blazen. Deze visuele observatie werd bevestigd door middel van een kwantitatieve analyse na chemische extractie: na een instillatie van 1 mM EB gedurende 2 uur, werd een 5,5 keer hogere concentratie waargenomen in tumorweefsel dan in gezond weefsel. Voornamelijk bij de hogere concentraties, werden echter ook plekken van blauwe kleuring aangetroffen in de gezonde blazen. Dit is waarschijnlijk te wijten aan ontstekingen of kleine wondjes ten gevolge van de catheterisatie procedure. In het geval van de tumorblazen werd vastgesteld dat de blauwe kleuring niet uniform verspreid was over de gehele binnenste blaaswand. Dit kan verklaard worden door een niet-uniforme verdeling van de AY-27 tumorcellen in de blaaswand of door de lokale regeneratie van normaal urotheel op de plaatsen met minder blauwe kleuring. Deze model-gerelateerde kwesties dienen verder onderzocht te worden in de toekomst.

Om lokale ongunstige effecten van intravesicaal geïnstilleerd EB na te gaan, werd deze kleurstof dagelijks toegediend in gezonde rattenblazen gedurende 7 opeenvolgende dagen. Histologische analyse toonde aan dat het urotheel volledig intact was na blootstellingen aan lage (1 mM) en hoge (5 mM) concentraties van EB. In sommige ratten werd een lichte ontsteking en oedeem waargenomen in de onderliggende lagen, de lamina propria en spierlaag. Aangezien dit soort ontsteking in dezelfde mate werd waargenomen in de controle blazen, veronderstellen we dat de onstekingen het gevolg waren van de dagelijkse instillatie procedure en niet van negatieve effecten geïnduceerd door EB zelf.

Tevens werd de hoeveelheid EB dat doorsijpelde vanuit de blaas tot in de bloedcirculatie onderzocht. Hiertoe werd EB geëxtraheerd vanuit rattenplasma. Dit experiment wees erop dat ongeveer 5 % van de oorspronkelijk toegediende EB de bloedcirculatie bereikte. Deze observatie zou vragen kunnen oproepen in verband met de veiligheid van EB instillaties. Echter, aangezien EB zeer frequent gebruikt werd als merker om het bloedvolume te bepalen in patiënten en er ten gevolge van deze toepassing geen ongunstige effecten werden gerapporteerd, kan het veiligheidsrisicio voor patiënten na een intravesicale toediening als zeer laag beschouwd worden.

Als laatste werd het mechanisme achter de specifieke opstapeling van EB in tumorweefsel verder onderzocht. Hiervoor werd de celadhesie tussen urotheelcellen nader bekeken op verschillende manieren. Ten eerste toonde transmissie elektronen microscopie (TEM) aan dat er ultrastructurele verschillen aanwezig waren tussen gezond en maligne urotheel. Cellen van gezond weefsel hingen zeer hecht aan elkaar en de aanwezigheid van normale cell adhesie juncties, dit zijn de zonula occludens, zonula adherens en de desmosomen, kon duidelijk worden waargenomen tussen deze cellen. In tumorstalen daarentegen waren de cellen los met elkaar verbonden en celadhesie structuren waren veel minder aanwezig. Ten tweede bleek uit immuunhistochemie dat desmogleïne-1, een belangrijk proteïne van de desmosomen, minder tot expressie kwam in maligne urotheel vergeleken met gezond urotheel. E-cadherine, een

belangrijke bouwsteen van de zonula adherens, werd niet differentieel tot expressie gebracht. Ten derde, toonde een transcriptoomanalyse van normaal en maligne urotheel aan dat veel genen gerelateerd aan celadhesie differentieel tot expressie werden gebracht. Dit werd voornamelijk waargenomen voor genen die coderen voor zonula occludens vorming en regulatie. Opmerkelijk genoeg wees een 'pathway' (PW) analyse van onze dataset eveneens op het belang van celadhesie, aangezien de categorieën 'zonula occludens PW' en 'zonula adherens PW' significant verrijkt waren.

CHAPTER 1

General introduction

PART I: Bladder cancer

1.1 Structure and function of the normal bladder

The urinary bladder is part of the urinary system, also called the renal system. Briefly, urine is produced in the kidneys by filtering the blood to excrete waste material and extra water. Urine travels through the ureters towards the bladder, which stores the urine until it is eliminated via the urethra.

The bladder is a hollow pear-shaped organ located in the pelvis between the pelvic bones. It is not a static structure, but can elastically change its shape according to the amount of collected urine. From inside to outside, the bladder wall consists out of four principal layers: the mucosa, composed of the urothelium and lamina propria, the submucosa, also known as muscularis mucosa, the muscularis (muscle layer) and the serosa (Figure 1.1).

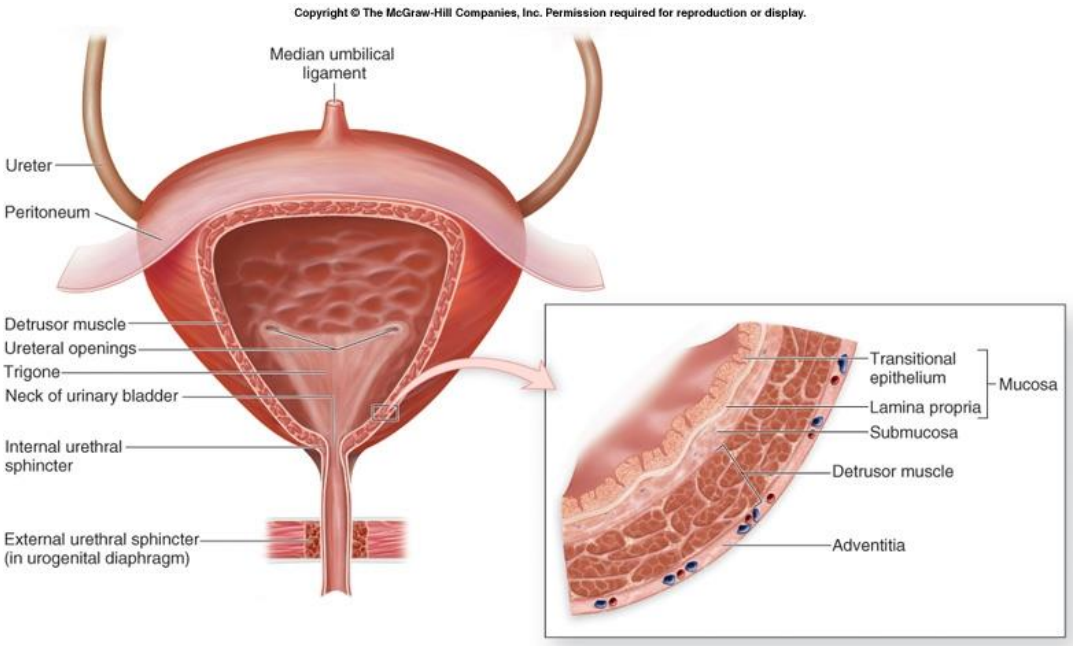

Figure 1.1: The human urinary bladder with the different layers of the bladder wall (Adopted from Miftahof et al, 2013)

The multilayered urothelium is the most specialized layer, consisting of three different cell types: (1) a cuboid-shaped basal cell layer, (2) an intermediate cell layer and (3) a superficial layer of umbrella cells. The umbrella-cell layer is in direct contact with the urine and is covered by a protective glycosaminoglycan layer (GAG). The urothelium has different functions: first of all, it serves as a barrier against urine constituents, infections, toxins and other irritants. In contrast to the old conception, the urothelium is much more than just a passive barrier, as it is also involved in some essential functions, like the micturition reflex, metabolic secretion, regulation of inflammation and afferent functions (Lazzeri, 2006). Defects in this layer can lead to pathological conditions like detrusor overactivity, inflammation, cell growth, differentiation and cancer.

1.2 Bladder cancer

1.2.1 Incidence

Bladder cancer (BC) is a major health problem worldwide. It is the 4th most common form of cancer in the male population of developed countries, following prostate, lung and colon cancer (Jemal et al, 2011). In the US, 74,690 new cases of bladder cancer were recorded accompanied with 15,580 deaths in 2014 (Malats & Real, 2015). In the European Union (EU-27), even higher numbers were registered in 2008 (110,500 new cases and 38,200 deaths) (Ferlay et al, 2010). A change in demographics has been noticed in recent years. In the past, bladder cancer was mainly a disease of the western societies, while nowadays more and more cases are arising in developing countries due to rising smoking prevalence and exposure to polluted or contaminated water sources (Ploeg et al, 2009; Noon & Catto, 2013).

1.2.2 Classification of bladder tumors

Most bladder cancers (over 90%) are transitional cell carcinomas (TCC), arising from transitional cells that line the bladder lumen, 5% of tumors are squamous cell carcinomas and less than 2% are adenocarcinomas (Kaufman et al, 2009). Transitional cell carcinomas are also known as urothelial cell carcinomas (UCC), the term that should preferentially be used according to the World Health Organization/International Society of Urological Pathology (WHO/ISUP) (Epstein et al, 1998).

Roughly, UCCs can be divided into 2 main groups: non-muscle-invasive bladder cancers (NMIBC) and muscle-invasive bladder cancers (MIBC). At first diagnosis, approximately 75% of detected lesions belong to the NMIBC group (Sharma et al, 2009). These kinds of tumors are characterized by low progression rates and patients often have a good long-term prognosis, although up to 45% of tumors will eventually progress to invasive tumors (van Rhijn et al, 2009). Patients presenting with MIBC have a higher mortality risk (Burger et al, 2013).

To determine the optimal treatment for the patients, NMIBC and MIBC are further subdivided according to the 'Tumor, Node, Metastasis' (TNM) classification system. This 2002 TNM classification system, approved by the Union for International Cancer Control (UICC), has been widely accepted and used. In 2009, this version was updated, but no changes for bladder cancer determination have taken place (Sobin et al, 2009). The 2009 TNM classification is given in Table 1.1.

The TNM system can be explained as follows: The T stands for staging and determines the depth of primary tumor invasion into the bladder wall (Figure 1.2): the majority (70%) of NMIBC are staged as Ta, which means that the tumors are papillary and confined to the urothelium. 20% of NMIBC are T1 tumors, invading the lamina propria, and 10 % are classified as carcinoma *in situ* (CIS), flat lesions confined to the urothelium. Muscle-invasive tumors are staged as T2 (invading the muscularis), T3 (infiltrating the perivesical tissue) or T4 (invading other organs). The N describes nearby lymph nodes that are possibly involved. There are 4 lymph node stages in

bladder cancer (Table 1.1). M stands for metastasis of the primary tumor. There are only 2 possibilities: either the cancer has spread to distant sites in the body (M1) or not (M0).

Table 1.1: The 2009 TNM classification system for bladder tumors

T - Primary tumour		
TX	Primary tumor cannot be assessed	
T0	No evidence of primary tumor	
Ta	Non-invasive papillary carcinoma	
Tis	Carcinoma *in situ* : 'flat tumor'	
T1	Tumor invades subepithelial connective tissue	
T2	Tumor invades muscle	
	T2a	Tumor invades superficial muscle (inner half)
	T2b	Tumor invades deep muscle (outer half)
T3	Tumor invades perivesical tissue:	
	T3a	Microscopically
	T3b	Macroscopically (extravesical mass)
T4	Tumor invades any of the following: prostate, uterus, vagina, pelvic wall, abdominal wall	
	T4a	Tumor invades prostate, uterus or vagina
	T4b	Tumor invades pelvic wall or abdominal wall
N - Lymph nodes		
NX	Regional lymph nodes cannot be assessed	
N0	No regional lymph node metastasis	
N1	Metastasis in a single lymph node in the true pelvis (hypogastric, obturator, external iliac, or presacral)	
N2	Metastasis in multiple lymph nodes in the true pelvis (hypogastric, obturator, external iliac, or presacral)	
N3	Metastasis in common iliac lymph node(s)	
M - Distant metastasis		
MX	Distant metastasis cannot be assessed	
M0	No distant metastasis	
M1	Distant metastasis	

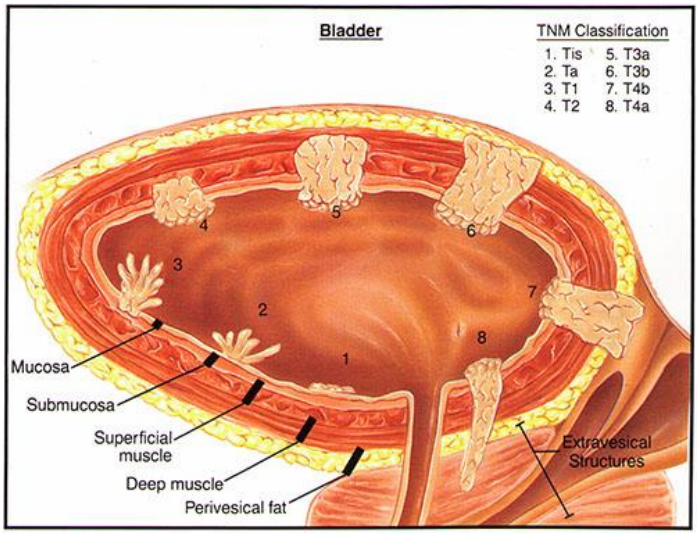

Figure 1.2: The different stages of bladder tumor invasion

Further characterization of bladder tumors is done by 'grading', which means that cancer cells are classified based on how they look under a microscope. Historically, the 1973 WHO classification, subdivided bladder tumors into 3 groups: grade 1 (well differentiated), grade 2 (moderately differentiated) and grade 3 (poorly differentiated). This system has been widely used, but the definition of the different grades was rather vague and did not take into account the specific histological criteria, which resulted in most tumors falling into the intermediate grading group (Miyamoto et al, 2010). To avoid this and to obtain a more universal staging system for bladder tumors, the WHO/ISUP developed a new classification system in 1998, which was revised in 2003 (Eble et al, 2004). In this new grading system, papillary urothelial neoplasms are divided into 4 groups: papilloma, papillary urothelial neoplasm of low malignant potential (PUNLMP), low grade papillary carcinoma and high grade papillary carcinoma. Each of these groups is accompanied with a detailed description of the architectural and cytological criteria. Among the flat lesions, the 2004 system identifies 5 groups: urothelial hyperplasia, reactive urothelial atypia, atypia of unknown significance, dysplasia and CIS. There is no one-to-one translation between the 1973 and 2004 classification system, as is illustrated in Figure 1.3. As a consequence, both classification systems are still used in the clinic.

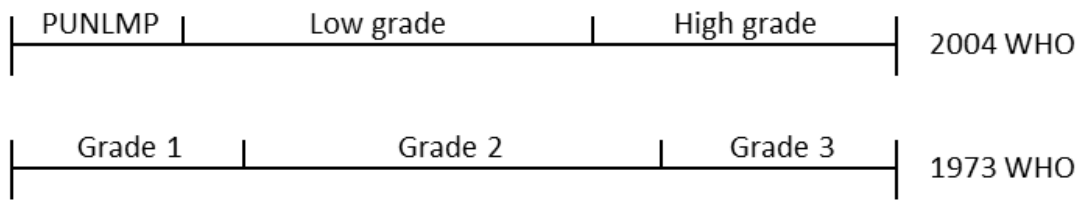

Figure 1.3: The WHO classification system of 1973 and 2004 compared (Adopted from Babjuk et al, 2013)

1.2.3 Risk factors

1.2.3.1 Smoking

Smoking is considered as the most important risk factor for developing bladder tumors and it is estimated to account for 50 % of bladder cancer cases (Freedman et al, 2011). Tobacco smoke contains compounds, like aromatic amines, such as β-naphthylamine, and polycyclic aromatic hydrocarbons that are known to cause bladder cancer. These compounds are inhaled and excreted through the renal system, thereby exposing the bladder wall. The time-frame between exposure to smoke compounds and the manifestation of tumors can be more than 30 years (Burger et al, 2013). This long latency time makes it difficult to predict the impact of smoking on bladder cancer in the future, especially since smoking habits are changing (for example: higher-educated people are more likely to quit) and the composition of tobacco products has also been adjusted over time. Over the years, less tar and nicotine are added but an increase in the concentration of β-naphthylamine and tobacco-specific nitrosamines has been found (Hoffmann et al, 2001). Several studies have mentioned higher relative risks for lung cancer associated with these newly constituted cigarettes (Thun et al, 1997) and a recent article from the New England

Bladder Cancer Study suggests that this might also be the case for bladder cancer (Baris et al, 2009).

1.2.3.2 *Occupational exposure*

The second most important risk factor for developing bladder cancer, accounting for an estimated 20 % of bladder tumors, is occupational exposure to carcinogens. Dangerous compounds in the working environment include aromatic amines, polycyclic aromatic hydrocarbons and chlorinated hydrocarbons (Burger et al, 2013). People working in industrial settings, processing paint, dye, metal, leather and petroleum products are often exposed to these compounds and different studies have indeed shown a higher incidence of bladder cancer in employees working in these particular environments (Sorahan et al, 1998; Kogevinas et al, 2003; Brown et al, 2012).

1.2.3.3 *Gender*

Men are 3-to-4 times more likely to develop bladder carcinomas than women, though women usually present with a more advanced form of the disease and have a worse prognosis (Fajkovic et al, 2011). No clear explanation for this gender difference has been found, but possible factors might be: unequal access to health care, delays in diagnosis and treatment, different exposures to carcinogens, anatomic and hormonal factors (sex steroids and receptors).

1.2.3.4 *Age*

The risk of developing bladder cancer rises with age. The mean age at diagnosis is approximately 67 years (Malats & Real, 2015).

1.2.3.5 *Schistosoma infection*

While smoking and occupational exposures are the most important risk factors in Western countries, chronic infection with the parasitic fluke *Schistosoma hematobium* causes most cases of bladder carcinoma in developing countries, mainly Africa and the Middle East. Schistosomiasis causes squamous cell carcinoma (SCC). The exact mechanism of the initiation and progression of SCC is not known, but it seems to be a combination of different factors: actions of the parasite, host immune response, co-infections, micronutrients and environmental exposure to toxins (Honeycutt et al, 2014). Recently, novel sterol-like metabolites and DNA-adducts were found in the urine of persons suffering from urogenital schistosomiasis. These reactive molecules are metabolized to active quinones that can modify DNA and hence, on the long term, induce tumors (Correia da Costa et al, 2014)

1.2.3.6 *Genetic predisposition*

Bladder cancer is known to occur more in certain families, though no clear Mendelian inheritance pattern can be found. However, some genes have been identified that play a role in de development of BC. The enzyme *N*-acetyltransferase 2 (NAT2), coded by the *NAT2* gene, is

responsible for the acetylation of aromatic and heterocyclic amine compounds, thereby detoxifying several bladder carcinogens. When the *NAT2* gene is mutated, the enzyme has a decreased capacity to detoxify aromatic amines, thereby increasing the risk to develop bladder cancer by 40 % (Garcia-Closas et al, 2005). Another gene related to bladder cancer is the *GSTM1* gene, encoding glutathione S-transferases. These enzymes detoxify several carcinogens, including polycyclic aromatic hydrocarbons. *GSTM1*-null genotypes are at increased risk to develop BC by an estimated 50 % (Garcia-Closas et al, 2005). Weak but evident associations with BC were found for some DNA repair gene SNPs (single nucleotice polymorphisms), e.g. *ERCC2* D312N, *NBN* E185Q and *XPC* A499V (Stern et al, 2009).

1.2.3.7 *Medication and radiation*

Cyclophosphamide, mainly used to treat certain cancers and some life-threatening auto-immune diseases, has been associated with an increased risk of BC. Likewise, phenacetin and chlornaphazine, two drugs frequently used in the past, are considered as risk factors for bladder cancer. These two latter drugs have been withdrawn from the market (Murta-Nascimento et al, 2007). Radiation therapy to treat cancers in the pelvic region (ovarian, cervical and prostate cancers) poses a risk in the development of BC (Murta-Nascimento et al, 2007).

1.2.4 Symptoms and diagnosis

Most often, the first symptom of bladder cancer is painless blood in the urine, called haematuria. Haematuria can be visible in the urine (macroscopic) or not visible (microscopic). Other symptoms, more specifically those associated with CIS, are urinary frequency, urgency and dysuria. When bladder tumors become more invasive, symptoms like flank, abdominal, pelvic or bone pain can occur.

The first step in the diagnosis of BC is the confirmation of haematuria by microscopic evaluation of the urine (urineanalysis). However, the presence of haematuria alone is not very specific for bladder cancer, but can also be caused by urinary tract or kidney infections, bladder/kidney stones or medications. Therefore, urine cytology is done in which the cells in the urine are examined under the microscope. Urine cytology has a high specificity (appr. 94 %), but has a low sensitivity, particularly for low-grade bladder carcinoma (25-57 % for low-grade, 53-92 % for high-grade bladder carcinoma) (Turco et al, 2011). Negative urine cytology therefore cannot exclude BC.

The "gold standard" for the diagnosis of BC is white-light (WL) cystoscopy. During this procedure, a rigid or flexible cystoscope is inserted through the urethra into the bladder to thoroughly investigate the bladder wall for tumors. All suspicious lesions are resected (called transurethral resection of the bladder or TURB) and investigated by a pathologist. WL cystoscopy can be used both as a diagnostic (detecting tumors) and therapeutic (resection of tumors) tool. However, this technique has some shortcomings. WL cystoscopy is operator-dependent, small papillary lesions and CIS are difficult to detect, inflamed and malignant regions are difficult to differentiate, margins of tumors are often not clear and grade and stage cannot be determined on the spot. These problems can lead to incompletely resected or even missed tumors, eventually causing recurrences and progression. After a first TURB, up to 30 to 80 % of

patients experience a recurrence of the disease, while a substantial amount of superficial lesions will eventually progress to invasive cancer (up to 45% within 5 years) (van Rhijn et al, 2009). To avoid this, patients require extensive follow-up, causing BC to have the highest lifetime treatment cost per patient of all cancers (Sievert et al, 2009).

In order to help the surgeon during cystoscopies, new imaging techniques are emerging.

1.2.4.1 *Fluorescence cystoscopy/photodynamic diagnosis (PDD)*

By instilling tumoritropic, (pro)-fluorescent compounds inside the bladder before cystoscopy, urothelial neoplasms can be visualized more clearly. The mechanism is the following: after instillation of the compound, it will selectively accumulate in malignant tissue. During cystoscopy, the bladder wall is illuminated with the correct wavelength, causing malignant tissue to emit a red fluorescence which makes it more distinguishable from healthy bladder tissue. The first compound used was 5-aminolevulinic acid (5-ALA), a precursor of the endogenous photosensitizer protoporphyrin IX (PpIX). To improve tissue penetration and to decrease drug dose and instillation time, a hexylester of 5-ALA, HAL (hexaminolevulinate; trade name Hexvix®/Cysview®) was developed. Other compounds used are hypericin and its derivative PVP (polyvinylpyrrolidone) -hypericin which is more water soluble. Hypericin and PVP-hypericin are direct photosensitizers, which means they accumulate directly into the tumor tissue.

HAL instillations were approved by the FDA (Food and Drug Administration) in 2010. The use of PDD is recommended by the European Association of Urology (EAU) when CIS or high-grade tumors are suspected (EAU guidelines, 2015).

Different studies investigated the efficacy of PDD over WL cystoscopy for NMIBC. A meta-analysis published in 2013 (Burger et al, 2013) concluded that blue-light cystoscopy with HAL improves detection of bladder tumors and reduces recurrence rates up to one year. The odds of detecting CIS were 12.4 times higher when using PDD instead of WLC.

1.2.4.2 *Narrow band imaging (NBI)*

Narrow band imaging is a technique in which light of specific blue (415 nm) and green wavelengths (540 nm) is used to investigate the bladder wall. The shorter wavelength penetrates the superficial layers of the mucosa; the 540 nm-wavelength penetrates deeper. Since these specific wavelengths are absorbed by hemoglobin in the vasculature, tumors, which are often highly vascularized, can be more easily detected. The malignant tissue appears as a dark green or brown color. Li et al (2013) published a meta-analysis to compare detection rates when NBI was used vs. WL cystoscopy. It was reported that an additional 24 % of tumors was detected in an additional 17 % of patients. False positive detection rates were similar to those observed with WL cystoscopy. Currently, a large international multicenter randomized trial, aiming to investigate recurrence rates at 1 year following TURB with white-light vs. TURB with NBI, is being conducted (Naito et al, 2013).

1.2.4.3 *Optical coherence tomography (OCT)*

This technique allows a surgeon to take a non-invasive real-time optical biopsy. Near-infrared light (890-1300 nm) is used to capture three-dimensional images of tissues via its scattering properties. Since different tissues have different cellular properties, the OCT signal differs for each tissue type which makes it possible to distinguish not only the different layers of the bladder wall (urothelium, lamina propria, muscularis propria) (Zagaynova et al, 2002) but also benign from malignant tissue and even non-invasive tumors (Ta) from invasive tumors (T1-T3) (Goh et al, 2008). OCT has several advantages for intravesical diagnostics. OCT can be easily integrated with the conventional endoscopes and can be composed with common optical fiber. Also, the system is compact and portable. However, before incorporating this technique in clinical practice, more *in vivo* studies/clinical trials should be performed to find out if OCT is able to differentiate between low-grade, high-grade and CIS tumors. Also parameters like sensitivity, specificity, and positive and negative predictive values need to be established more thoroughly (Bus et al, 2015).

1.2.4.4 *Storz Professional Imaging Enhancement System (SPIES)*

Very recently, a new imaging device has been developed by the Karl Storz company, called Storz Professional Imaging Enhancement System. The big advantage of SPIES is that the endoscopic view can be monitored in four different ways and two images are projected on the screen, a white-light image and an enhanced image (Villa et al, 2015). The four modes of endoscopic viewing are the SPECTRA A and B, CLARA and CHROMA mode. With the two SPECTRA modes, specific color renderings are projected that enhance local contrasts in the bladder tissue. The CLARA mode provides a better visualization of dark regions, while the CHROMA mode increases the clearness of anatomical structures. It is believed that by generating clearer images of the bladder wall, more tumors are detected and a more complete resection of the detected tumors can be performed. Currently, the effectiveness of SPIES vs. WL cystoscopy in NMIBC is investigated in a clinical trial (Gravas & Stenzl, 2014).

1.2.4.5 *Urinary biomarkers*

At present, no diagnostic technique is able to replace invasive cystoscopy. Much research has been done to look for urinary biomarkers for BC detection. Ideally, a test for surveillance and screening for BC needs to be fast, easy to perform, non-invasive and have high sensitivity and specificity values. Many markers have been described in literature, but few have been approved for clinical use. An overview of some biomarkers under investigation can be found in Table 1.2. The main problem with most of these markers is a too low specificity/sensitivity level (see Table 1.3). To date, no biomarker has been accepted in the guidelines of the EAU (EAU guidelines, 2015).

Table 1.2: Urinary biomarkers for bladder cancer (adopted from Smith & Guzzo, 2013)

Test (Manufacturer)	Marker detected	Assay type	FDA approval
Cytology	Tumor cells	Microscopy	N/A
BLCA-4 (Eichrom Technologies)	Nuclear matrix protein	Sandwich ELISA (rabbit polyclonal antibody)	-
BTA stat® (Polymedco)	Complement factor H-related protein and complement factor H	Immunoassay or point-of-care	For diagnosis & follow-up
BTA TRAK® (Polymedco)	Complement factor H-related protein and complement factor H	Sandwich ELISA	For diagnosis & follow-up
CYFRA 21-1 (Bio International; Roche Diagnostics)	Cytoskeletal protein (cytokeratin 19)	Immunoradiometric assay or ELISA	-
DD23 (UroCor Labs)	185-kDa tumor associated antigen	Immunocytochemistry	-
NMP22/BladderChek® (Alere)	Nuclear mitotic apparatus protein	Sandwich ELISA or point-of-care	For diagnosis & follow-up
Survivin (Fujirebio Diagnostics)	Inhibitor of apoptosis gene	Bio-dot test (rabbit polyclonal antibody)	-
UBC™ (IDL Biotech)	cytoskeletal proteins (cytokeratin 8 and 18)	Sandwich ELISA or point-of-care	-
ImmunoCyt™/uCyt+™ (Scimedx)	Carcinoembryonic antigen, two bladder tumo cell-associated mucins	Immunocytochemistry	For follow-up
UroVysion™ (Abbott, Vysis)	Alterations in chromosomes 3, 7, 17 and 9p2	FISH	For diagnosis & follow-up

Table 1.3: Sensitivity and specificity levels of some urinary biomarkers (adopted from Smith & Guzzo, 2013)

Test	Surveillance		Screening	
	Sensitivity (%)	Specificity (%)	Sensitivity (%)	Specificity (%)
Cytology	22-52	96-98	15-55	81-99
BLCA-4	89-96	100	-	-
BTA stat®	53-83	67-72	90	76
BTA TRAK®	66-72	51-75	-	-
CYFRA 21-1	67-97	67-89	79	89
DD23	70-81	60	-	61-86
NMP22/BladderChek®	47-100	60-90	55-97	29-85
Survivin	64-100	87-93	-	-
UBC™	66-82	83-90	-	-
ImmunoCyt™/uCyt+™	50-100	69-79	-	-
UroVysion™	36-100	89-98	-	-

Recently, an article described the possibility to use a multicomplex biomarker panel for the detection of BC. Five highly sensitive and specific biomarkers were combined and tested on urine samples of BC patients and patients with benign urological conditions, chronic diseases or other cancers. The biomarkers were the following: Corinin-1A, Apolipoprotein A4, Semenogelin-2, γ-synuclein and DJ-1/PARK7. The combination of these 5 biomarkers lead to higher specificity/sensitivity values compared to commercially available tests (Kumar et al, 2015).

1.2.5 Management of bladder cancer

Treatment options for bladder cancer strongly depend on grade and stage of the cancer at initial diagnosis. A general scheme can be found in Figure 1.4.

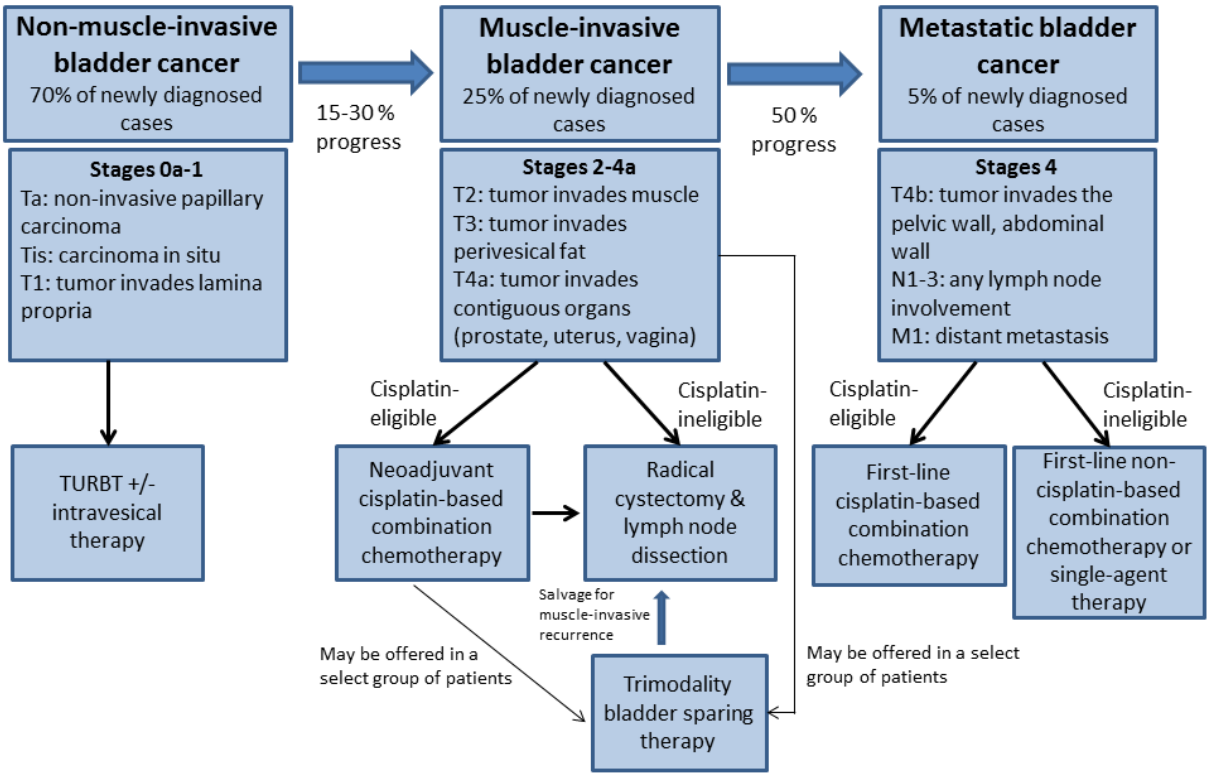

Figure 1.4: Treatment scheme for bladder cancer (adopted from Park et al, 2014)

1.2.5.1 *Non-muscle-invasive bladder cancer*

Treatment of NMIBC aims to prevent recurrences and progression, to avoid loss of the urinary bladder and to enhance survival of the patients. The standard initial therapy for non-muscle-invasive bladder cancer consists of a complete transurethral resection of the tumor(s) (TURBT), including a part of the underlying muscle. This resection allows pathologists to stage the tumor(s) and make decisions about the treatment plan. If necessary (incomplete resection, no muscle in specimen), a reresection is performed. Also, in case of T1 and/or grade 3 tumors (with the exception of CIS alone), a second TURBT is carried out after 2 to 6 weeks to restage the tumor(s). Since non-muscle-invasive bladder tumors have a high tendency for recurrence and/or progression after TURBT, intravesical instillation therapy is often recommended. The EAU has created guidelines of instillation therapy for NMIBC according to the risk stratification. These recommendations are listed in Table 1.4.

Intravesical instillation is performed with either chemotherapeutic agents or by immunotherapy. Mitomycin and thiotepa are often used as chemotherapeutics, while bacillus Calmette-Guérin (BCG) is used in immunotherapy.

Table 1.4: Treatment recommendations for NMIBC after TURB (adopted from Weijers et al, 2015)

Risk category	Definition	Treatment Recommendation
Low	Primary, solitary, Ta, G1 (low grade), <3 cm, no CIS	One immediate instillation of chemotherapy
Intermediate	All cases not defined in the 2 adjacent categories	One immediate instillation of chemotherapy followed by further instillations, either chemotherapy for a maximum of 1 y or 1 y full-dose BCG
High	Any of the following: • T1 • G3 (high grade) • CIS • Multiple and recurrent and large (>3 cm) TaG1-2 tumors (all conditions must be presented)	Full-dose BCG instillations for 1-3 y or cystectomy (in highest risk tumors)

Abbreviations : BCG, bacillus Calmette-Guérin; TaG, tumor stage "a" grade

1.2.5.2 *Muscle-invasive bladder cancer*

Standard treatment for MIBC is a radical cystectomy with pelvic lymph node dissection. However, the 5-year survival rate after a cystectomy stays low (50-70 % depending on tumor stage), despite a 90 % 5-year local control rate (Kaufman, 2006). This observation indicates the presence of micrometastases at the time of surgery and requires additional treatments. Different studies indicate that neoadjuvant cisplatin-based combination chemotherapy increases the survival in patients with MIBC (Grossman et al, 2003; International Collaboration of Trialists, 2011; Advanced Bladder Cancer Meta-analysis Collaboration, 2003; Winquist et al, 2004). Despite the fact that this combination chemotherapy seems to give good outcomes, not all patients are good candidates. Excluded are patients that suffer from hearing loss or dysfunction, cardiac dysfunction, poor performance status and particularly renal insufficiency (Park et al, 2014). Neoadjuvant radiotherapy alone does not give a firm therapeutic benefit (Cole et al, 1995; Crawford et al, 1987). Adjuvant chemotherapy is recommended for patients at high risk for recurrence.

As an alternative to radical cystectomy, different bladder-sparing strategies have been developed. These can be surgical (TURBT, partial cystectomy) or non-surgical (radiation, chemotherapy). Single treatment options, however, are often suboptimal. Therefore a trimodal strategy with the combined power of surgery, radiation and chemotherapy has been tested in clinical trials and shows promising outcomes (Rödel et al, 2002; Kaufman et al, 2000; Elmunt et al, 2012).

PART II: Preclinical models in bladder cancer research

2.1 Cell lines in bladder cancer research

"Normal urothelial cell lines" are cell lines originating from healthy urothelium, which can be used as a control in bladder cancer research. These cell lines have been established by a variety of methods including organ cultures (Knowles et al, 1983; Scriven et al, 1997), primary cultures (de Boer et al, 1996), subcultured cell lines and urothelial cell-stroma recombinants (Scriven et al, 1997).

Bladder cancer cell lines are usually derived from immortalized cell lines, since primary cultures are difficult to obtain and often fail in culture over time. Especially low-grade superficial bladder cancers, the majority of newly diagnosed cases, are difficult to establish in culture (Seifert et al, 2007). Therefore, most human TCC cell lines are derived from high-grade, poorly differentiated cancers, which can be seen in table 1.5.

Table 1.5: Overview of commonly used cell lines in bladder cancer research (adopted from Gabriel et al, 2007)

Cell line	Origin of biopsy	Clinical stage of disease	Established in	Gender
5637	Primary TCC	n.a.	1974	Male
BC-3C	Invasive, solid TCC	G4, C	1998	Female
CAL-29	Invasive, metastatic TCC	G4, T2	1985	Female
HT-1376	Invasive TCC	T2, G3	1977	Female
HT-1197	Recurrent invasive TCC	T2, G4	1977	Male
KU-19-19	Invasive TCC	pT3b, G3	1993	Male
RT4	Recurrent TCC	G1, T2	1968	Male
RT112/84	Primary TCC	G2	1973	Female
T24	Primary TCC	G3	1970	Female
U-BLC1	Primary TCC spontaneously immortal	min. pT2, G3	1998	Female
UM-UC 3	TCC	n.a.	1982	Male

Most studies on cell lines are performed on cells grown in monolayers. This technique is easy and cost-effective, but has several limitations, the most important one being the fact that they do not mimic the *in vivo* situation very well. A solution is 3D cell culture, which is gradually becoming more and more applied by laboratories in the world. In 3D cell culture, cells are allowed to grow as spheroids (cell colonies that grow in 3 dimensions) by different techniques. The general idea behind the generation of spheroids is to minimize interactions between cells and substrate and to maximize cell-cell interactions. Common techniques include: hanging drop method, liquid overlay cultures, continuous spinning techniques and scaffolding techniques. 3D cell culture has many advantages compared with 2D cell culture. The multicellular aggregates show similar characteristics as the 3D original tissue mass, like their histoarchitecture, nutrient gradients, oxygen levels, proliferation rate, pH, response to stimuli, cell-cell communication etc. (Antoni et al, 2015). Also, very importantly, the genotype displayed by 3D spheroids is significantly more relevant to the *in vivo* situation compared to 2D cultures (Smith et al, 2012). A more practical advantage is that cells grow in 3D can be cultured up to 4 weeks versus only 1 week for monolayer cultures due to confluency.

2.2 Animal models in bladder cancer research

Animal models are an essential step in the final preclinical testing procedure before continuing to clinical trials. To increase the chances of a drug working in humans, animal models must resemble the human situation. In rodents, the lower urinary tract shows a remarkable structural and functional similarity to that of humans (Oyasu, 1995). Also, induced bladder neoplasms in rodents are histologically similar to the human disease and even share similar genetic pathways during the development of the tumors (Williams et al, 2008). In the next section, different animal models of bladder cancer will be reviewed.

2.2.1 Orthotopic models

In an orthotopic model, the cancer will grow at the normal place in the body, in our case in the bladder.

2.2.1.1 *Spontaneous models*

Spontaneous development of bladder tumors in rodents is a rare event, but is very common in dogs, affecting tens of thousands of dogs each year worldwide (Fulkerson & Knapp, 2015). Dogs most often suffer from invasive urothelial carcinoma, which closely resembles invasive TCC in humans and therefore might form an opportunity to investigate this disease and translate its findings to the human situation. Dogs are often used to study genetic and environmental risk factors for the development of TCC, but also to test new therapies (Knapp et al, 2014). One example of a promising new therapy for bladder cancer is folate-targeted therapy. It has been shown that certain cancers have a high uptake of folate (vitamin B9) and folate drug conjugates due to an up-regulation of folate receptor (FR) expression. Clinical trials are ongoing to test folate-targeted therapy in humans with ovarian and lung cancer. The potential value of this therapy for bladder cancer was tested in a dog study with promising results (Dhawan et al, 2013).

2.2.1.2 *Chemically induced models*

Exposure to chemical carcinogens (like aromatic amines, polycyclic aromatic hydrocarbons and chlorinated hydrocarbons) is an important risk factor for the development of bladder cancer in humans and this is also the case in rodents. Therefore, by exposing them to carcinogens under the appropriate conditions, bladder tumors can be generated. Most agents used to induce BC in rodents have aromatic amine components, like FANT (*N*-[4-5-nitro-2-furyl-2-thiazolyl]-formamide), BBN (*N*-butyl-*N*-(4-hydroxybutyl)nitrosamine) and MNU (*N*-methyl-*N*-nitrosurea). These carcinogens are usually administered orally to the animals, but injections, intravesical instillations or other methods are also possible.

BBN is the most popular agent to be used due to its lack of systemic toxicity and the exclusive development of urothelial carcinoma (Bertram et al, 1972). The carcinogen is added orally, either by gavage or added to the drinking water, in concentrations of 0.01 to 0.05% for a period of 16 to 30 weeks. Nearly 100% of animals fed with BBN display bladder tumors after treatment (Wu et al, 2000). Importantly, the treatment generates different kind of tumors in mice versus rats: in mice, the formed tumors are often muscle-invasive and metastatic, while in rats the tumors are mostly low-grade, papillary and non-muscle-invasive (DeGraff et al, 2012). Formed tumors are genetically and pathologically similar to the human disease.

2.2.1.3 *Orthotopic xenograft and syngeneic models*

In orthotopic xenograft models, human urothelial cancer cells are injected into the bladders of immunodeficient rodents, while in the syngeneic models, syngeneic mice/rats cancer cells are implanted in immunocompetent animals. The technique for tumor implantation is the same for both models: single cell suspensions are injected into the bladder either via an abdominal incision or after catheterization. The tumor take rate with this method ranges from 30-100%, but can be optimized in different ways. When instilling more tumor cells, increasing the duration time of tumor contact with the bladder wall or mechanically/chemically disrupt the bladder mucosa before injection of tumor cells, tumor take rates are reported to increase significantly (Chan et al, 2009). With these techniques, tumors are already formed after <1 week-2 weeks, which is much faster than in the chemically induced models. The xenograft model is not suitable to test responses to immune therapies, which is often applied to treat bladder cancer, due to the use of immunodeficient animals.

2.2.2 Heterotopic models

In heterotopic models, tumor cells (either animal-specific or primary human cells) are implanted at another place in the body than the urinary bladder. Tumor cells are injected subcutaneously, usually in the flank or hind leg of the mouse/rat. Again, when working with human cells, immunodeficient rodents are needed. Major drawbacks of this model are the low tumor take rate, which is only about 35 % for urothelial carcinomas (DeGraff et al, 2013), and the unnatural environment for the tumors to grow in. Again, when working with human cells, no immunoresponses can be investigated. On the other hand, tumors grow quickly and can be detected already 1 week after tumor implantation. Also, tumor growth can be detected by palpation, which is easier compared to detecting orthotopic tumor growth (e.g. by MRI or histology after sacrifice) (Gabriel et al, 2007).

2.2.3 Genetically engineered models

The generation of transgenic mice or genetically engineered mice (GEM) is a relative new field in bladder cancer research. The first transgenic mouse model was generated in 1999 by Zhang et al. In these mice, simian virus 40 (SV40) large T antigen was expressed under the control of an urothelium-specific promotor, uroplakin 2 (*UpkII*). Transgenic mice were found to develop CIS (low copy number of SV40T transgene) or CIS accompanied with invasive and metastatic disease (high copy number of SV40T transgene) (Zhang et al, 1999). Another possible promotor to drive urothelium-specific expression is the *Krt19* promotor. Besides SV40 large T antigen, other oncogenes that have been expressed in the urothelium in transgenic mice are *Hras*, *Egfr* and cyclin D1 (Kobayashi et al, 2015).

A UPKII-driven Cre mouse strain was developed that was able to target genes flanked by loxP-sites. Some examples of gene targeting with this technique are the following: removal of tumor suppressors p53 and/or pRb (He et al, 2009); activation of β-catenin via deletion of loxP-flanked exon 3 (Ahmad et al, 2011) and deletion of *Ncstn* thereby interfering with Notch-signaling

(Rampias et al, 2014). Due to the use of the *UPKII*-promotor, all alterations are urothelium-specific. Another means to specifically alter gene expression in the urothelium, is delivering Cre-recombinase-expressing adenovirus into the urothelium, which can delete rodent genes flanked by loxP-sites. The delivery of adenovirus is managed through catheterization of the bladder.

PART III: Evans blue

3.1 Chemical and physical properties

Evans blue (EB), also named T-1824 or Direct blue 53, is a water-soluble poly-aromatic diazo dye, discovered by the American chemist Herbert McLean Evans. Its full IUPAC name is the following: tetrasodium (6*E*,6'*E*)-6,6-[(3,3'-dimethylbiphenyl-4,4'-diyl)di(1*E*)hydrazin-2-yl-1-ylidene]bis(4-amino-5-oxo-5,6-dihydronaphthalene-1,3-disulfonate). Azo compounds contain the functional group R-N=N-R'. The aromatic side groups around the azo bond makes many of the azo compounds colored due to absorption of visible light, which is also the case for EB. This dye features a very intense blue color with a molar absorption coefficient of 78,100 $M^{-1}cm^{-1}$ at 626 nm (Roberts & Palade, 1995).

EB has a molecular weight of 960.81 g/mol and a λ_{max} of 605-613 nm (in water). The chemical structure and absorption spectrum of EB is given in Figure 1.5. Evans blue appears as a black powder or as blue crystals with a green-bronze gloss. The compound is soluble in water from 10 to 50 mg/ml (at 24.5 °C) (NTP, 1992) and emits a bright red fluorescence upon excitation (λ_{ex}: 470 and 540 nm; λ_{em}: 680 nm) (Jaffer et al, 2013).

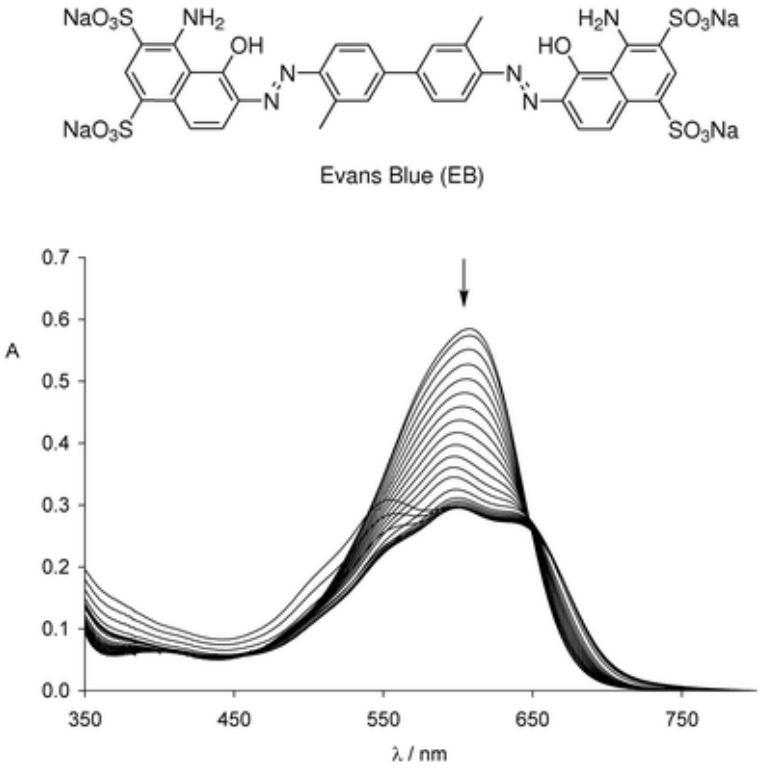

Figure 1.5: Chemical structure and absorption spectra of Evans blue (EB was dissolved in a buffered aqueous solution (MOPS, pH 7)) (adopted from Müller-Graff et al, 2010)

3.2 Clinical use

Evans blue has been used in the past for the determination of the blood volume in humans due to its high binding affinity for the plasma protein albumin. The first dye method to determine plasma and blood volumes was introduced by Keith et al in 1915. They used a red dye, vital red, to calculate plasma volumes. In 1920, Dawson et al tested over 60 different dyes for their possible use in blood volume determinations. They found Evans blue to be the best choice. Advantages of using EB are that this compound is very slowly eliminated from the blood capillaries due to the intense binding with albumin, EB is also non-toxic in high concentrations and, very importantly, it is easier to measure the blue color in the plasma compared to the red, especially when the sample is hemolyzed. The first reliable method to determine plasma volumes with EB was described by Gibson & Evans (1937). Briefly, a measured quantity of the dye is injected into the blood stream. After some time intervals (minimum 10 min after injection), blood is withdrawn and centrifuged to obtain the plasma. Subsequently, the blue color is measured using a spectrophotometer set at 620 nm. Control (undyed plasma) samples undergo the same process. Based on the reads of the photometer, plasma volumes can then be calculated. Intravenously injected EB solutions were found to be non-toxic in doses up to 20 mg/kg in rats (Gibson & Gregerson, 1935).

Evans blue has been used as the standard plasma marker (with some improvements in the technique) until the use of radioisotopes was introduced 20 years later. Main reasons to switch to radioisotopes were reports of sensitivity reactions and patient discolorations. However, in some cases (pregnant women, children) the use of radiolabeled compounds is not appropriate. Therefore, in recent years, the Evans blue dye method has been renewed to a more user-friendly method, e.g. same venous site for dye-injection and collection of samples and an easy way to correct for hemolysis and turbidity of plasma samples (Jones & Wardrop, 2000). Other uses of EB in clinical practice involve the detection of aspirated materials in patients with tracheostomy (Belafsky et al, 2003), dye imaging in cardioscopy (Kanai et al, 2000) and, in the past, Evans blue was injected into the amniotic sac to diagnose premature rupture of the membranes (Atlay & Sutherst, 1970).

AIMS AND OUTLINE OF THE STUDY

At present, white-light (WL) cystoscopy remains the gold standard for bladder cancer detection during transurethral resection of the bladder (TURB). However, inspection of the bladder wall with white light is not a 100% effective, causing underdiagnoses of small lesions and flat carcinoma *in situ* (CIS). As a consequence, many patients experience recurrences and progression to a more advanced stage of the cancer. It is believed that a better detection at initial diagnosis leads to fewer recurrences, thereby improving the outcome for patients. For example, it has been studied that, by using fluorescence cystoscopy after instillation of fluorescent, tumoritropic compounds, detection of bladder tumors improves, decreasing recurrence rates up to one year (Burger et al, 2013). Despite its proven efficacy, fluorescence cystoscopy is not routinely used in clinical practice, mostly because specific, expensive material is required. An ideal solution would be to use a very intensely colored tumoritropic dye in combination with WL cystoscopy. Such a compound, Evans blue (EB), was previously investigated by our group. Using spheroids composed of normal and malignant urothelial cells, it was shown that EB accumulated to a higher extent in the spheroids composed of malignant cells. It was concluded that the compound is a possible promising tool as a clinical diagnostic for bladder cancer.

The general objectives of this project were:

- To investigate the tumoritropic characteristics of EB in an *in vivo* orthotopic AY-27 rat bladder urothelial cell carcinoma model and hence the feasibility to use EB for the detection of non-muscle-invasive bladder cancer
- To examine the safety of EB intrabladder instillations
- To gain more insight into the underlying mechanisms of selective EB uptake in tumor tissue

To address the general objectives, the current study has been divided in the following chapters:

A general introduction is provided in **Chapter 1**.

In **Chapter 2**, the biodistribution of EB in the different layers of the bladder wall (urothelium, submucosa and muscle) was compared in normal and tumor-bearing rat bladders after intravesical instillation of EB. For this purpose, an orthotopic rat bladder urothelial cell carcinoma model was generated by inoculating AY-27 tumor cells into pre-treated rat bladders. Ultrastructural differences between healthy and malignant urothelium were investigated by means of transmission electron microscopy (TEM). Finally, immunohistochemistry was performed to check the differential expression of E-cadherin, desmoglein-1 and claudin-1 in the two urothelial tissue types.

In **Chapter 3**, the differential accumulation of EB in normal and malignant rat bladders was further investigated. The inner walls of the bladders were visually inspected for the presence of blue staining after intravesical instillations of EB. Also, the concentrations of EB present in the bladder homogenates was quantified after an extraction procedure. Furthermore, the amount of EB present in the plasma after intravesical instillations was investigated, as well as the possible histological adverse effects of repeated EB instillations. Finally, a transcriptomic analysis of malignant and normal rat urothelium was performed with a specific focus on cell adhesion.

In **Chapter 4**, the general conclusions and future perspectives are discussed.

CHAPTER 2

Biodistribution of Evans blue in an orthotopic AY-27 rat bladder urothelial cell carcinoma model: implication for the improved diagnosis of non-muscle-invasive bladder cancer (NMIBC) using dye-guided white-light cystoscopy

Elsen S[1], Lerut E[2], Van Cleynenbreugel B[3], Van der Aa F[3], Van Poppel H[3], de Witte P[1]

[1] Laboratory for Molecular Biodiscovery, Faculty of Pharmaceutical Sciences, KULeuven, B-3000 Leuven, Belgium

[2] Laboratory of Translational Cell and Tissue Research, Faculty of Medicine, KULeuven, B-3000 Leuven, Belgium

[3] Department of Urology, University Hospital Leuven, B-3000 Leuven, Belgium

BJU International (2015) 116, 468-77. Epub 2015 Apr 30.

ABSTRACT

Objectives: To investigate the possibility of using Evans blue (EB) as a novel diagnostic tool to detect bladder tumors with white-light (WL) cystoscopy, in this preclinical study we examined the biodistribution of the compound in the different layers (urothelium, submucosa, muscle) of a normal rat bladder and a rat bladder bearing a malignant urothelium composed of syngeneic AY-27 tumor cells.

Materials and methods: EB was instilled into both normal as well as tumor-bearing rat bladders. Following instillation, bladders were removed and snap frozen in liquid nitrogen. The distribution of EB in the different layers was quantified using fluorescence microscopy. To gain more insight into the mechanism underlying the selective accumulation of EB in tumor tissue, bladder sections were prepared for ultrastructural investigations by means of transmission electron microscopy (TEM). Besides, we also examined the expression of E-cadherin, claudin-1 and desmoglein-1 by immunohistochemistry to study the integrity of the bladder wall as these molecules are key constituents of adherens junctions, tight junctions and desmosomes, respectively.

Results: In most cases the accumulation of EB in malignant bladders was substantially higher than in healthy bladders, at least when 1 mM EB instillations were used. In case of a 1 mM EB instillation for 2 hrs, the EB-associated fluorescence in malignant urothelial tissue was 55 times higher as compared to the fluorescence found in normal urothelium. Ultrastructurally, malignant tissue displayed wider intercellular spaces and a decreased number of cell junction components as compared to normal tissue, pointing to defects in the urothelial barrier. No differences in expression of E-cadherin were found, whereas desmoglein-1 staining was stronger in the membranes of healthy bladder urothelium compared to tumor tissue. Claudin-1 expression was negative in all samples tested.

Conclusion: EB is selectively taken up by tumor tissue after intravesical instillations in rats bearing bladder tumors. The lower expression of desmoglein-1 in tumor samples, together with the decreased presence of desmosomes observed with TEM, likely imply that desmosomes play an important role in the ultrastructural differences between healthy rat urothelium and tumor tissue, and secondary to that, to the differential uptake of EB in both tissues. We believe that our findings can be useful for future clinical developments in the field of diagnostics for bladder cancer.

1. INTRODUCTION

Bladder cancer is a common cancer worldwide, affecting mostly the male elderly population. In the western world, this disease is the 4th most common form of cancer in men, following prostate, lung and colon cancer [1]. In the US, 73,510 new cases of bladder cancer were recorded accompanied with 14,880 deaths in 2012 [2]. In the European Union (EU-27), even higher numbers were registered in 2008 (110,500 new cases and 38,200 deaths) [3].

At first diagnosis, approximately 75% of detected lesions are classified as non-muscle-invasive bladder cancer (NMIBC) originating from the urothelium (urothelial cell carcinoma, UCC) [4]. These lesions are generally resolved by endoscopic removal of cancerous tissue from the bladder, called transurethral resection (TUR). Disappointingly, after a first TUR, up to 30 to 80% of patients experience a recurrence of the disease, while a substantial amount of superficial lesions will eventually progress to invasive cancer (up to 45% within 5 years) [5]. As a consequence, bladder cancer patients require extensive follow-up, which explains the high treatment cost from diagnosis to death [6].

Nowadays, the 'gold standard' for the visualization of suspicious lesions during TUR is white-light (WL) cystoscopy. In general, this technique works well in detecting exophytic lesions, but small papillary lesions and flat lesions such as carcinoma *in situ* (CIS) are often underdiagnosed. Since the latter superficial lesions are characterized by their malignant potential to progress and invade other tissues, efforts need to be made to improve their detection during TUR procedures. Recently, the use of fluorescence-guided diagnosis or photodynamic diagnosis (PDD) with different tumoritropic compounds (like hexaminolevulinate (HAL) and hypericin) was introduced in the urology clinic [7-8]. A recent review investigated the efficacy of PDD over WL cystoscopy for NMIBC [9]. It was concluded that PDD significantly improves detection of bladder cancer and is more effective for the diagnosis of CIS. A meta-analysis conducted in 2013 confirmed that blue-light cystoscopy with HAL improves detection of bladder tumors and reduces recurrence rates up to one year [10].

Despite the many advantages of using PDD over WL cystoscopy, the widespread use and implementation of this technique is hampered by the requirement of specific, expensive equipment. An interesting alternative to PDD would be the use of WL cystoscopy in combination with a dye. One of the compounds under investigation by our group is Evans blue (EB), also known as Direct Blue 53 or T-1824, a poly-aromatic water-soluble diazo dye (Figure 2.1) that has a very intense blue color. Positive results regarding the tumorotropic accumulation of this dye using an *in vitro* spheroid model [11], lead us to investigate EB as a NMIBC tool in an established syngeneic orthotopic rat bladder tumor model [12]. The specific accumulation of EB in tumor versus healthy urothelium was considered as well as the mechanisms underlying this accumulation. The results show that EB accumulated significantly more in malignant urothelium compared to healthy urothelium and this specific accumulation was due to defects in the urothelial barrier. We believe that EB in combination with WL cystoscopy might be used as a clinical application to increase the detection of NMIBC.

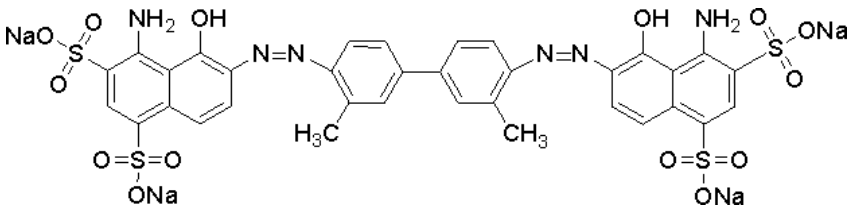

Figure 2.1: Chemical structure of Evans blue.

2. MATERIAL AND METHODS

2.1 Animals

Female Fisher rats (F-344) weighing 160-200g were used in all experiments (Charles River Laboratories, Lyon, France). Rats were kept in standard filter-top cages and were provided with purine chow and water *ad libitum*. Room temperature was kept constant at 22°C and a 12 hrs dark/light cycle was maintained. All animal procedures were performed in compliance with national and European regulations and were approved by the animal care and Ethics Committee of the University of Leuven (approval number 053/2010).

2.2 Orthotopic AY-27 rat bladder tumor model

AY-27 cells were used for tumor implantation experiments. Culturing methods and the technique used for tumor implantation were described previously by Vandepitte et al [13]. Briefly, rats were anesthetized with an intraperitoneal injection of 45 mg/kg sodium pentobarbital (Nembutal) and placed on an animal board kept at 25°C to retain body temperature. Rat bladders were then catheterized via the urethra with a plastic 18-gauge intravenous catheter. Bladders were emptied and flushed once with 0.3 ml PBS. Subsequently, the bladder mucosa was mildly disrupted by performing an acid/base treatment: first 0.3 ml of a 0.1 N HCl solution was injected for 20 s, followed by an injection of 0.3 ml of a 0.1 N NaOH solution for 20 s. Afterwards, the bladder was flushed several times thoroughly with 0.3 ml PBS. AY-27 cells (4 x 10^6 cells/0.3 ml) were inoculated into the bladder for one hour. Rats were turned 90° every 15 min to expose the whole bladder wall to the tumor cells. After the procedure, the catheter was removed and rats were able to void spontaneously. For all injections, syringes of one ml and 18-gauge needles were used. Importantly, prior to trypsinization, cells were incubated for 30 min with the green fluorescent cell tracker 3,3'-dioctadexyloxacarbocyanine perchlorate (DiO, Molecular Probes Inc, OR, USA) in the tumor accumulation experiments to visualize the cells after implantation.

To obtain an intact and superficial non-muscle-invasive bladder tumor, in our hands malignant cells needed to grow for one to three days after cell inoculation [13]. Therefore, all experiments were performed two days after the inoculation of AY-27 cells into the rat bladder.

2.3 Biodistribution experiment

2.3.1 *Bladder instillation of Evans blue*

Evans blue powder (Sigma-Aldrich) was dissolved in PBS before intrabladder application. Rats were anesthetized with an intraperitoneal injection of 45 mg/kg sodium pentobarbital and catheterized with an 18-gauge catheter. Afterwards, 0.3 ml of an EB solution was instilled. Different concentrations and different instillation times were tested during preliminary experiments (50 μM, 1, 2.5, 5 mM – 0.5, 1, 2 hrs). Finally, three instillation conditions were investigated into more detail: 1 mM EB for 1 and 2 hrs, and 2.5 mM EB for 1 hr. For each experiment, 24 rats were divided into 4 groups: a tumor bladder group, instilled with EB (n=6), a tumor bladder group instilled with PBS (n=6), a normal bladder group, instilled with EB (n=6) and a normal bladder group, instilled with PBS (n=6). After the instillation of EB or PBS, rats were euthanized, the bladders were dissected, cut open and immediately embedded into Tissue Tek medium (Miles Inc, Elkart, IN, USA). Consequently, the bladders were snap-frozen in isopentane-cooled liquid nitrogen. Cryostat microtomy was performed to obtain 5-μm bladder sections.

2.3.2 *Imaging of fluorescence*

Pictures of the bladder wall sections were taken with an Axioskop 2 plus fluorescence microscope (Carl Zeiss, Göttingen, Germany), illuminated by a 100-W mercury lamp. Fluorescence images were taken using a light-sensitive charge-coupled device (CCD) digital camera (Axiocam HR, Carl Zeiss, Göttingen, Germany). To maintain uniformity concerning fluorescence intensities, study parameters such as objective lenses, excitation and emission filters and exposure time were kept constant.

Fluorescence imaging of EB was done using a filter set with a 510-560 nm band-excitation filter and a 590 nm long-pass emission filter. The fluorescence of DiO marked the presence of tumor tissue and could be visualized with a different filter set (450-490 nm band-pass excitation filter and 515-565 nm band-pass emission filter).

After capturing the fluorescence, the sections were stained with a standard hematoxylin and eosin (H&E) staining for histological examination.

2.3.3 *Quantification of fluorescence*

For each rat, two randomly selected places in the bladder were examined. From each of those sections, histological intact regions (minimum of two, size appr. 2 mm on 500 μm) were delineated and the fluorescence of the different bladder layers (urothelium, submucosa, muscle) was quantified using ZEN 2012 (version 1.1.0.0, Carl Zeiss Microscopy GmbH) quantification software. Corrections for autofluorescence were made by subtracting fluorescence values measured in tissue of control animals.

2.3.4 *Statistical analysis*

Results are expressed as means + SEM. To compare the fluorescence of EB in tumor rat bladders versus healthy rat bladders, a non-parametric Mann-Whitney U test was performed (GraphPad prism software, significance level of 0.05).

2.4 Transmission electron microscopy

Bladders were removed from one control rat and one tumor-instilled rat. Small pieces of the bladders were cut out and fixed in cold 2% glutaraldehyde, buffered at pH 7.3 with 50 mM Na-cacodylate and 150 mM sucrose for 20 hrs. Postfixation was done in 2% osmium tetroxide in the same buffer. After the fixation steps, tissues were dehydrated in a graded acetone series, after which they were embedded in Araldite and sectioned with a Leica EMUC6 ultramicrotome. Sections of 1 μm thickness were obtained, stained with methylene blue and thionin and examined under a light microscope (Carl Zeiss, Göttingen, Germany). 70 nm-thin sections were stained twice with lead citrate and uranyl acetate and examined using a Zeiss EM 900 electron microscope.

2.5 Immunohistochemistry

Control (n=4) and bladders bearing a malignant urothelium (n=4) were examined for the presence of E-cadherin, claudin-1 and desmoglein-1. These specific molecules were chosen as they are key constituents of adherens junctions, tight junctions and desmosomes, respectively. Following primary antibodies were used: rabbit polyclonal anti-E-cadherin antibody, dilution of 1/500 (ab53226; Abcam, Cambridge, UK), rabbit polyclonal anti-claudin-1 antibody, dilution of 1/100 (ab15098; Abcam, Cambridge, UK) and rabbit polyclonal anti-desmoglein-1 antibody, dilution of 1/200 (sc-20114; Santa Cruz Biotechnology). Immunohistochemistry was performed on paraffin sections according to the protocol described in the BOND polymer refine detection kit. As a positive control, rat skin was used. Background staining was tested by adding the secondary antibody ('dual envision') without the primary antibody. Semi-quantitative analysis was performed by a trained histologist by scoring the intensity of expression as absent, weak, moderate or strong. Also the localization of expression was considered as present in the membranes, cytoplasm or nucleus.

3. RESULTS

3.1 Biodistribution experiment

All animals instilled with AY-27 tumor cells (n=36) survived the implantation procedure and were found to have a superficial form of bladder cancer after two days of tumor growth. This was confirmed by the histological analysis and the presence of the fluorescent tumor marker DiO. More specifically, pathological examination indicated that tumors generated were high-grade carcinoma *in situ*. No invasions in underlying tissue were seen, while nuclei were enlarged, variable in size and arranged disorderly (anisokaryosis). Also a loss of polarization was noticed. Examples of H&E stained 5-μm sections are depicted in Figure 2.2.

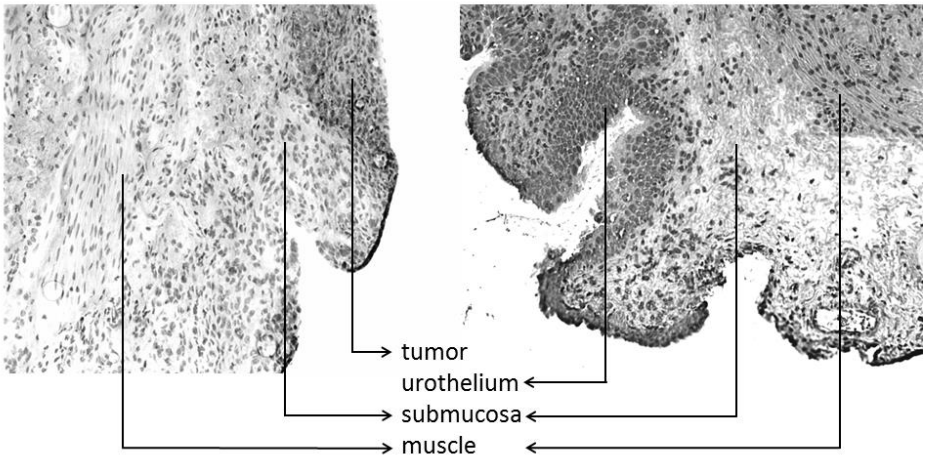

Figure 2.2: Example of H&E staining.
The different layers of a tumor rat bladder (left side) and a normal rat bladder (right side) are depicted in this picture. Original magnification = 200x.

Control and tumor-inoculated rat bladders were instilled with EB. EB emits a bright red fluorescence upon excitation, and since the blue color in the 5-μm sections of rat bladders is too weak to be quantified, the biodistribution of the compound as present in the different layers of the bladder (urothelium, submucosa, muscle) was investigated by fluorescence microscopy.

Figure 2.3 depicts some representative pictures of the 5-μm bladder sections after a 2-hrs instillation of EB (1 mM). The fluorescence of the compound is shown with the corresponding H&E stainings of the 5-μm samples. The red fluorescence is weak and confined to the outside of the bladder wall in control bladders (2.3A), while a clear accumulation in the superficial tumor cells is visible in the tumor samples (2.3E). Also in the deeper muscle layer significant fluorescence is visible (2.3G). In control samples, no fluorescence of EB is noticed in the muscularis (2.3C). Since AY-27 tumor cells can be visualized by the green fluorescent cell tracker DiO, the superficial nature of the tumor is evident (2.3I). Importantly, areas of green fluorescence (tumor) and red fluorescence (EB) show a good correlation (2.3J).

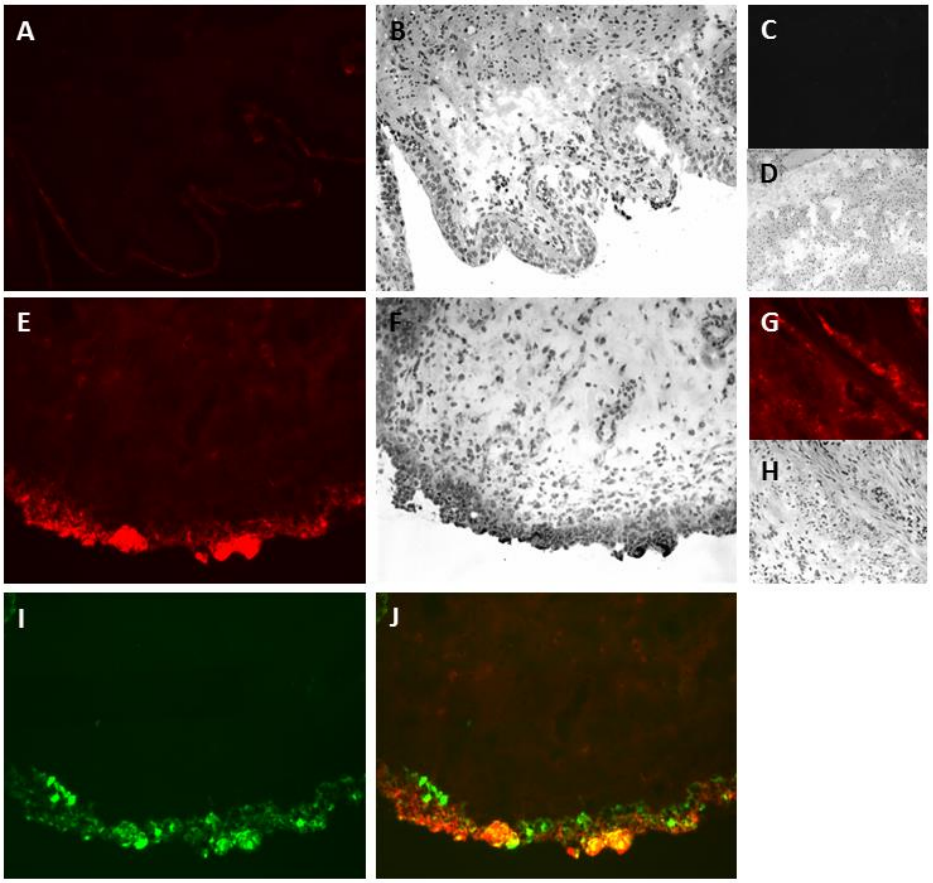

Figure 2.3: 5-µm sections of rat bladders after instillation of Evans blue.
Fluorescence photomicrographs and the corresponding H&E stainings of the frozen 5-µm sections after a 2 hrs instillations of Evans blue (1 mM) in control (A-D) and tumor-instilled rat bladders (E-J). Figures A and B visualize the urothelium and underlying submucosa, figures C and D the deeper muscle layer of healthy rat bladders. Figures E and F show the tumor layer and submucosa, figures G and H the muscle layer of tumor-instilled rat bladders. Visualization of tumor cells by DiO (I) and the overlay of DiO fluorescence and Evans blue fluorescence (J). Red = fluorescence of Evans blue; green = fluorescence of DiO, which marks the presence of tumor cells; yellow = overlap of the fluorescence of EB and DiO.
Original magnification = 200x, gain = 3, exposure time = 200 ms.

Figure 2.4 compares quantitatively the accumulation of EB in the different layers, as measured by the fluorescence present, after an instillation of 1 mM EB for 1 and 2 hrs, and an instillation of 2.5 mM EB for 1 hr. All 72 animals were included in the analysis (n = 24 for each graph, i.e. 12 animals in case of tumor conditions and 12 animals in case of healthy bladder conditions). The accumulation in tumor urothelium is in line with the conditions tested, i.e. a higher accumulation was found using 1 mM EB in the 2 hrs-condition as compared to the 1-h condition, and using the 2.5 mM condition as compared to the 1 mM condition (both 1 h incubation). The concentrations in the underlying tissues (submucosa, muscle) in general follow this pattern. With a longer instillation time (2 hrs) EB piles up in the muscle layer of the tumor bladders. In most

cases the accumulation of EB in the tissues of healthy bladders is substantially lower than in the malignant conditions, at least when 1 mM EB instillations were used. In one condition (2.4B) EB fluorescence in malignant urothelial tissue was 55 times higher as compared to the fluorescence found in normal urothelium. Comparable high concentrations (although still statistically different) were found in the tissues of both healthy and tumor bladders in the 2.5 mM condition (2.4C).

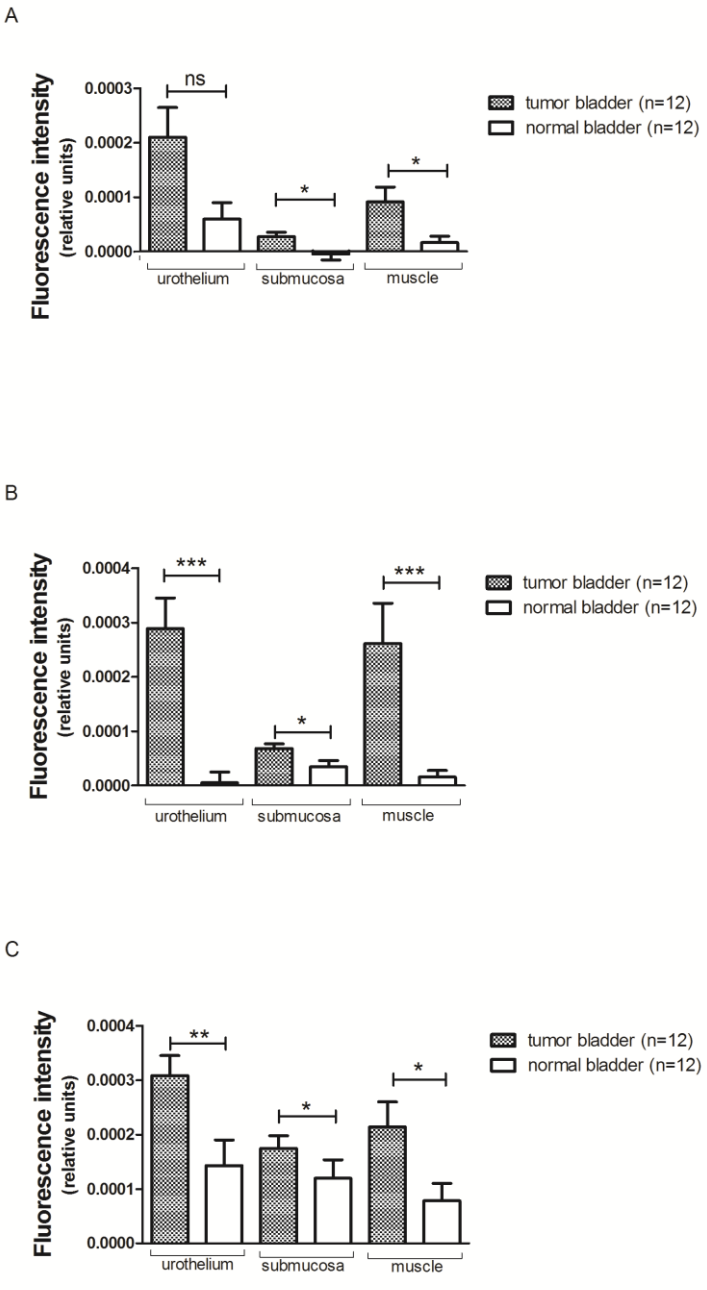

Figure 2.4: Quantification of fluorescence after Evans blue instillation.
The fluorescence intensity in the different layers of normal rat bladders vs tumor-bearing rat bladders is compared. Conditions: (A) 1 mM EB, 1 hr instillation, (B) 1 mM EB, 2 hrs instillation, (C) 2.5 mM, 1 hr instillation. Means + SEM are shown. *** = p-value < 0.0001, ** = p-value < 0.01, * = p-value < 0.05.

3.2 Transmission electron microscopy

In order to explain the differential accumulation of EB in both bladder types, ultrastructural differences were investigated using TEM (Figures 2.5 and 2.6).

From Figure 2.5 it is clear that cells of the urothelium from normal bladders are tightly interconnected. Components of the junctional complex can easily be found: tight junctions, adherens junctions and desmosomes can be distinguished from the apical to the basal surface. These cell adhesion structures are omnipresent and evident. In contrast, the photomicrographs of the tumor samples (Figure 2.6) show a very different image: tumor cells are loosely attached to each other and clear cell adhesion structures are difficult to find. This first might seem as an incompetence of the tumor cells to properly attach to each other. However, joining tumor cells are also characterized by the presence of many microvillar extensions thereby enlarging the connecting surface between tumor cells.

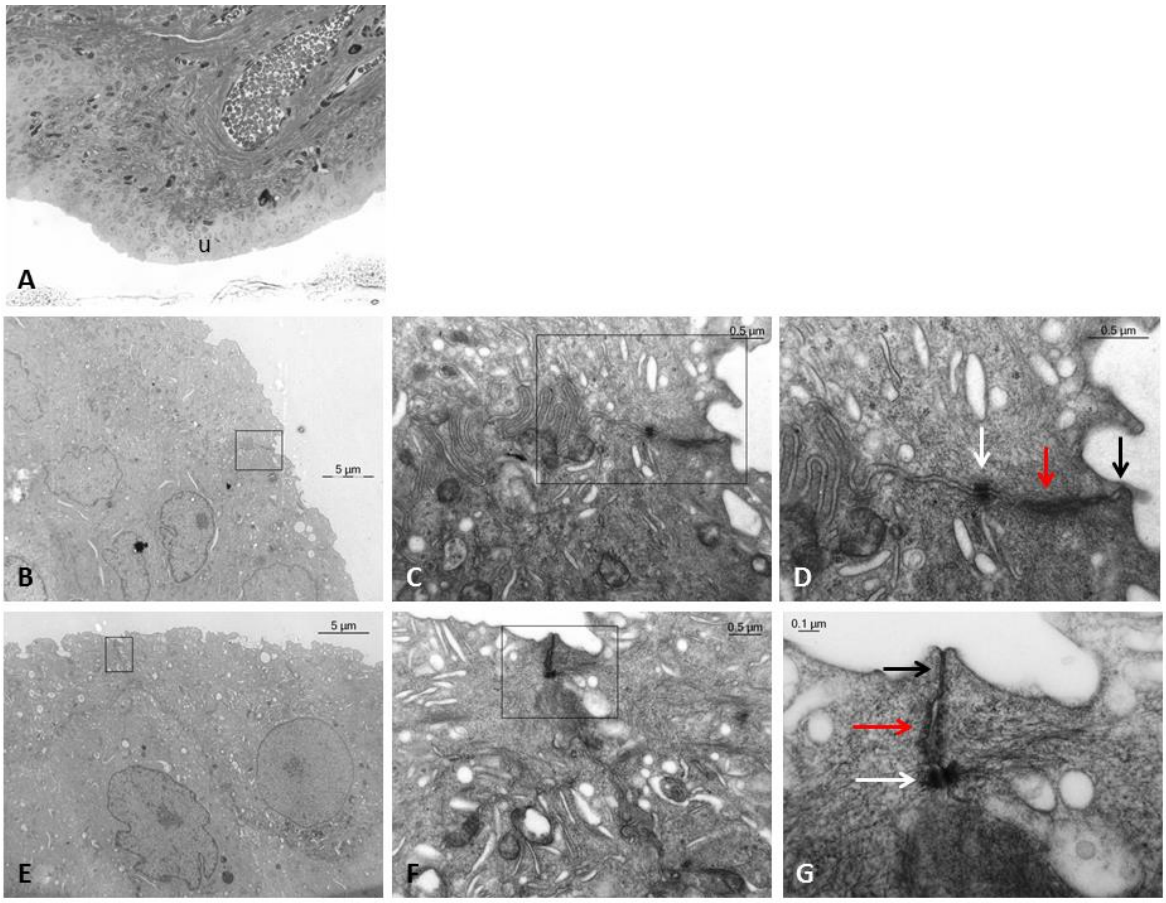

Figure 2.5: Transmission electron photomicrographs of normal rat bladder.
(A) Overview photomicrograph (light microscopy) of methylene blue and thionin-stained bladder wall (original magnification = 400x, u = urothelial cell layer); (B,E) Electron photomicrographs of uranyl acetate and lead citrate-stained urothelium (1100x), the boxed areas are shown at higher TEM magnification (7000x) in C and F, respectively. (D, G) Close-ups of the junctional complexes are given (D, 12000x; G, 20000x). Arrows point to different components of the junctional complex: white arrows = desmomes, red arrows = adherens junctions and black arrows = tight junctions.

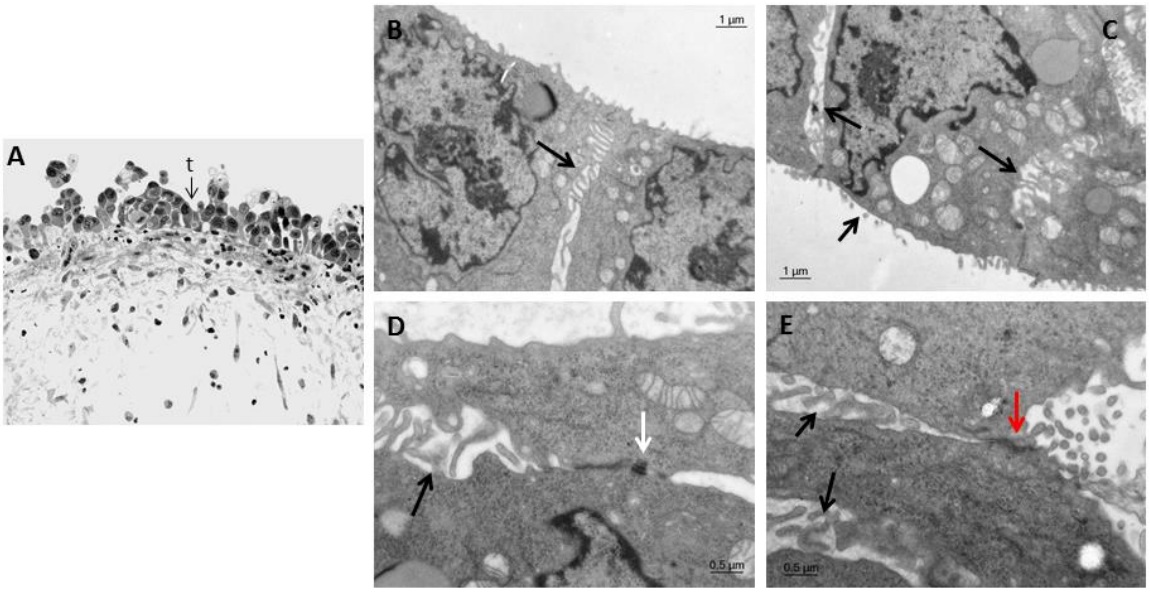

Figure 2.6: Transmission electron photomicrographs of tumor rat bladder.
(A) Overview photomicrograph (light microscopy) of methylene blue and thionin-stained bladder wall (original magnification = 400x, t = proliferating tumor cells). (B-E) Electron photomicrographs of uranyl acetate and lead citrate-stained cell adhesion sites between tumor cells; magnifications: 3000x (B, C) and 7000x (D, E); Arrows point to different components of the junctional complex: white arrow = desmosome, red arrow = adherens junction, black arrows = microvillar extensions

Immunohistochemistry

No differences in E-cadherin immunostaining were found between the tumor bladder samples and the control bladder samples. All eight samples showed a weak membrane staining in the deeper layers of the urothelium and a stronger staining of the membranes in the superficial urothelial layers (Fig. 2.7A-B). Claudin-1 staining was negative in all samples tested (data not shown), while a clear difference was observed between healthy rat bladder urothelium and tumor tissue for desmoglein-1 (Fig. 2.7C-D): healthy bladder urothelium is characterized by a strong staining of the membranes, while membranes of tumor tissue stain only weakly positive.

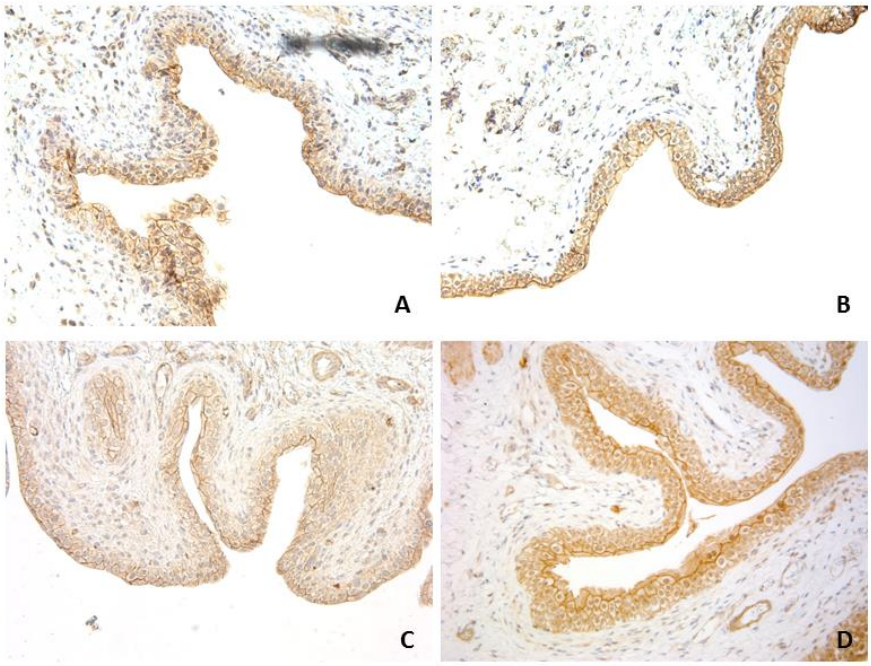

Figure 2.7: Photomicrographs of bladder urothelium immunostainings
Representative photomicrographs of the rat bladder urothelium after immunostaining with E-cadherin (A-B) and Desmoglein-1 (C-D). A and C represent pictures of malignant urothelium; B and D show pictures of healthy urothelium. Original magnification = 200x.

4. DISCUSSION

To investigate the possibility of using the water-soluble dye Evans blue (EB) as a novel diagnostic tool to detect bladder tumors with white-light (WL) cystoscopy, we examined the biodistribution of the compound in the different layers (urothelium, submucosa, muscle) of a normal rat bladder and a rat bladder bearing a malignant urothelium composed of syngeneic AY-27 tumor cells. In this preclinical study we exploited the bright fluorescence of EB to be able to assess the relative amount of EB in thin sections (5-µm) of the different layers of the bladder. However, the fluorescence-based methodology applied for this purpose does not preclude the possibility to use EB as a visual marker of malignant bladder lesions in combination with WL cystoscopy in the clinic. EB features a very intense blue color (molar absorption coefficient = 78,100 $M^{-1}cm^{-1}$ at 626 nm) and we anticipate that its accumulation in multiple layers of malignant cells will results in a true "staining" of the tissue which can be observed by white-light (WL) cystoscopy.

In all cases, EB accumulated substantially more in malignant urothelial tissue as compared to normal urothelium. However, instillations of EB in rat tumor bladders also resulted in some accumulation of EB in the inner layers of the bladder, i.e. the muscle layer. This was observed especially when applying longer instillation times. We hypothesize that the formation of tumor cells disturbs the normal barrier function of the urothelium, causing EB to penetrate by passive diffusion. With time, the EB eventually accumulates in the muscle layer of the bladder for which

the compound seems to exhibit a higher affinity than for submucosal tissue. This is not necessarily a problem and might even aid to detect bladder tumors. The human bladder wall is only a few mm thick (3.35 mm on average [14]) and it is anticipated that the accumulation of EB in the muscle layer below malignant lesions will also be picked up by cystoscopy, thereby increasing the chance of detection of bladder tumors.

Interestingly, an identical AY-27 tumor bladder rat model as employed in this study was used to examine the accumulation of PVP (polyvinlypyrrolidone)-hypericin and HAL-induced PpIX (protoporphyrin IX) in the rat bladder wall [15-16]. PVP-hypericin showed a 3.5-fold difference of accumulation in tumor urothelial tissue versus normal urothelium. In case of 8 mM HAL instillations, PpIX quantities extracted from tumor bearing bladders were ca. 3.75-fold higher than the amount found in normal bladders. Since hypericin but especially HAL are routinely used in the urologic clinic for bladder instillation followed by PDD, and since similar to higher differential concentrations were observed in this study using EB, we anticipate that EB could become an interesting candidate for dye-guided WL cystoscopy.

Moreover, of critical importance, multiple studies mention the use of EB in clinic practice without adverse reactions. Clinical use of this dye include the determination of blood volume [17], evaluation of blood vessel and cellular membrane permeability [18], detection of aspirated materials in patients with tracheostomy [19] and guidance during amniocentesis [20]. The widespread use of EB for different applications in the clinic indicates that the risks in using this compound are minimal.

To gain more insight into the mechanism underlying the selective accumulation of EB in tumor tissue, bladder sections were prepared for ultrastructural investigations. The urothelium of healthy rat bladders compared to tumor rat bladders show clear differences. Healthy urothelium is characterized by the presence of clear and distinct cell junction components. This is in line with the usual arrangement found in human bladder samples [21]. Conversely, in tumor samples, cells were found to be loosely attached to each other. Cell junction components are sometimes present, but not in an orderly manner as found in healthy urothelium. Similar ultrastructure characteristics, i.e. wide intercellular space and decreased number of cell junction components (including desmosomes), were noticed in spheroids composed of malignant cells derived from established bladder cancer cell lines [11] and also in clinical samples of superficial bladder tumors [22-23]. These morphologic characteristics might point to a loss of cohesiveness in bladder carcinoma and might explain the penetration of EB into the barrier-defective tumor cells of our rat model. Furthermore, most tumor cells in our experiments are characterized by the presence of microvillar-like extensions, the function of which is unclear. In the study of Arum et al [24], it is proposed that these microvilli might serve to prevent tumor eradication by the host immune system. Another article suggests that a greater number of microvilli appear on tumor cells that have a higher growth potential and metastatic ability [25].

Next to the characterization of ultrastructural aspects, the expression of three different cell adhesion molecules was investigated immunohistochemically. The cell adhesion molecules were chosen based on their presence in different kind of junctions: E-cadherin as a component of adherens junctions, claudin-1 as an element of tight junctions and desmoglein-1 as a component of desmosomes. No differences in expression of E-cadherin were found, whereas desmoglein-1

staining was stronger in the membranes of healthy bladder urothelium compared to tumor tissue. Claudin-1 expression was negative in all samples tested.

At first sight, our findings therefore contradict the results of the study of Arum et al [24]. In their work, the expression of E-cadherin and desmoglein$_{1+2}$ was investigated in sections of AY-27 cell inoculated rat bladders. The authors found that E-cadherin is expressed in normal epithelia but not in tumor tissue, while desmoglein$_{1+2}$ expression was negative in healthy as well as tumor bladder. The reason for this discrepancy might be the use of different periods of tumor growth: to obtain a superficial form of bladder cancer, tumor cells proliferated for only 2 days in our study, whereas in the study by Arum et al tumors grew for one to three weeks. It is possible that the decrease of E-cadherin expression only occurs later during tumor progression (the so-called cadherin switching), an observation that is also found in studies of the human bladder [26]. Studies on the expression of desmoglein-1 in bladder cancer are rare. It is however known that a reduced or negative expression of desmoglein-1 is associated with malignant properties in carcinoma of the skin and squamous cancers [27-28].

The lower expression of desmoglein-1 in tumor samples, together with the decreased presence of desmosomes observed with TEM, might imply that desmosomes play an important role in the ultrastructural differences between healthy rat urothelium and tumor tissue, and secondary to that, to the differential uptake of EB in both tissues. Presumably, other factors also play a role. Clearly, these aspects need to be investigated further in order to understand better the mechanism of accumulation of EB in bladder tumor tissue.

We believe that our findings can be useful for future clinical developments in the field of diagnostics for bladder cancer. Most importantly, EB is already used for years in a clinical setting for other kinds of applications without adverse reactions. If these positive results using EB can also be repeated in a human setting, we expect a substantial benefit for patients and society by implementing the protocol of EB instillations combined with WL cystoscopy in comparison with the expensive PDD procedure.

ACKNOWLEDGMENTS

We would like to thank prof. Johan Billen for his help with the transmission electron microscope. This project was funded by the KU Leuven (OT project nr OT/11/075).

REFERENCES

1. Jemal A, Bray F, Center MM, Ferlay J, Ward E, Forman D. Global cancer statistics. *CA Cancer J Clin* (2011) 61, 69-90
2. Siegel R, Naishadham D, Jemal A. Cancer Statistics 2012. *CA Cancer J Clin* (2012) 62, 10-29
3. Ferlay J, Parkin DM, Steliarova-Foucher E. Estimates of cancer incidence and mortality in Europe in 2008. *Eur J Cancer* (2010) 46, 765-81
4. Sharma S, Ksheersagar P, Sharma P. Diagnosis and treatment of bladder cancer. *Am Fam Physician* (2009) 80, 717-23

5. van Rhijn BW, Burger M, Lotan Y, Solsona E, Stief CG, Sylvester RJ, Witjes JA, Zlotta AR. Recurrence and progression of disease in non-muscle-invasive bladder cancer: from epidemiology to treatment strategy. *Eur Urol* (2009) 56, 430-42
6. Sievert KD, Amend B, Nagele U, Schilling D, Bedke J, Horstmann M, Hennenlotter J, Kruck S, Stenzl A. Economic aspects of bladder cancer: what are the benefits and costs? *World J Urol* (2009) 27, 295-300
7. Lange N, Jichlinski P, Zellweger M, Forrer M, Marti A, Guillou L, Kucera P, Wagnières G, van den Bergh H. Photodetection of early human bladder cancer based on the fluorescence of 5-aminolaevulinic acid hexylester-induced protoporphyrin IX: a pilot study. *Br J Cancer* (1999) 80, 185-93
8. D'Hallewin MA, Kamuhabwa AR, Roskams T, De Witte PA, Baert L. Hypericin-based fluorescence diagnosis of bladder carcinoma. *BJU Int* (2002) 89, 760-3
9. Cordeiro ER, Anastasiadis A, Bus MT, Alivizatos G, de la Rosette JJ, de Reijke TM. Is photodynamic diagnosis ready for introduction in urological clinical practice? *Expert Rev Anticancer Ther* (2013) 13, 669-80
10. Burger M, Grossman HB, Droller M, Schmidbauer J, Hermann G, Dragoescu O, Ray E, Fradet Y, Karl A, Burgués JP, Witjes JA, Stenzl A, Jichlinski P, Jocham D. Photodynamic diagnosis of non-muscle-invasive bladder cancer with hexaminolevulinate cystoscopy: a meta-analysis of detection and recurrence based on raw data. *Eur Urol* (2013) 64, 846-54
11. Roelants M, Huygens A, Crnolatac I, Van Cleynenbreugel B, Lerut E, Van Poppel H, de Witte PA. Evans blue as a selective dye marker for white-light diagnosis of non-muscle-invasive bladder cancer: an in vitro study. *BJU Int* (2012) 109, 300-5
12. Xiao Z, McCallum TJ, Brown KM, Miller GG, Halls SB, Parney I, Moore RB. Characterization of a novel transplantable orthotopic rat bladder transitional cell tumour model. *Br J Cancer* (1999) 81, 638-46.
13. Vandepitte J, Maes J, Van Cleynenbreugel B, Van Poppel H, Lerut E, Agostinis P, de Witte PA. An improved orthotopic rat bladder tumor model using DiI-loaded fluorescent AY-27 cells. *Cancer Biol Ther* (2010) 9, 986-93
14. Hakenberg OW, Linne C, Manseck A, Wirth MP. Bladder wall thickness in normal adults and men with mild lower urinary tract symptoms and benign prostatic enlargement. *Neurourol Urodyn* (2000) 19, 585-93
15. Vandepitte J, Van Cleynenbreugel B, Hettinger K, Van Poppel H, de Witte PAM. Biodistribution of PVP-hypericin and hexaminolevulinate-induced PpIX in normal and orthotopic tumor-bearing rat urinary bladder. *Cancer Chemotherapy Pharmacol* (2011) 67, 775-81
16. El Khatib S, Dedelon J, Leroux A, Bezdetnaya L, Notter D, D'Hallewin M. Kinetics, biodistribution and therapeutic efficacy of hexylester 5-aminolevulinate induced photodynamic therapy in an orthotopic rat bladder tumor model. *J Urol* (2004) 172, 2013-17
17. Brown MA, Mitar DA, Whitworth JA. Measurement of plasma volume in pregnancy. *Clin Sci (Lond)* (1992) 83, 29-34
18. Kaya M, Ahishali B. Assessment of permeability in barrier type of endothelium in brain using tracers: Evans blue, sodium fluorescein, and horseradish peroxidase. *Methods Mol Biol* (2011) 763, 369-82
19. Brady SL, Hildner CD, Hutchins BF. Simultaneous videofluoroscopic swallow study and modified evans blue dye procedure: an evaluation of blue dye visualization in cases of known aspiration. *Dysphagia* (1999) 14, 146-49

20. Wolf DA, Scheible FW, Young PE, Matson MR. Genetic amniocentesis in multiple pregnancy. *J Clin Ultrasound* (1979) 7, 208-10
21. Khandelwal P, Abraham SN, Apodaca G. Cell biology and physiology of the uroepithelium. *Am J Physiol Renal Physiol* (2009) 29, 1477-501
22. Kakudo K, Itatani H, Uematsu K. Non-papillary carcinoma in situ of the urinary bladder. An electron microscopic study. *Acta Pathol Jpn* (1984) 34, 345-53
23. Fellows GJ. Permeability of normal and diseased human bladder epithelium. *Proc R Soc Med* (1972) 65, 299-300
24. Arum CJ, Anderssen E, Viset T, Kodama Y, Lundgren S, Chen D, Zhao CM. Cancer immunoediting from immunosurveillance to tumor escape in microvillus-formed niche: a study of syngeneic orthotopic rat bladder cancer model in comparison with human bladder cancer. *Neoplasia* (2010) 12, 434-42
25. Ren J, Hamada J, Okada F, Takeichi N, Morikawa K, Hosokawa M, Kobayashi H. Correlation between the presence of microvilli and the growth or metastatic potential of tumor cells. *Jpn J Cancer Res* (1990) 81, 920-26
26. Bryan RT, Atherfold PA, Yeo Y, Jones LJ, Harrison RF, Wallace DM, Jankowski JA. Cadherin switching dictates the biology of transitional cell carcinoma of the bladder: ex vivo and in vitro studies. *J Pathol* (2008) 215, 184-94
27. Wong MP, Cheang M, Yorida E, Coldman A, Gilks CB, Huntsman D, Berean K. Loss of desmoglein 1 expression associated with worse prognosis in head and neck squamous cell carcinoma patients. *Pathology* (2008) 40, 611-16
28. Li G, Schaider H, Satyamoorthy K, Hanakawa Y, Hashimoto K, Herlyn M. Downregulation of E-cadherin and desmoglein 1 by autocrine hepatocyte growth factor during melanoma development. *Oncogene* (2001) 20, 8125-35

CHAPTER 3

Evans blue-mediated white-light detection of non-muscle-invasive bladder cancer: a preclinical feasibility and safety study using a rat bladder urothelial cell carcinoma model

Elsen S[1], Lerut E[2], Van der Aa F[3], Van Cleynenbreugel B[3], Van Poppel H[3], de Witte P[1]

[1] Laboratory for Molecular Biodiscovery, Faculty of Pharmaceutical Sciences, KULeuven, B-3000 Leuven, Belgium

[2] Laboratory of Translational Cell and Tissue Research, Faculty of Medicine, KULeuven, B-3000 Leuven, Belgium

[3] Department of Urology, University Hospital Leuven, B-3000 Leuven, Belgium

Submitted to BJU International

ABSTRACT

Purpose: Photodynamic diagnosis (PDD, also known as fluorescence cystoscopy) improves the detection of non-muscle-invasive bladder cancer (NMIBC). Nonetheless, white-light (WL) cystoscopy remains the technique routinely used in the urological clinic. A cheaper but equally performant alternative to PDD might encompass the use of a tumoritropic dye with an intense color in combination with WL cystoscopy. Using a preclinical setting, we investigated in this study some practical aspects of the use of Evans blue (EB) for the possible future detection of NMIBC using WL cystoscopy.

Materials and methods: A solution of 1 mM and 5 mM EB was instilled into healthy and AY-27 tumor-bearing rat bladders for 2 h and 1 h, respectively. Bladders were then rapidly dissected and inner walls were inspected for EB using WL stereomicroscopy. EB present in the bladders and the plasma was also quantified using HPLC analysis. To assess the effects of repeated instillations on normal rat bladders, EB was instilled for seven consecutive days, after which the bladder wall was investigated histologically. To gain insight into the mechanism underlying the selective accumulation of EB in malignant urothelium, RNA sequencing of LCM-dissected urothelial tissue and subsequent comparative analysis were performed, with a specific focus on cell adhesion.

Results: In both conditions tested, concentrations of EB were substantially higher in malignant bladders in comparison with healthy bladders, matching the blue staining of the inner bladder wall observed by WL stereomicroscopy. In case of a 1 mM EB instillation for 2 h, EB concentrations were 5.5-fold higher in the tumor condition. EB was equally present in the plasma of healthy subjects and tumor-bearing subjects, though at low concentrations. EB did not cause any abnormalities in the urothelium after a 7-day repeated instillation in normal rats. RNA sequencing of the urothelium indicated an abnormal expression of many genes related to cell adhesion in malignant urothelium compared with the normal situation, an observation that was confirmed by the KEGG enrichment analysis.

Conclusion: We believe that our findings can be important for future clinical developments in the field of diagnostics for bladder cancer. Implementing the cheaper protocol of EB instillations in combination with WL cystoscopy might offer a benefit for patients and society in comparison with the expensive photodynamic procedure.

1. INTRODUCTION

Bladder cancer is an important health issue worldwide, with an estimated 429,000 new cases accompanied with 165,000 deaths in 2012 [1]. Importantly, the management of bladder cancer contributes enormously to medical costs, with bladder cancer having the highest lifetime treatment cost per patient for all cancers [2]. This is mainly due to the high recurrence rates of the disease, expensive treatments and the necessity for frequent surveillances [3]. Little progress has been made in research to understand and treat bladder cancer causing the outcomes of this disease to have changed very little in the past three decades. This is in stark contrast with the significant progress in the 5-yr survival rates for other urothelial malignancies, like kidney and prostate cancer, during this period [4].

At initial diagnosis, 70-75% of bladder cancers are classified as non-muscle-invasive urothelial cell carcinomas, tumors from urothelial origin confined to the mucosa or submucosa [5]. The standard treatment for these lesions is an endoscopic removal of the malignant tissue, called transurethral resection of the bladder (TURB). Usually, a white-light cystoscope is used during TURB to visualize the tumors. White-light (WL) cystoscopy works sufficiently for the detection of exophytic tumors, but small papillary tumors and flat tumors such as carcinoma *in situ* (CIS) are often missed during the procedure, leading to underdiagnosis and eventually causing recurrences and progression. Up to 30 to 80 % of patients experience a recurrence of bladder cancer after a first TURB, while up to 45 % of patients are faced with progression to invasive cancers [6]. The main goal of future non-muscle-invasive bladder cancer (NMIBC) treatments is to reduce recurrences and progression, thereby decreasing the costs of extensive follow-ups and improving the outcomes for patients with bladder cancer. To achieve this goal, detection during TURB procedures needs to be improved. Fluorescence-guided diagnosis or photodynamic diagnosis (PDD) after instillation of tumoritropic (pro-) fluorescent compounds has been shown to improve detection of tumors in clinical practice. The compound most often used for this purpose is hexaminolevulinate (HAL, Hexvix®/Cysview®). A recent review investigated the efficacy of PDD over WL cystoscopy for NMIBC [7]. It was concluded that PDD significantly improves detection of bladder cancer and that this technique is more effective for the diagnosis of CIS. A meta-analysis conducted in 2013, including 10 publications, confirmed that blue-light cystoscopy with HAL improves detection of bladder tumors and reduces recurrence rates up to 1 year [8]. Despite proven efficacy of PDD and recommendations by experts when CIS or high-grade tumors are expected [9], WL cystoscopy remains the technique routinely used in the urological clinic. This is mainly due to the expensive, specific equipment that is needed to perform PDD.

A possible alternative to PDD would be to use a tumoritropic dye with an intense color in combination with WL cystoscopy. Such a compound, Evans blue (EB), was previously investigated *in vitro* and *in vivo*. In the study of Roelants et al [10], EB accumulated significantly more in spheroids composed of malignant urothelial cells compared to spheroids derived from normal human urothelial cells. Elsen et al [11] studied the accumulation of EB in an orthotopic rat NMIBC model. The biodistribution of EB was examined in the different layers of healthy rat bladders and rat bladders bearing a malignant urothelium by quantifying the fluorescence of EB. It was concluded that EB is selectively taken up in tumor tissue when using a 1 mM instillation

concentration and that this specific accumulation is possibly due to urothelial defects in tumor rat bladders.

In this study, the feasibility to use EB for the detection of NMIBC in the orthotopic rat model was further investigated using a 1 mM and a 5 mM instillation concentration. We applied WL stereomicroscopy at low magnification to visually inspect the accumulation of EB in the inner malignant and the normal bladder wall, and quantified the amount of EB present in homogenates of tumor bladders and healthy bladders. Furthermore, the amount of EB present in the plasma after intravesical instillation was investigated, as well as the possible histological adverse effects of repeated EB instillations. The rat NMIBC tumor model was characterized into more detail by a transcriptome analysis of malignant and normal rat urothelium with a specific focus on cell adhesion. The aim of this analysis was to further investigate our previous hypothesis [11] that EB is able to selectively accumulate in tumor tissue due to defects in the urothelial barrier.

2. MATERIAL AND METHODS

2.1 Animals

Female Fisher rats (F-344) weighing 160-200g were used in all experiments (Charles River Laboratories, Lyon, France). Rats were kept in standard filter-top cages and were provided with purine chow and water *ad libitum*. Room temperature was kept constant at 22°C and a 12 hrs dark/light cycle was maintained. All animal procedures were performed in compliance with national and European regulations and were approved by the animal care and Ethics Committee of the University of Leuven (approval number 142/2014).

2.2 Chemicals and reagents

Evans blue (EB), naphtol blue black (NBB), ureum, 2-mercapto-ethanol, tetrabutylammonium hydroxide and tetrabutylammonium dihydrogen phosphate were purchased from Sigma-Aldrich. Chloroform was obtained from Acros Organics, 2-propanol from Chem-Lab and acetonitrile from Fisher Chemical. EB powder was dissolved in ultrapure water (milli-Q®) immediately before instillation.

2.3 Sedation and catheterization of animals

For all experiments, rats were anesthetized with an intraperitoneal injection of 45 mg/kg sodium pentobarbital (Nembutal) and placed on an animal board kept at 25 °C to retain body temperature. Rat bladders were then catheterized via the urethra with a plastic 18-gauge intravenous catheter (22-gauge catheters were used in the repeated instillation experiment).

2.4 Orthotopic AY-27 rat bladder tumor model

2.4.1 *Tumor cell line*

AY-27 cells, originally developed by Dr. S. Selman and Dr. J. Hampton (Ohio Medical College, USA), were cultured in 175 cm^2 culture flasks at a temperature of 37 °C in a humidified atmosphere, containing 5% CO_2 and 95% air. Cells were grown as a monolayer in minimal

essential medium (MEM) with Earle's salts, supplied with 2 mM L-glutamine, 1% antibiotic/antimycotic solution, 1% non-essential amino acids, tylosine (60 μg/ml) (Eli Lilly, Brussels, Belgium) and 10% fetal calf serum (FCS). Cell culture medium and supplements were purchased from Invitrogen (Belgium).

Cells were used for animal experiments between passage 5 and 15. After reaching confluency, cells were washed twice with PBS (pH 7.4), trypsinized and collected after centrifugation. Cells were counted with a Coulter Z1 particle counter (Coulter Electronic, Luton, UK) and resuspended in MEM in a concentration of 4 x 10^6 cells/0.3 ml.

2.4.2 *Tumor model*

Subsequently, the AY-27 cells were used for inoculation in our rat bladder tumor model. Rats were anesthetized and catheterized as described in the section above. Afterwards, bladders were emptied and flushed once with 0.3 ml PBS. The bladder mucosa was then mildly disrupted by performing an acid/base treatment: first 0.3 ml of a 0.1 N HCl solution was injected for 20 s, the solution was removed and immediately followed by an injection of 0.3 ml of a 0.1 N NaOH solution for 20 s. After removal of the NaOH solution, the bladder was flushed several times thoroughly with 0.3 ml PBS. AY-27 cells (4 x 10^6 cells/0.3 ml) were inoculated into the bladder for one hour. Rats were turned 90° every 15 min to expose the whole bladder wall to the tumor cells. After the procedure, the catheter was removed and rats were able to void spontaneously. For all injections, syringes of one ml and 18-gauge needles were used.

To obtain an intact, high-grade non-muscle-invasive bladder tumor, malignant cells needed to grow for two days after cell inoculation [11]. Therefore, all experiments were performed two days after the inoculation of AY-27 cells into the rat bladder.

2.5 Accumulation of EB in rat bladders and plasma after intravesical instillation

2.5.1 *EB administration and visual inspection of inner wall rat bladder*

After sedation and catheterization of the animals, the EB solution was instilled in the bladders. Two conditions were tested: 1 mM EB instillation during 2 hrs and 5 mM EB instillation during 1 h in healthy rats (n = 5 per condition) and rats with bladder tumors (n = 5 per condition). In case of a 2-hrs instillation period, rat were turned 90° every 30 min, in case of a 1-hr instillation period, this was done every 15 minutes. After the instillation periods, rat bladders were thoroughly flushed with PBS to remove all EB residues in the bladder. Rats were then euthanized, bladders were rapidly dissected and the inner wall was visually inspected for blue dye accumulation using WL stereomicroscopy (Leica MZ10 F) at low magnification. Pictures were taken with a DFC310 FX digital camera run by Leica Application Suite software (version 3.6.0). Afterwards, the bladders were extracted (see further).

2.5.2 *Blood sampling*

Healthy (n = 3 per condition) and tumor-bearing rats (n = 3 per condition) were instilled with 1 mM EB for 2 hrs or with 5 mM EB as described in the section above. Immediately after the 1 or

2 hrs-instillation periods, bladders were flushed thoroughly and blood was taken via the tail vein of living animals using a wing needle (Venoflux, 0.5 mm G25). Blood was collected into 200 µl tubes with lithium-heparin (Microvette®, Sarstedt) to prevent coagulation of blood. The tubes were subsequently centrifuged at 2000 rpm for 15 min to separate plasma from blood cells. Three hours after the first blood sampling, blood was collected a second time from the same rats and processed as described before. After the second blood sampling, rats were euthanized.

2.5.3 *Extraction procedure*

The extraction procedure was based on the method described by Gardner [12]. Shortly, in case of extraction from bladder samples, the procedure was as follows: the bladder was transferred in a 50-ml falcon tube and 100 µl/100 mg bladder of a 15 µg/ml aqueous solution of the internal standard (IS), naphtol blue black, was added. Napthol blue black (NBB) was chosen as an internal standard because of its structural similarity with the analyte. Then, 100 µl/100 mg bladder of an 8 M ureum/2-mercaptoethanol (125:1) solution was added to the mixture. After vortexing, 200 µl/100 mg bladder of a 0,1 M tetrabutylammonium hydroxide solution was added, followed by 6 ml/100 mg bladder of chloroform/2-propanol (83:17). This mixture was homogenized with a T25 basic Ultra-Turrax® (IKA-WERKE). After homogenization, the tubes were shaken vigorously for 15 min and centrifuged at 500 g for 5 min. The upper layer was removed with a pipette and the remaining organic layer, containing EB and NBB, was transferred to a new 15-ml falcon tube. Subsequently, the samples were evaporated with a slow stream of nitrogen at 30 °C.

For plasma samples, the extraction procedure was identical as described above, with 100 µl plasma corresponding to 100 mg bladder tissue. The homogenization step was omitted from the procedure.

2.5.4 *Preparation of samples for HPLC analysis*

Dried samples were redissolved in 500 µl or 200 µl of ultrapure water (milli-Q®) in case of bladder or plasma samples, respectively. The solution was vortexed and transferred to 500 µl tubes that were centrifuged for 5 min at 12,000 rpm. From the clear supernatant, 20 µl was manually injected into the HPLC system.

2.5.5 *HPLC method for determination of EB*

The samples were analyzed on LaChrom *Elite* HPLC system (VWR Hitachi) equipped with diode array detection (L-2450). Chromatographic separation was performed on a Phenomenex reversed phase column, type Luna 3u C18 [150 x 4.6 mm 3 µm] attached to a Phenomenex guard column C18 (4 x 3 mm). The column was operated at a flow rate of 1 ml/min at 40 °C (detection wavelength: 614 nm). Acetonitrile: phosphate buffer (pH 7, 0.067 M) (45:55) with 2 mM tetrabutylammonium dihydrogen phosphate was used as mobile phase.

2.5.6 *Validation of HPLC method*

A calibration curve was generated to test the linearity of the method. Seven different solutions of EB were made in ultrapure water (milli-Q®), with concentrations of EB ranging from 0.25 to 16 μg/ml. NBB was added to yield a final concentration of 15 μg/ml. The standard solutions were injected three times and analyzed according to described procedures.

To test the recovery of EB, fetal calf serum (FCS) (n=4) was spiked with EB and NBB to obtain final concentrations of 8 μg/ml and 7.5 μg/ml, respectively. After addition of EB and NBB, samples were incubated at 37 °C for 1 h to enable binding between EB and albumin present in FCS. After the incubation period, samples were extracted according to the procedure described above for plasma samples. Subsequently, samples were injected and analyzed. The theoretical concentration of EB was compared with the concentration obtained by the HPLC method.

2.5.7 *Statistical analysis*

Results are expressed as means + SEM. To compare the concentration of EB in the different conditions, a non-parametric Mann-Whitney U test was performed (GraphPad prism software, significance level of 0.05).

2.6 Repeated intrabladder instillation of Evans blue

Healthy rats were instilled with EB instillation solutions for 7 consecutive days. Concentrations of 1 mM and 5 mM were tested, PBS instillations served as a control (n = 3 per condition). Each day, rats were anesthetized and catheterized via the urethra with a plastic 22-gauge intravenous catheter. Bladders were emptied and flushed once with 0.3 ml PBS. Subsequently, 0.3 ml of the EB solution was injected into the bladder. Rats were turned 90° every 15 min to expose the whole bladder wall to the EB solution. After a 1-hour period, EB was removed and the bladder was flushed several times with 0.3 ml PBS. The catheters were removed and rats were allowed to void spontaneously. After the last instillation on day 7, rats were euthanized, bladders were removed, cut open and immediately transferred into Tissue Tek medium (Miles Inc, Elkart, IN, USA). Consequently, the bladders were snap-frozen in isopentane-cooled liquid nitrogen. Cryostat microtomy was performed to obtain 5-μm bladder sections.

Bladder sections were stained with a standard hematoxylin and eosin (H&E) staining to examine the bladder wall histologically. Afterwards, bladder sections were blindly analyzed by a trained histo-pathologist. Photomicrographs of the bladder cryosections were taken at different magnifications with a Zeiss light microscope (Carl Zeiss, Göttingen, Germany).

2.7 RNA sequencing experiment

2.7.1 *Specimen collection and laser capture microdissection (LCM)*

Four healthy rats and six rats bearing a malignant urothelium were anesthetized. Subsequently, rats were euthanized, the bladders were dissected, cut open and immediately embedded into Tissue Tek medium (Miles Inc, Elkart, IN, USA). The bladders were then snap-frozen in isopentane-cooled liquid nitrogen. Cryostat microtomy was performed to obtain 10 μm bladder

sections that were mounted onto DNAse- and RNAse-free PET-membrane-coated metal frame slides (1.4 μm, Leica). Immediately before performing LCM, the cryosections were stained with a standard H&E staining.

Based on the H&E staining, healthy and malignant urothelial tissue was microdissected using a Leica DM60000B microscope (Leica Microsystems). The lasered fragments were captured on the cap of 200 μl PCR tubes (Greiner bio-one), filled with 25 μl RLT plus buffer (Qiagen) + 1% 2-mercaptoethanol. After the microdissection, PCR tubes were closed, centrifuged for 30 sec and stored at -80 °C until further processing. For each rat, four cryosections were microdissected. An overview picture of a stained cryosection was taken with the Leica microscope.

2.7.2 *RNA extraction, quality control and sequencing*

Microdissected tissue from the same rats was pooled together, after which RNA was extracted according to the protocol described in the RNeasy plus microkit. RNA concentration and purity were determined spectrophotometrically using the Nanodrop ND-1000 (Nanodrop Technologies) and RNA integrity was assessed using a Bioanalyser 2100 (Agilent). Per sample, an amount of 1 ng of total RNA was used as input for the SMART-Seq v4 Ultra Low Input RNA protocol (version "040215") from Clontech Laboratories Inc. Subsequently, 1 ng of purified cDNA was sheared to 300 bp using the Covaris M220. From the sheared material, sequencing libraries were prepared with the NEBNext Ultra DNA Library Prep Kit for Illumina (version 2.0 -1/15), according to the manufacturer's protocol including a size selection to 250 bp insert size with the following minor modifications: only half of the library was subjected to a 15 cycle PCR in the final library amplification step. Sequence-libraries of each sample were finally equimolarly pooled and sequenced on ½ NextSeq500 flow-cell at 1x75 bp.

2.7.3 *Data analysis*

After cleaning and adapter removal, preprocessed reads were mapped to the *Rattus norvegicus* reference genome (rnor50) with Tophat v2.0.13. The number of reads in the alignment, overlapping with gene features, were counted using featureCounts 1.4.6 [13]. Subsequently, genes with less than 1 count-per-million were removed and normalization was performed for GC content, library size and RNA composition using EDASeq package from Bioconductor [14]. Principal component analysis (PCA) was carried out to identify expression patterns in the dataset. To obtain the differentially expressed genes between the two conditions, statistical comparative analysis was performed with EdgeR 3.4.0 (Bioconductor Package) [15]. The resulting p-values were corrected for multiple testing with Benjamini-Hochberg to control the false discovery rate (FDR) [16]. Results are given as log2 fold change and a FDR p-value below 0.05 was considered as significant. Genes with a log2-ratio < -1 and > 1 were considered as down- and up-regulated, respectively.

Special interest was shown for genes related to cell adhesion. Cell adhesion genes were identified by means of a thorough literature search [17-19] and using the 'Pathway Unification Database' website [20]. Following keywords were entered: 'cell adhesion molecules', 'tight junction', 'adherens junction', 'tight junction interactions' and 'adherens junctions interactions'.

2.7.4 *Functional enrichment analysis*

In order to comprise the dataset into more biologically interpretable data, a functional enrichment analysis was performed. Since the rat's pathways are poorly annotated and most databases are made for human genes, the putative orthologous genes in human were extracted for the 14,115 genes annotated in the rat genome used for the statistical analysis. 10,740 orthologous genes were obtained using one-2-one orthologous relationship from Ensembl (BioMart Portal v0.9). The gene enrichment analysis was performed online with WebGestalt (WEB-based Gene SeT AnaLysis Toolkit) [21] using our sets of differentially expressed genes. The pathway analysis was performed using the annotated pathways of KEGG (Kyoto Encyclopedia of Genes and Genomes) database with default significance level of 0.05 (FDR corrected p-values).

3. RESULTS

3.1 Accumulation of EB in rat bladders and plasma after intravesical instillation

3.1.1 *Visual inspection of inner wall rat bladder*

Figure 3.1 shows representative pictures of the inner wall of rat bladders after instillations of 1 mM EB for 2 hrs and 5 mM EB for 1 hr, as visualized by WL stereomicroscopy at low magnification. In healthy bladders instilled with the lowest concentration of EB, the blue staining is almost non-existent (3.1A), while a clear blue but non-homogeneous staining is visible in the tumor bladders (3.1B). Healthy bladders instilled with the highest concentration show some non-specific blue staining (3.1C), the tumor bladders exhibit an intense blue color (3.1D). In both conditions, the healthy rat bladders are less stained when compared with the tumor conditions.

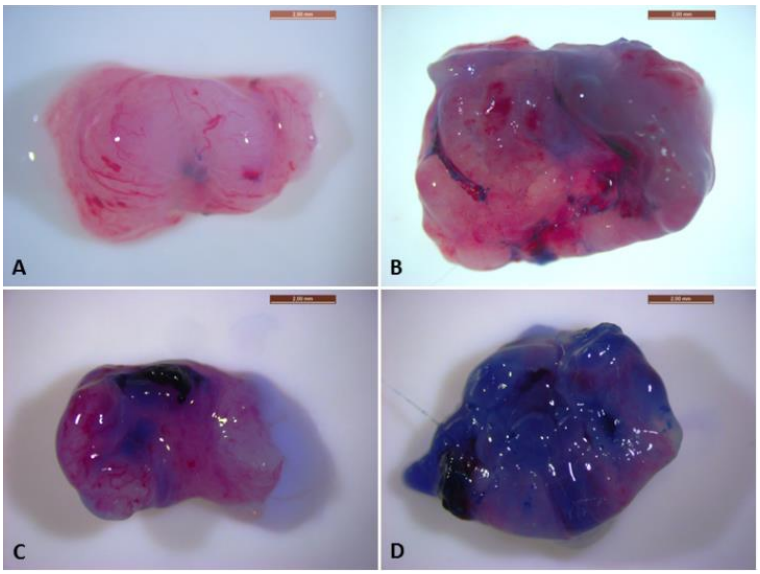

Figure 3.1: Representative pictures of cut-open rat bladders

Pictures of the inner wall of rat bladders after a 2 hrs instillation of 1 mM EB (A-B) and a 1 hr instillation of 5 mM EB (C-D) as visualized by WL stereomicroscopy. Figures A and C show

healthy rat bladders, figures B and D rat bladders with a malignant urothelium. Original magnification = 1.25x

In order to compare the amount of EB present in healthy and malignant rat bladders after intravesical instillation, EB was extracted and quantified using a HPLC method.

3.1.2 *Validation of HPLC method*

Selectivity. The method for the chromatographic analysis of rat bladder samples and rat plasma samples showed no interference from endogenous components at the retention times of EB (2.0 min) and IS (3.5 min). A typical chromatogram is given in Figure 3.2.

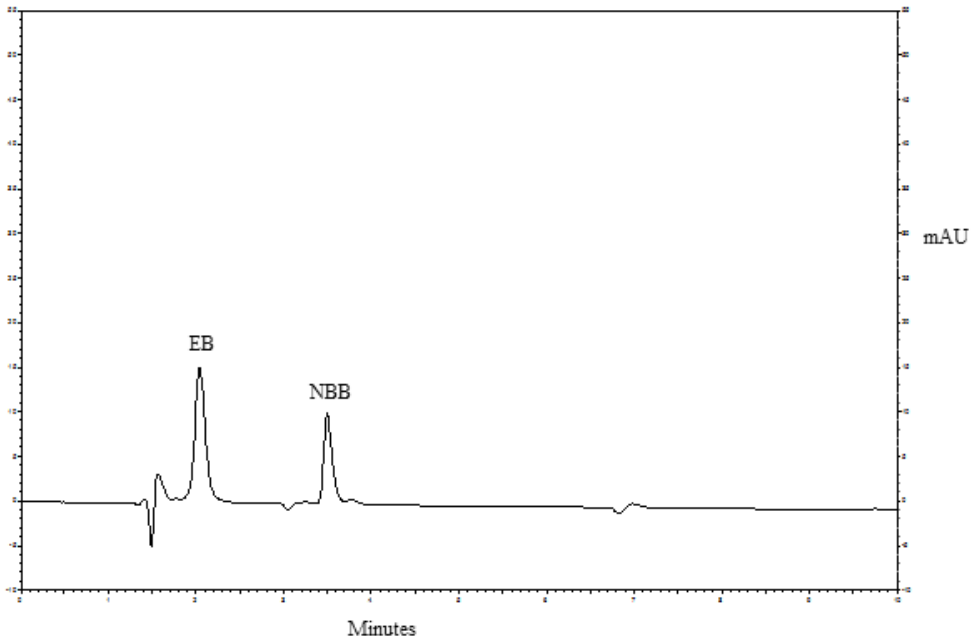

Figure 3.2: Representative chromatogram showing peaks of EB and NBB
Chromatogram of a plasma sample spiked with EB and NBB, final concentrations of 8 μg/ml and 7.5 μg/ml, respectively. EB = Evans blue, NBB = napthol blue black, the internal standard

Linearity. The calibration curve of EB from standard solutions was linear over the concentration range of 0.25 to 16 μg/ml (n=3, r_{mean} = 0.998). The mean equation of the 3 curves was the following: 'y = 262321 x – 73868' with x = EB concentration and y = area under the curve.

Recovery. The mean (± SD) recovery of EB from FCS was 77.4 ± 8.8 %.

3.1.3 *Determination of Evans blue in rat bladder homogenates after intravesical instillation*

Figure 3.3 compares quantitatively the concentration of EB in bladder homogenates after instillation of the compound in healthy rat bladders and in bladders with a malignant urothelium. The graph from Figure 3 indicates that in both conditions tested, more EB was taken up in the tumor bladders as compared to healthy bladders, though this difference was only found to be significant in the 1 mM-2hrs condition. On average, the concentration of EB in tumor bladder

homogenates was 5.5 times higher than in healthy bladder homogenates in the 1 mM-2hrs condition. In the 5 mM-1hr condition, a 3.2-fold increase could be observed. These findings match the observations of blue color in the bladder samples, as visualized in Figure 3.1.

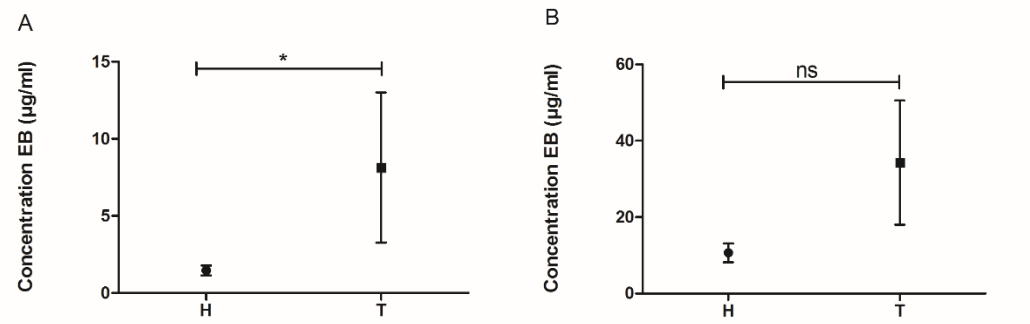

Figure 3.3: Concentration of EB in bladder homogenates after intravesical instillation
The concentration of EB found in homogenates of healthy bladders (H) and bladders bearing tumors (T) after intravesical instillation is compared. Two conditions were tested: 1 mM instillation of EB for 2 hrs (A) and 5 mM instillation of EB for 1 hr (B) n = 5 for each condition. Means + SEM are shown. * = p-value < 0.05.

3.1.4 *Determination of Evans blue in rat plasma after intravesical instillation*

To determine the amount of EB that evades from the bladder into the circulatory system, the concentration of EB in rat plasma was quantified after intravesical instillation in both healthy and malignant rat bladders. Determination of EB concentrations was also investigated 3 hrs after removal of the catheters to examine the retention of EB in rat blood. As Figure 3.4 shows, there were no significant differences in EB concentrations in plasma of normal rats compared to rats with a malignant urothelium after instillation of EB in all conditions tested (1 mM-2hrs-5hrs, 5 mM-1hr-4hrs). As expected, a 5 mM instillation led to a higher concentration of EB in the plasma compared to a 1 mM instillation (3 to 4- fold increase). The highest mean concentration in rat plasma, 7 µg/ml, was observed for the 5 mM-1hr condition in healthy rat bladders. After a 3 hrs EB instillation-free period, EB concentrations did not significantly change.

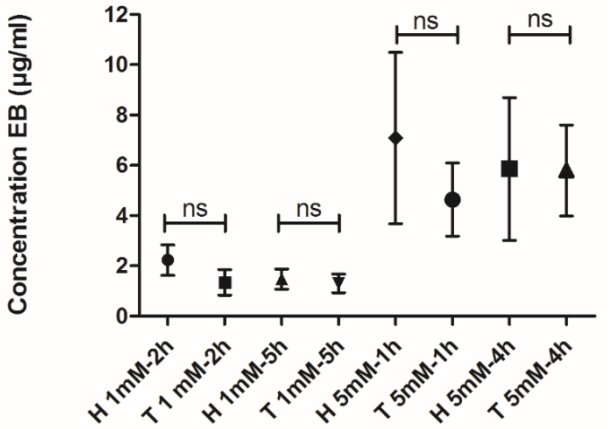

Figure 3.4: Concentration of EB in bladder plasma after intravesical instillation

The concentration of EB found in rat plasma after intravesical instillation in healthy bladders (H) and bladders bearing tumors (T) is compared. Four conditions were tested: 1 mM EB instillation for 2 hrs (1mM-2h), 5 mM EB instillation for 1 hr (5mM-1h) and the blood samples taken 3 hrs after the end of instillation (1mM-5h and 5 mM-4h). n = 3 for each condition. Means + SEM are shown.

3.2 Repeated intrabladder instillation of Evans blue

EB solutions or PBS (control) were instilled for 7 consecutive days in normal rat bladders to examine possible adverse effects of EB on the bladder wall. In the control PBS samples (Figure 3.5C), the urothelium appeared normal in all 3 rat bladders, while in 2 bladders a purulent inflammation was found in the muscularis. In the third rat, oedema was present in the lamina propria. The histological injuries seen in these control conditions are likely due to the repeated instillation procedure.

A 7-day repeated instillation of 1 mM EB did not show any more signs of adverse effects observed within the bladder wall as compared to the control conditions (Figure 3.5A). Histologic analysis showed that the urothelium was normal in all cases. Slight inflammation and oedema was noticed in the lamina propria and 1 bladder showed a purulent inflammation in the muscularis. Also in case of the 5 mM EB instillations, the urothelium of the 3 rat bladders was normal (Figure 3.5B), while inflammation and oedema was noticed in the lamina propria and in the muscularis of 2 rats.

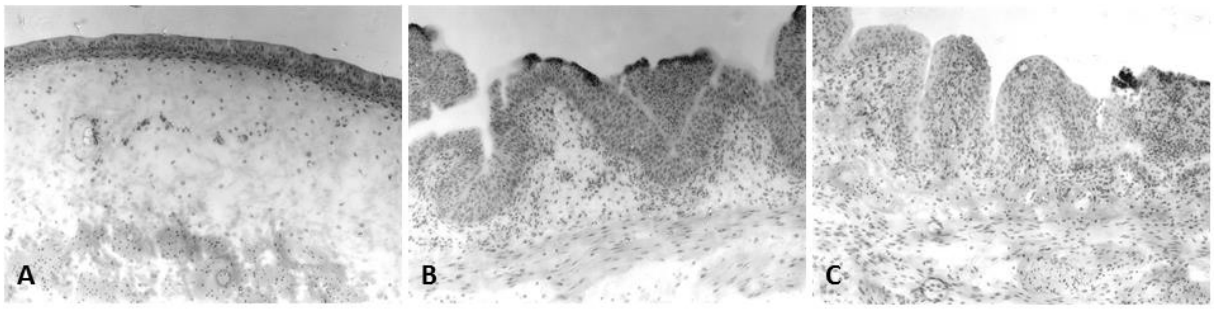

Figure 3.5: Representative H&E stainings of 5-µm sections of rat bladders
Photomicrographs of the H&E stained sections after a daily 1-hr instillation of EB or PBS for 7 consecutive days. (A) 1 mM EB, (B) 5 mM EB, (C) PBS; Original magnification = 100x

3.3 RNA sequencing experiment

In order to better understand the differential accumulation of EB in urothelial tumor tissue versus healthy tissue, a RNA sequencing experiment was designed to specifically look at the gene expression of urothelial tissue. To isolate the urothelium, laser capture microdissection was performed. A picture of a rat bladder cryosection is given in Figure 3.6, in which the dotted line separates the urothelium (above) from the underlying layers (under).

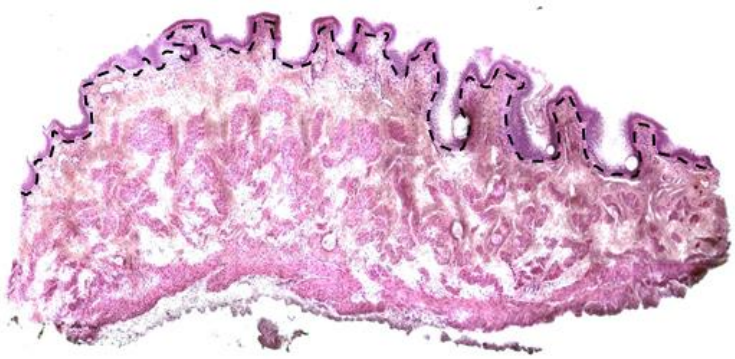

Figure 3.6: Picture of a healthy rat bladder cryosection after H&E staining. The dotted line separates the urothelium (above) from the underlying layers (under)

3.3.1 *Comparative analysis between tumor samples and healthy samples*

Principal component analysis demonstrated that one tumor sample did not cluster well with the other five tumor samples. This sample was therefore considered as an outlier and was left out of the comparative analysis. Comparative analysis of the remaining tumor samples and the four healthy samples showed that 2441 genes were down-regulated (log_2-ratio < -1) and 2244 genes were up-regulated (log_2-ratio > 1) in tumor vs. healthy samples ($p < 0.05$), as visualized by a Volcano plot (Figure 3.7).

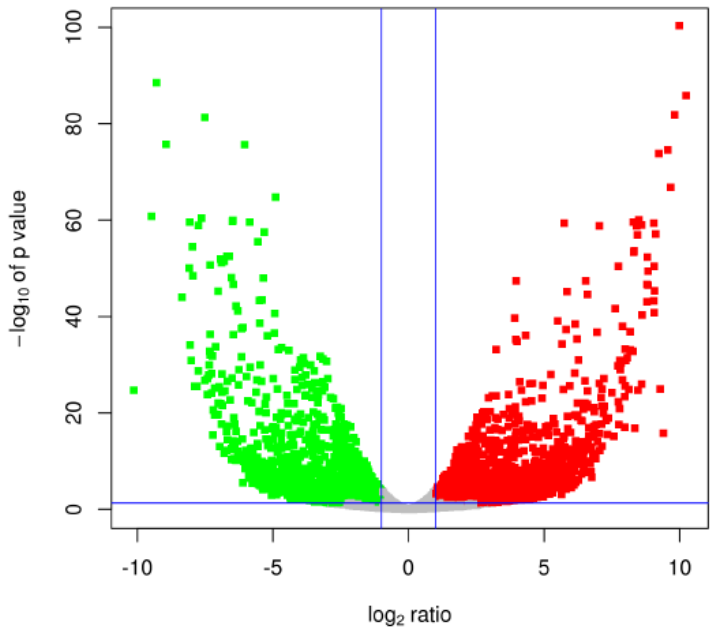

Figure 3.7: Volcano plot for tumor samples vs. healthy samples.
The vertical lines correspond to a log_2-fold change of -1 and 1, while the horizontal line indicates a p-value of 0.05. The dots are colored green or red if classified as down- or up-regulated, respectively.

Since we hypothesized before that EB specifically accumulates in tumor tissue due to defects in the urothelial barrier [11], genes correlated to cell-cell adhesion were selected and the expression levels analyzed. The focus was set on genes belonging to or correlated to the three typical cell

adhesion structures: tight junctions, adherens junctions and desmosomes. The results can be found in Table 3.1. This table clearly shows that many genes related to cell adhesion were differentially expressed in malignant urothelium compared with normal urothelium. When looking at genes related to tight junctions (TJs), 13 genes were found to be down-regulated, 8 genes were up-regulated. These genes include 5 different kinds of claudins, the major building blocks of TJs. It is also clear that many of these genes were up- or down-regulated at a very high level, e.g. *Cldn3* was 237-fold up-regulated, *Cldn 23* was 110-fold down-regulated in tumor urothelium vs. normal urothelium, respectively. Also genes encoding proteins involved in adherens junctions (AJ) were differentially expressed, though at a lower level compared to the TJ-related genes. Highest levels of up-regulation were seen for *Cdh17* (18-fold), of down-regulation for *Pvrl3* (13-fold). Three genes correlated to desmosomes were detected, e.g. *Dsc2, Dsp* and *Pkp1*.

Table 3.1: Differential expression of cell adhesion genes in tumor samples vs. healthy samples. Down-regulated genes are indicated in green, up-regulated genes in red. Corrected p-values were used, LogFC = the $\log_2$-ratio as calculated by EdgeR.

Tight junctions			**Adherens junctions**			**Desmosomes**		
Gene ID	LogFC	p-value	Gene ID	LogFC	p-value	Gene ID	LogFC	p-value
Amotl1	-4,45	1,86E-07	*Acp1*	1,11	0,00527	*Dsc2*	1,99	4,13E-06
Cldn3	7,89	9,90E-39	*Actb*	3,00	3,51E-07	*Dsp*	-1,64	0,00120
Cldn8	-6,78	3,00E-25	*Actg1*	2,55	0,00552	*Pkp1*	1,16	0,00179
Cldn11	-2,90	0,00956	*Actn1*	3,18	3,05E-07			
Cldn18	3,85	0,00786	*Actn4*	1,32	1,42E-06			
Cldn23	-5,07	2,14E-13	*Baiap2*	1,51	6,38E-06			
F11r	-1,22	7,62E-05	*Cdh3*	2,01	0,00576			
Inadl	-1,51	0,0238	*Cdh4*	-3,42	0,0187			
Jam2	-2,99	0,00219	*Cdh17*	4,18	0,00247			
Jam3	-2,35	0,0400	*Cdh18*	-2,97	0,0168			
Magi3	-1,33	0,00173	*Csnk2b*	-1,39	1,21E-07			
Mpdz	2,74	0,00940	*Ctnnd1*	-1,26	0,00193			
Pard6a	4,02	4,76E-05	*Insr*	-1,90	0,0150			
Pard6b	1,63	2,03E-05	*Ptpn1*	1,92	1,19E-06			
Pard6g	-4,48	1,13E-13	*Ptprb*	-3,54	0,00075			
Prkca	1,92	0,00302	*Ptprf*	-1,41	4,90E-06			
Prkch	-1,97	0,00018	*PVR*	2,11	4,36E-11			
Prkci	-1,26	0,00011	*Pvrl1*	-3,13	0,00099			
Prkcq	-6,70	5,77E-13	*Pvrl3*	-3,68	0,00333			
Rab3b	4,33	0,00065	*Pvrl4*	-2,43	9,39E-07			
Ybx3	1,63	1,18E-06	*Snai2*	-2,76	0,00619			
			Was	4,01	0,00055			
			Wasl	-1,17	9,02E-05			

3.3.2 *Functional enrichment analysis*

To identify enriched pathways (PWs), our gene set was compared to predefined categories of the KEGG database. This analysis showed that the up-regulated differentially expressed genes were

related to 99 KEGG pathways (see supplemental Table S3.1). A top 10 of these up-regulated enriched PWs is given in Table 3.2. Notably, this table shows that the most significantly enriched PW is the cell cycle pathway. In relation to this PW, also DNA replication and MAPK signaling PWs are included in the top 10. Alongside this top 10, other interesting categories that were significantly enriched are the bladder cancer PW (R = 5.21, p = 0.0054), tight junction PW (R = 3.34, p = 0.0025) and adherens junction PW (R = 3.62, p = 0.012).

When analyzing the down-regulated differentially expressed genes, 53 different pathways were enriched (see Supplemental Table S3.1). The top 10 is shown in Table 3.2. Interestingly, many of the PWs in this top 10 are related to catabolism, in which the cells break down molecules into smaller units to release energy: lysosome PW, peroxisome PW and endocytosis PW are among this category. The PPAR signaling, terpenoid backbone synthesis, fatty acid metabolism and SNARE interactions in vesicular transport PWs also play an indirect role in the catabolic metabolism of the cells. Other interesting categories that were significantly enriched are the tight junction PW (R = 3.36, p = 0.0055) and the p53 signaling PW (R = 3.92, p = 0.017).

Table 3.2: Top 10 enriched categories in the up- and down-regulated genes using the KEGG database. For each pathway, the number of genes found in that category as well as in our gene set is given, together with the total number of genes in that category. Also the ratio of enrichment and corrected p-values are shown.

Top 10 enriched categories in the up-regulated genes

KEGG pathway	# differentially expressed genes	# genes in category	ratio of enrichment	p-value
Cell cycle	33	124	11,72	9,28E-24
Metabolic pathways	74	1130	2,88	4,76E-14
Small cell lung cancer	18	85	9,33	2,48E-11
DNA replication	13	36	15,91	2,48E-11
Pathways in cancer	33	326	4,46	3,46E-11
Focal adhesion	25	200	5,51	1,61E-10
Oocyte meiosis	19	122	7,47	2,10E-10
MAPK signaling pathway	27	268	4,44	2,55E-09
Regulation of actin cytoskeleton	24	213	4,96	2,55E-09
RNA transport	20	151	5,83	4,34E-09

Top 10 enriched categories in the down-regulated genes

KEGG pathway	# differentially expressed genes	# genes in category	ratio of enrichment	p-value
Metabolic pathways	92	1130	3,62	3,51E-23
Lysosome	18	121	6,61	2,06E-08
Valine, leucine & isoleucine degradation	11	44	11,10	1,39E-07
Peroxisome	12	79	6,75	7,65E-06
PPAR signaling	11	70	6,98	1,38E-05
Endocytosis	17	201	3,76	8,95E-05
Fatty acid metabolism	8	43	8,26	9,92E-05
Terpenoid backbone synthesis	5	15	14,81	2,00E-04
SNARE interactions in vesicular transport	7	36	8,64	2,00E-04
Glutathione metabolism	8	50	7,11	2,00E-04

4. DISCUSSION

Using a preclinical setting, we investigated in this study some practical aspects of the use of EB for future applications as a diagnostic dye in the detection of NMIBC in combination with WL cystoscopy. Besides, by performing transcriptome analysis of malignant and normal rat urothelium, we set out to mechanistically understand the accumulation of the compound in malignant bladder urothelium.

Our results show that the total amount of EB accumulating in rat bladders bearing a malignant urothelium surpassed clearly the one found in healthy bladders, at least in case of a 1 mM EB instillation. The data therefore are in line with a previous study using an identical tumor model that quantified the fluorescence of EB at a microscopic level in the different layers of the bladder wall [11]. As a consequence, a differential uptake of EB in the malignant and normal inner bladder could also be observed by using WL stereomicroscopy. The previous study [11] showed as well that EB penetrates readily through the malignant urothelium reaching and afterwards accumulating in the deeper muscle layers, and hence the perpendicular stereomicoscopic view at the surface of the inner wall (as in case of a cystoscope) likely visualizes both. The images furthermore show a non-homogenous distribution of the blue color which probably reflects the variable proliferation of the AY-27 cells after inoculation, as observed before [11].

Although differences in accumulation of EB in tumor vs. healthy bladders were clear, this was not the case for the EB plasma levels. We expected to find less EB in the plasma of healthy rats due to the presence of a functional urothelial barrier as compared to the disrupted barrier in the rats bearing bladder tumors. However, it is possible that the catheterization procedure, also in control conditions, caused small injuries which enabled EB to penetrate into the blood stream without the need to pass through the urothelial barrier. Obviously this possibility should be investigated further using larger animals with bladders that are easier accessible.

Approximately 5 % of the amount of EB instilled was able to pass into the blood stream in the conditions tested. Although this quantity might be an overestimation due to the specific instillation conditions used, the absorption across the bladder wall of EB into the blood stream could raise some safety concerns. At this point, it should be mentioned that EB has been frequently used as a dye marker to determine blood volume in humans [22-25]. To that end, EB is injected directly into the blood stream. Based on an average blood volume of 5 l for a person weighing 70 kg [26], the final concentration of EB inside the circulatory system in humans ranges between 6.36 μg EB/ml plasma [25] and 12.73 μg EB/ml plasma [23] after intravenous injections. These values are in the range of the highest mean concentration found in this study (7 μg/ml). Moreover, Gibson & Gregerson [27] concluded that doses of EB up to 20 mg/kg are non-toxic when administered intravenously to growing rats. For a person of 70 kg, this dose would result in a plasma concentration of ca. 500 μg EB/ml plasma, which is a 70-fold higher than the highest mean concentration observed in our study. Other uses of EB in clinical practice include the detection of aspirated materials in patients with tracheostomy [28] and imaging in cardioscopy [29]. Overall, the widespread use of EB for different applications in the clinic seems to indicate that even when intravesically instilled EB leaks into the bloodstream, the safety risk for the patients is deemed very low.

Of particular interest, no adverse effects on the urothelium were found after a daily instillation of EB for 7 days, not even after intravesical application of concentrations of EB as high as 5 mM. Since the urothelium is directly exposed to the EB solutions, these data again point to the fact that the compound possesses a high non-toxic profile. This characteristic might be partially due to the fact that the compound is not likely to accumulate intracellularly as it features a high molecular mass (M_r: 960) in combination with four sulphonic substituents that are completely ionized at physiological pH. However, some inflammation was noticed in the other layers, e.g. lamina propria and muscularis, of some, but not all, rat bladder samples. Since these injuries were also present in the control bladders, we hypothesize that the inflammation observed was due to the repeated instillation procedure and not to adverse effects induced by EB itself.

We previously assumed that EB selectively accumulates paracellularly in tumor tissue due to defects in the urothelial barrier [11]. To investigate this hypothesis into more detail, transcriptome analysis of the urothelium was performed and the differential expression between healthy and malignant urothelium was analyzed. It is clear from the data that many genes related to cell adhesion were differentially expressed, especially genes related to tight junctions. Also genes that are associated with adherens junctions and desmosomes were found to be significantly up- or down-regulated.

A first important observation is the presence of 5 claudin genes, differentially expressed with high values. Claudin proteins are the most important components of TJs. A study investigating the expression of claudins in normal and neoplastic human tissues concluded that most claudin genes are decreased in tumors, except for *CLDN3*, *CLDN4* and *CLDN7*, which are elevated in some kinds of cancer, including bladder cancer [30]. This conclusion matches our results, in which *Cldn8, 11* and *23* were significantly down-regulated in malignant urothelium, while *Cldn3* was 237 times up-regulated. The *AMOTL1* gene, coding for the junctional adhesion molecule A (JAM-A), is involved in the regulation of TJ development between epithelial cells. Different studies have indicated that down-regulation of this protein is linked to invasion, metastasis, poor prognosis and progression in pancreatic cancer [31], renal cell carcinoma [32] and breast cancer [33-34]. This correlates with the 22-fold down-regulation of the *Amotl1* gene seen in our data set and highlights the high-grade character of our rat tumor model. Another gene of interest, down-regulated 104-fold in tumor tissue in our data set, is the *Prkcq* gene, coding for protein kinase C θ protein. This protein plays a key role in the activation and survival of T-cells and is also required for effective anti-tumor immune surveillance *in vivo* [35], which would explain the lower expression in a tumor environment as a strategy to inhibit eradication by the host immune system. On the other hand, inhibition of this protein has been shown to maintain the integrity of TJs in cardiac endothelial cells [36], which is contradictory to our theory of decreased cell adhesion. However, since PRKCQ is involved in many processes, it is difficult to draw a clear conclusion in relation to its involvement in cell adhesion in our tumor model. PARD6G has a known tumor-suppressor function and is therefore often down-regulated or even deleted in epithelial cancers [37], which is also observed in our dataset. RAB3B is a member of the RAS oncogene family and is observed to be up-regulated in this study.

When looking into more detail at the differentially expressed genes correlated to adherens junctions, four different cadherins and one catenin, the major building blocks of AJs [17], are noticed. The best studied cadherin is E-cadherin (CDH1), the most important mediator of cell-cell adhesion in epithelial tissues and also an important tumor suppressor [38]. It is well

documented that, during the epithelial-to-mesenchymal transition (EMT), an important first step of cancer metastasis, a cadherin switch occurs. In different malignancies, it is observed that the expression of E-cadherin decreases, while the expression of N-cadherin (CDH2) and/or P-cadherin (CDH3) increases [39]. In the case of bladder cancer, a transition to N-cadherin and P-cadherin has also been observed, though the exact timing and combination of expression of the three cadherins remains to be elucidated [39]. When these studies are regarded in the light of our study, we can see that P-cadherin is indeed significantly up-regulated four times in tumor tissue as compared to healthy tissue, but the expression of E-cadherin and N-cadherin was not significantly different. This observation might be explained in two ways: it is possible that in our tumor model, the cadherin switch starts with an increased expression of P-cadherin and that a decreased E-cadherin expression starts later in the tumorigenesis. Another possibility is that the EMT has not started yet and that the P-cadherin expression should be regarded separately. Bryan et al [40] studied the expression of P-cadherin *in vivo* and concluded that even in the presence of normal E-cadherin expression, an increased expression of P-cadherin was associated with a more malignant phenotype of bladder cancer. The protein expression of E-cadherin in an identical animal model was previously investigated by our group by means of immunohistochemistry [11]. It was concluded that no differences in expression of E-cadherin were found, confirming the gene expression of the *Cdh1* gene in this study. Two other proteins were investigated by Elsen et al [11]: claudin-1 and desmoglein-1. The *Cld1* gene and *Dsg1* were not differentially expressed in our gene analysis, but we did find a decreased expression of desmoglein-1 in malignant urothelium in the previous study [11].

Interestingly, the enrichment analysis points to the involvement of cell adhesion as well: the tight junction PW was enriched in the up- as well as the down-regulated genes, the adherens junction PW in the up-regulated genes. The cell-cycle PW was the most significantly enriched PW coming out of the analysis, confirming the observations of different other authors investigating human bladder samples [41-43]. In the study of Shen et al [41], 256 human samples were analyzed, including healthy bladder mucosa, recurrent NMIBC and primary bladder tumors. KEGG enrichment analysis revealed 7 significantly enriched up-regulated PWs, 5 of which were also found in our study, and 47 significantly enriched down-regulated PWs, 8 of which recur in this study. Arum et al [44] performed PW analysis of bladder tumors, grown for 14 days in an AY-27 rat bladder tumor model, and found 20 significantly enriched up-regulated KEGG PWs, 15 PWs recurring in our study. In none of the aforementioned studies the TJ or AJ pathways were observed in the enrichment analysis, though the pathway 'cell adhesion molecules' was enriched in Arum et al [44]. However, in our study, RNA was specifically isolated from the urothelium, the outer layer which forms the barrier of the bladder wall and therefore the layer that will be altered in terms of cell adhesion. In the other studies, whole tumors (NMIBC or MIBC)/whole rat bladders were investigated, which might explain the absence of cell adhesion PWs in the enrichment analysis.

Taken together, the data show that many genes involved in cell adhesion are differentially expressed in healthy and malignant urothelium, pointing strongly to defects in the urothelial barrier. Although the relative expression of genes does not necessarily reflect the abundance of the corresponding proteins, it is anticipated that also at the level of protein expression major defects are present. Indeed, our results are fully in line with the previously observed

ultrastructural defects, as malignant tissue displayed wider intercellular spaces and a decreased number of cell junction components compared with normal tissue [11].

In conclusion, we have shown that EB is selectively taken up by tumor tissue after intravesical instillations in rats bearing bladder tumors compared with normal rats. EB instillations do not harm the bladder wall and penetration into the circulatory system is limited, especially when low concentrations are used. The selective uptake of EB is probably due to defects in the urothelial barrier, as shown by differential expression of cell adhesion genes and by pathway analysis.

If these preclinical results on EB can be confirmed in a human setting, we believe that our findings can be important for future clinical developments in the field of diagnostics for bladder cancer. Implementing the cheaper protocol of EB instillations in combination with WL cystoscopy might offer a benefit for patients and society in comparison with the expensive photodynamic procedure.

ACKNOWLEDGMENTS

This project was funded by the KU Leuven (OT project nr OT/11/075). Library preparation, sequencing and statistical analysis were performed by VIB Nucleomics Core (www.nucleomics.be).

REFERENCES

1. Ferlay J, Soerjomataram I, Dikshit R, Eser S, Mathers C, Rebelo M, Parkin DM, Forman D, Bray F. Cancer incidence and mortality worldwide: sources, methods and major patterns in GLOBOCAN 2012. *Int J Cancer* (2015) 136, E359-86
2. Sievert KD, Amend B, Nagele U, Schilling D, Bedke J, Horstmann M, Hennenlotter J, Kruck S, Stenzl A. Economic aspects of bladder cancer: what are the benefits and costs? *World J Urol* (2009) 27, 295-300
3. Svatek RS, Hollenbeck BK, Holmäng S, Lee R, Kim SP, Stenzl A, Lotan Y. The economics of bladder cancer: costs and considerations of caring for this disease. *Eur Urol* (2014) 66, 253-62
4. Kaplan AL, Litwin MS, Chamie K. The future of bladder cancer care in the USA. *Nat Rev Urol* (2014) 11, 59-62.
5. Park JC, Citrin DE, Agarwal PK, Apolo AB. Multimodal management of muscle-invasive bladder cancer. *Curr Probl Cancer* (2014) 38, 80-108
6. van Rhijn BW, Burger M, Lotan Y, Solsona E, Stief CG, Sylvester RJ, Witjes JA, Zlotta AR. Recurrence and progression of disease in non-muscle-invasive bladder cancer: from epidemiology to treatment strategy. *Eur Urol* (2009) 56, 430-42
7. Cordeiro ER, Anastasiadis A, Bus MT, Alivizatos G, de la Rosette JJ, de Reijke TM. Is photodynamic diagnosis ready for introduction in urological clinical practice? *Expert Rev Anticancer Ther* (2013) 13, 669-80
8. Burger M, Grossman HB, Droller M, Schmidbauer J, Hermann G, Drăgoescu O, Ray E, Fradet Y, Karl A, Burgués JP, Witjes JA, Stenzl A, Jichlinski P, Jocham D. Photodynamic diagnosis of non-muscle-invasive bladder cancer with hexaminolevulinate cystoscopy: a meta-analysis of detection and recurrence based on raw data. *Eur Urol* (2013) 64, 846-854

9. European Association of Urology – Babjuk M, Böhle A, Burger M, Compérat E, Kaasinen E, Palou J, Rouprêt M, van Rhijn BWG, Shariat S, Sylvester R, Zigeuner R. Guidelines on non-muscle-invasive bladder cancer (Ta, T1 and CIS) (2015); http://www.uroweb.org/guidelines
10. Roelants M, Huygens A, Crnolatac I, Van Cleynenbreugel B, Lerut E, Van Poppel H, de Witte PA. Evans blue as a selective dye marker for white-light diagnosis of non-muscle-invasive bladder cancer: an in vitro study. *BJU Int* (2012) 109, 300-5
11. Elsen S, Lerut E, Van Cleynenbreugel B, Van der Aa F, Van Poppel H, de Witte PA. Biodistribution of Evans blue in an orthotopic AY-27 rat bladder urothelial cell carincinoma model: implication for the improved diagnosis of non-muscle-invasive bladder cancer (NMIBC) using dye-guided white-light cystoscopy. *BJU Int* (2015) 116, 468-77
12. Gardner MJ. Micromethod for the analysis of Evans blue in plasma using ion-pair high-performance liquid chromatography. *J Chromatogr* (1986) 5, 295-303
13. Liao Y, Smyth GK, Shi W. FeatureCounts: An efficient general purpose program for assigning sequence reads to genomic features. *Bioinformatics* (2014) 30, 923-30
14. Risso D, Schwartz K, Sherlock G, Dudoit S. GC-content normalization for RNA-seq data. *BMC Bioinformatics* (2011) 12: 480
15. Robinson MD, Smyth GK. Moderated statistical tests for assessing differences in tag abundance. *Bioinformatics* (2007) 23, 2881-87
16. Benjamini Y, Hochberg Y. Controlling the false discovery rate: a practical and powerful approach to multiple testing. *J R Stat Soc Ser B* (1995) 57, 289-300
17. Ishiyama N, Ikura M. The three-dimensional structure of the cadherin-catenin complex. *Subcell Biochem* (2012) 60, 39-62
18. Van Itallie CM, Anderson JM. Architecture of tight junctions and principles of molecular composition. *Semin Cell Dev Biol* (2014) 36, 157-65
19. Kowalczyk AP, Green KJ. Structure, function, and regulation of desmosomes. *Prog Mol Biol Transl Sci* (2013) 116, 95-118
20. PathCards database. http://pathcards.genecards.org/
21. Wang J, Duncan D, Shi Z, Zhang B (2013). WEB-based GEne SeT AnaLysis Toolkit (WebGestalt): update 2013. *Nucleic Acids Res* (2013) 41, W77-83
22. Gibson JG, Evans WA. Clinical studies of the blood volume. I. Clinical application of a method employing the azo dye "Evans blue" and the spectrophotometer. *J Clin Invest* (1937) 16, 301-16
23. Crooke AC, Morris CJ. The determination of plasma volume by the Evans blue method. *J Physiol* (1942) 101, 217-23
24. Brown MA, Mitar DA, Whitworth JA. Measurement of plasma volume in pregnancy. *Clin Sci (Lond)* (1992) 83, 29-34
25. Farquhar WB, Hunt BE, Taylor JA, Darling SE, Freeman R. Blood volume and its relation to peak O(2) consumption and physical activity in patients with chronic fatigue. *Am j Physiol Heart Circ Physiol* (2002) 282, H66-71
26. Boulpaep EL. Chapter 18: Arteries and veins. In: Boron WF, Boulpaep EL (ed.) *Medical physiology*, Elsevier Inc (2005), p 447-462
27. Gibson JG, Gregersen MI. Toxicity of two vital dyes used in plasma volume determinations. *Am J Physiol (Proc)* (1935) 113: 50
28. Belafsy PC, Blumenfeld L, LePage A, Nahrstedt K. The accuracy of the modified Evan's blue dye test in predicting aspiration. *Laryngoscope* (2003) 113, 1969-72

29. Kanai M, Sakurai T, Yoshinaga K, Aoyagi K, Hitsumoto T, Yoshinuma M, Uchi T, Noike H, Ohsawa H, Kawamura K, Tokuhiro K, Takahashi M, Ebihara T, Tachihara K, Uchida Y. Percutaneous dye image cardioscopy for detection of endocardial lesions. *Diagn Ther Endosc* (2000) 7, 29-33
30. Hewitt KJ, Agarwal R, Morin PJ. The claudin gene family: expression in normal and neoplastic tissues. *BMC Cancer* (2006) 6: 186
31. Fong D, Spizzo G, Mitterer M, Seeber A, Steurer M, Gastl G, Brosch I, Moser P. Low expression of junctional adhesion molecule A is associated with metastasis and poor survival in pancreatic cancer. *Ann Surg Oncol* (2012) 19, 4330-6
32. Gutwein P, Schramme A, Voss B, Abdel-Bakky MS, Doberstein K, Ludwig A, Altevogt P, Hansmann ML, Moch H, Kristiansen G, Pfeilschifter J. Downregulation of junctional adhesion molecule-A is involved in the progression of clear cell renal cell carcinoma. *Biochem Biophys Res Commun* (2009) 380, 387-91
33. McSherry EA, Brennan K, Hudson L, Hill AD, Hopkins AM. Breast cancer cell migration is regulated through junctional adhesion molecule-A-mediated activation of Frap1 GRPase. *Breast Cancer Res* (2011) 13, R31
34. Gotte M, Mohr C, Koo CY, Stock C, Vaske AK, Viola M, Ibrahim SA, Peddibhotla S, Teng YH, Low JY, Ebnet K, Kiesel L, Yip GW. miR-145-dependent targeting of junctional adhesion molecule A and modulation of fascin expression are associated with reduced breast cancer cell motility and invasiveness. *Oncogene* (2010) 29, 6569-80
35. Anel A, Aquiló JI, Catalán E, Garaude J, Rathore MG, Pardo J, Villalba M. Protein kinase C-θ (PKC-θ) in natural killer cell function and anti-tumor immunity. *Front Immunol* (2012) 3: 187
36. Li Z, Abdullah CS, Jin ZQ. Inhibition of PKC-θ preserves cardiac function and reduces fibrosis in streptozotocin-induced diabetic cardiomyopathy. *Br J Pharmacol* (2014) 171, 2913-24
37. Marques E, Englund JI, Tervonen TA, Virkunen E, Laakso M, Myllynen M, Mäkelä A, Ahvenainen M, Lepikhova T, Monni O, Hautaniemi S, Klefström J. Par6G suppresses cell proliferation and is targeted by loss-of-function mutations in multiple cancers. *Oncogene* (2015) [Epub ahead of print]
38. Jeanes A, Gottardi CJ, Yap AS. Cadherins and cancer: how does cadherin dysfunction promote tumor progression? *Oncogene* (2008) 27, 6920-29
39. Bryan RT, Tselepis C. Cadherin switching and bladder cancer. *J Urol* (2010) 184, 423-31
40. Bryan RT, Atherfold PA, Yeo Y, Jones LI, Harrison RF, Wallace DM, Jankowski JA. Cadherin switching dictates the biology of transitional cell carcinoma of the bladder: ex vivo and in vitro studies. *J Pathol* (2008) 215, 184-94
41. Shen Y, Wang X, Jin Y, Lu J, Qju G, Wen X. Differentially expressed genes and interacting pathways in bladder cancer revealed by bioinformatic analysis. *Mol Med Rep* (2014) 10, 1746-52
42. Canturk KM, Ozdemir M, Can C, Öner S, Emre R, Aslan H, Cilingir O, Ciftci E, Celayir FM, Aldemir O, Özen M, Artan S. Investigation of key miRNAs and target genes in bladder cancer using miRNA profiling and bioinformatic tools. *Mol Biol Rep* (2014) 41, 8127-35
43. The Cancer Genome Atlas Research Network. Comprehensive molecular characterizations of urothelial bladder carcinoma. *Nature* (2014) 507, 315-22
44. Arum CJ, Anderssen E, Tommeras K, Lundgren S, Chen D, Zhao CM. Gene expression profiling and pathway analysis of superficial bladder cancer in rats. *Urology* (2010) 75, 742-9

SUPPLEMENTAL DATA

Table S3.1: Enriched categories in the up- and down-regulated genes using the KEGG database

Enriched KEGG PWs for the up-regulated genes in order of significance	Enriched KEGG PWs for the down-regulated genes in order of significance
Cell cycle	Metabolic pathways
Metabolic pathways	Lysosome
Small cell lung cancer	Valine, leucine & isoleucine degradation
DNA replication	Peroxisome
Pathways in cancer	PPAR signaling
Focal adhesion	Endocytosis
Oocyte meiosis	Fatty acid metabolism
MAPK signaling pathway	Terpenoid backbone synthesis
Regulation of actin cytoskeleton	SNARE interactions in vesicular transport
RNA transport	Glutathione metabolism
Osteoclast differentiation	Propanoate metabolism
Leukocyte transendothelial migration	Biosynthesis of unsaturated fatty acids
Chemokine signaling pathway	Protein processing in endoplasmic reticulum
Spliceosome	Drug metabolism - cytochrome P450
Cytokine-cytokine receptor interaction	Metabolism of xenobiotics by cytochrome P450
Leishmaniasis	Tryptophan metabolism
Progesterone-mediated oocyte maturation	Sphingolipid metabolism
p53 signaling pathway	Steroid hormone biosynthesis
Pyrimidine metabolism	TGF-beta signaling pathway
NOD-like receptor signaling pathway	Fatty acid elongation in mitochondria
Chronic myeloid leukemia	Steroid biosynthesis
Purine metabolism	Tight junction
Protein processing in endoplasmic reticulum	Cysteine and methionine metabolism
Glioma	Insulin signaling pathway
Homologous recombination	Circadian rhytm-mammal
Pancreatic cancer	Basal cell carcinoma
Apoptosis	Hedgehog signaling pathway
Hematopoietic cell lineage	Inositol phosphate metabolism
Amoebiasis	Phosphatidylinositol signaling system
Prostate cancer	Melanogenesis
Neurotrophin signaling pathway	Aldosterone-regulated sodium reabsorption
Jak-STAT signaling pathway	Collecting duct acid secretion
Rheumatoid arthritis	Pathways in cancer
T cell receptor signaling pathway	p53 signaling pathway
Nucleotide excision repair	Amino sugar and nucleotide sugar metabolism
Shigellosis	Epithelial cell signaling in Helicobacter pylori infection
Ribosome biogenesis in eukaryotes	Adipocytokine signaling pathway
Mismatch repair	Fc gamma R-mediated phagocytosis
ECM-receptor interaction	Other glycan degradation
Base excision repair	Glyoxylate and dicarboxylate metabolism
Phagosome	Calcium signaling pathway
Toxoplasmosis	Pancreatic secretion
Arginine and proline metabolism	Regulation of actin cytoskeleton
Adipocytokine signaling pathway	Amoebiasis
Non-small cell lung cancer	Pyruvate metabolism
Fc gamma R-mediated phagocytosis	Retinol metabolism
Pathogenic Escherichia coli infection	Proximal tubule bicarbonate reclamation
Galactose metabolism	Glycolysis/Gluconeogenesis
Fc epsilon RI signaling pathway	Salivary secretion
Toll-like receptor signaling pathway	Lysine degradation
Colorectal cancer	Vascular smooth muscle contraction
Proteasome	Synthesis and degradation of ketone bodies
Chagas disease (American trypanosomiasis)	Vasopressin-regulated water reabsorption

Hypertrophic cardiomyopathy (HCM)
Glycolysis/Gluconeogenesis
Tight junction
Glutathione metabolism
Dilated cardiomyopathy
Malaria
Ubiquitin mediated proteolysis
Bacterial invasion of epithelial cells
Melanoma
Insulin signaling pathway
Vibrio cholerae infection
Arrhythmogenic right ventricular cardiomyopathy (ARVC)
B cell receptor signaling pathway
Cytosolic DNA-sensing pathway
VEGF signaling pathway
Arachidonic acid metabolism
Glycerophospholipid metabolism
Endocytosis
Bladder cancer
Glycosphingolipid biosynthesis - lacto and neolacto series
TGF-beta signaling pathway
Natural killer cell mediated cytotoxicity
Glycosphingolipid biosynthesis - ganglio series
Complement and coagulation cascades
Viral myocarditis
RNA degradation
Glycerolipid metabolism
RIG-I-like receptor signaling pathway
Adherens junction
Amyotrophic lateral sclerosis (ALS)
Staphylococcus aureus infection
Acute myeloid leukemia
Hepatitis C
Nitrogen metabolism
ErbB signaling pathway
Protein export
Type I diabetes mellitus
Epithelial cell signaling in Helicobacter pylori infection
Renal cell carcinoma
Folate biosynthesis
RNA polymerase
Histidine metabolism
Axon guidance
Drug metabolism - other enzymes
Endometrial cancer
mTOR signaling pathway

CHAPTER 4

General discussion and conclusion

4.1 Evans blue as a new diagnostic tool for bladder cancer

Treatment of bladder cancer (BC) remains a challenging problem for urologists. Urothelial cell carcinomas can be roughly divided into two groups: non-muscle-invasive-bladder cancers (NMIBC) and muscle-invasive bladder cancers (MIBC). Treatment options depend very strongly on the grade and stage of the cancer at initial diagnosis, with the majority of patients (approximately 75 %) presenting with NMIBC (Sharma et al, 2009). Although the 5-year survival rate for NMIBC is relatively high (>90%) (American Cancer Society, 2015), 30 to 80 % of patients experience a recurrence of the disease after initial treatment and up to 45 % of patients will develop invasive cancer within 5 years (van Rhijn et al, 2009). Therefore, patients require extensive follow-up, causing BC to have the highest lifetime treatment cost per patient of all cancers (Sievert et al, 2009).

To minimize recurrences and progression, detection of tumors needs to be improved. The standard method to diagnose BC is white-light (WL) cystoscopy. In general, exophytic lesions are easily detectable using this technique, but small papillary lesions and especially flat carcinoma *in situ* (CIS), exhibiting a very malignant invasive character, are underdiagnosed. New imaging techniques have been developed with the aim to solve this problem: photodynamic diagnosis (PDD), narrow band imaging (NBI), optical coherence tomography (OCT) and very recently SPIES (Storz Professional Imaging Enhancement System). Despite these interesting developments, only the use of PDD has been implemented in the guidelines of the European Association of Urology (EAU) (EAU guidelines, 2015), but even so, the investment of specific, expensive equipment and the high costs of the instillation agent Hexvix®/Cysview® hampers the widespread use of PDD in clinical practice.

Conversely, the use of a dye that specifically accumulates in or between tumor cells would be an ideal solution. The advantages of PDD could then be combined with the less expensive WL cystoscopy protocol. After *in vitro* investigating different compounds with high absorption coefficients in the visible light spectrum, Evans blue (EB) was selected as the only dye showing the desired tumoritropic characteristics as revealed with spheroids composed of malignant urothelial cells (Roelants et al, 2012). It was concluded that the compound is a possible promising tool as a clinical diagnostic for bladder cancer. The tumor-accumulating properties of EB have already been investigated before by other groups. By injecting EB intravenously in mice, the compound accumulated specifically in different kind of tumors (skin tumors, mammary, neurofibrosarcoma, ovarian carcinoma) (Moore et al, 1943; Maeda, 2012). The accumulation of EB in this type of tumors is due to the 'enhanced permeability and retention' effect, a unique phenomenon of solid tumors (Fang et al, 2011). Basically, since tumor tissue is highly vascularized and large gaps are present between the endothelial cells, macromolecules are able to selectively accumulate in solid tumors. However, the use of EB as a marker for tumor tissue has never been investigated for superficial forms of bladder cancer.

In this preclinical study, the possible use of EB as a diagnostic tool for bladder cancer was investigated using an *in vivo* orthotopic AY-27 rat bladder cancer model. This preclinical model, originally developed by Xiao et al (1999), consists of high-grade UCC tumors that invade the muscularis at some time point after inoculation. To obtain an intact and superficial non-muscle-invasive bladder tumor, in our hands malignant AY-27 cells were allowed to grow for two days

after inoculation (Vandepitte et al, 2010). At this time point, pathological examination indicated that the tumors generated were high-grade carcinoma in situ. No invasion in underlying tissues was seen, the nuclei were enlarged, variable in size and arranged disorderly (anisokaryosis). Also a loss of polarization was noticed. Additionally, the green fluorescent cell tracker DiO demonstrated the superficial nature of the tumors generated.

To evaluate the tumoritropic behavior of EB using the AY-27 rat model, two experiments were performed. First, the fluorescent properties of EB were used to quantify the accumulation of this compound in the different layers of the bladder wall (urothelium, submucosa, muscularis). Three conditions were tested: 1 mM EB instillation for 1 h and 2 hrs and 2.5 mM EB instillation for 1 h. For the 1 mM concentrations, the accumulation of EB in tumor bladders was substantially higher compared with healthy bladders. When instilling 1 mM EB for 2 hrs, the fluorescence in malignant urothelium was found to be 55 times higher than in the healthy urothelium. This is a remarkable result, since in an identical rat tumor model, the fluorescence of the NMIBC-diagnostic PVP-hypericin was only 3 to 4 times higher in malignant urothelium compared with the normal situation, while PpIX-related fluorescence after HAL instillations was even almost equal in normal and malignant tissue (Vandepitte et al, 2011). With a longer instillation time (2 hrs), EB also accumulated in the muscle layer of the tumor bladders, which was not seen in the case of PVP-hypericin. The red fluorescence of EB correlated well with the green fluorescence of the tumor tracker DiO, except for the red fluorescence found in the deeper muscle layer.

The future goal of this research is to apply EB in combination with WL cystoscopy without the need for fluorescence imaging. Therefore, in a second experiment we visually inspected by stereomicroscopy the level of staining of the inner bladder wall after intrabladder instillation of EB. Ideally, healthy rat bladder walls should not exhibit any blue appearance, whereas tumor walls should show a uniform blue coloring. However, especially in case of the highest EB concentration (5 mM), healthy rat bladders presented with spots with intense blue staining, an outcome that was also observed in case of the tumor-bearing bladders. Although the origin of these blue areas is not known and definitely deserves to be investigated further, it is possible that, due to inflammation or small injuries as a consequence of catheterization, some of the EB was able to locally penetrate into the bladder wall. In case of the tumor-inoculated bladders, in general a more intense blue color could be noticed as compared to the normal bladders. This difference was also investigated and confirmed by quantitative analysis after chemical extraction. The non-uniform distribution of the dye observed in the malignant inner walls is possibly due to an equally non-uniform proliferation of the local AY-27 tumor cells in the bladder wall, as has been noticed before by the use of DiO-labelled tumor cells and fluorescence microscopic analysis of the inner bladder wall (see pictures in Chapter 2). Conversely, according to Vandepitte et al (2010), the inoculated AY-27 cells exist for up to only 1 to 3 days as an intact NMIBC after tumor cell inoculation, and it is also conceivable that normal urothelium locally regenerated and replaced the tumoral lesions, resulting in less EB accumulation. Future work will have to further investigate into detail the relationship between the local EB coloration and presence/thickness of malignant tissue of the inner bladder wall. This can be done for instance by taking small biopsies for further microscopic analysis from selected and color-predetermined zones of the inner bladder walls.

4.2 Safety of Evans blue instillations

To investigate local adverse effects, EB was instilled in healthy rat bladders for up to 7 consecutive days. Histologic analysis showed that the urothelium, the outer layer of the bladder wall, was completely intact in case of exposure to 1 mM and 5 mM concentrations of EB. In some of the rats, slight inflammation and oedema was noticed in the underlying layers, e.g. in the lamina propria and muscularis. Since this kind of inflammation was also present in the control rat bladders, we hypothesize that the inflammation was caused by the daily catheterizations and not by harmful effects of EB. In humans, long-term catheterization is often associated with a typical form of mucosal irritation, commonly referred to as polypoid cystitis (Norlén et al, 1988). Polypoid cystitis is characterized by a polypoid ('resembling a polyp') urothelium of normal thickness, an oedematous lamina propria and inflammation. The mucosal irritation is probably caused by mechanical irritation and/or pressure exerted by the catheter (Norlén et al, 1988; Sun et al, 2011). Our histological observations of the bladder wall correlated well with the characteristics of polypoid cystitis (e.g. normal thickness of urothelium, oedema in the lamina propria, inflammation), thereby strengthening our hypothesis.

As discussed in the introduction, EB has been frequently used as a marker for blood volume determinations. Using this method, EB was injected directly into the blood stream, reaching concentrations ranging between 6.36 μg EB/ml plasma (Farquhar et al, 2002) and 12.73 μg EB/ml plasma (Crooke & Morris, 1942) (See discussion Chapter 3). The concentrations found in rat plasma after intravesical instillations ranged between 1.3 and 2.3 μg EB/ml plasma and 4.6 and 7 μg EB/ml plasma after instillations of 1 mM and 5 mM, respectively. In case of 1 mM instillations, the best condition in the tumor accumulation experiments, the concentrations found in rat plasma are thus lower compared to typical concentrations used for blood volume determinations in humans. Gibson and Gregersen (1935) concluded that in rats, IV injections up to 20 mg EB/kg body weight were non-toxic and did not slow the growth of the animals. This observation was later confirmed in monkeys. A single intravenous dose of below 25 mg EB/kg body weight was non-toxic and the animals exhibited a normal behavior during the observation period of five weeks (Malaowall & Fong, 1962). A dose of 25 mg EB/kg would lead to appr. 800 μg EB/ml plasma in a rat weighing 160 g, thus exceeding by a 100-fold the highest concentrations found in this study (7 μg/ml). We can conclude that the concentrations found in rat plasma after intravesical instillations are much lower than the concentrations considered as 'safe' after intravenous injection of EB.

After an instillation-free period of 3 hrs, concentrations of EB had not significantly decreased in the plasma. This can be explained by the firm binding of EB to albumin in the blood stream after injection, causing a very slow elimination of the dye from the blood. According to the disappearance curves of EB in human and dog plasma (Gibson & Evans, 1937; Miller 1947), 80-90 % of the original amount of dye is still detectable in the blood stream 3 hrs after an intravenous injection.

Contradictory to our expectations, there were no differences in the concentrations of EB found in the plasma of rats with normal bladders and rats with tumor bladders after intravesical application, despite the clear difference of accumulation in the bladder tissues. It thus seems that Evans blue was able to reach the circulatory system in equal amounts, irrespective of the presence

of tumor cells. Interestingly, also HAL instillations in healthy bladders have been shown to reach the blood stream. In the study of Klem et al (2006), healthy volunteers were intravesically instilled with radioactively labeled HAL. Seven percent of the amount instilled could be retrieved in the blood stream. This percentage agrees very well with the 5 % obtained in this study.

4.3 Mechanisms behind the selective accumulation of EB in tumor tissue

Normal urothelium forms a tight barrier against different kinds of external factors: urine constituents, irritants, toxins etc. Therefore, the cells of this outer layer are very tightly interconnected by means of adhesion between the urothelial cells. In normal urothelium, different kinds of specialized junctions are present (see Figure 4.1), each composed of specific proteins. The tight junctions (TJs) are formed near the apical surface of epithelial cells. The major building blocks of TJs are claudins, occludins and ZO (zonula occludens) proteins. Adherens junctions (AJs) usually occur more basal than the TJs and are composed of cadherins and catenins. A third important type of junction is the desmosome. Desmosomes are localized most basally and are built from desmogleins, desmocollins and desmoplakins. The main function of TJs is to tightly link the cells together and act as a selective permeability barrier, thus regulating the paracellular permeability. AJs and desmosomes are mechanical linkers of epithelial cells (Alberts et al, 2002), but AJs also play an important role in the formation of TJs (Hartsock & Nelson, 2008).

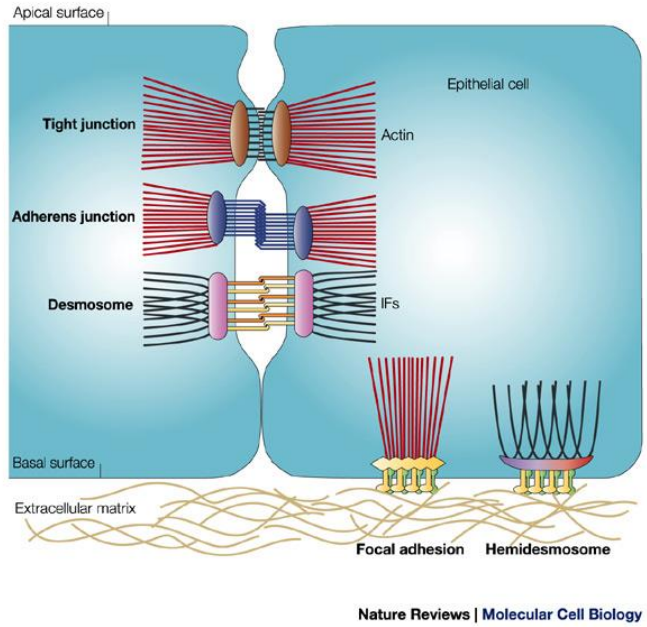

Figure 4.1: Cell adhesion structures between epithelial cells (adopted from Jefferson et al, 2004)

It was hypothesized before (Roelants et al, 2012) that abnormalities in cell adhesion might play an important role in the selective uptake of EB in spheroids composed of malignant urothelial cells. This hypothesis was explored into more detail in this study. EB, a highly hydrophilic compound, normally is not able to pass the urothelium via transcellular transport and prefers the paracellular route between the cells. In normal urothelium, cells are very tightly linked together through the presence of intact junctions and EB cannot penetrate. In tumor tissue, cells are more loosely

attached due to abnormalities in the cell adhesion structures. In this situation, EB is able to penetrate via the paracellular route. This 'defect barrier' hypothesis is visualized in Figure 4.2.

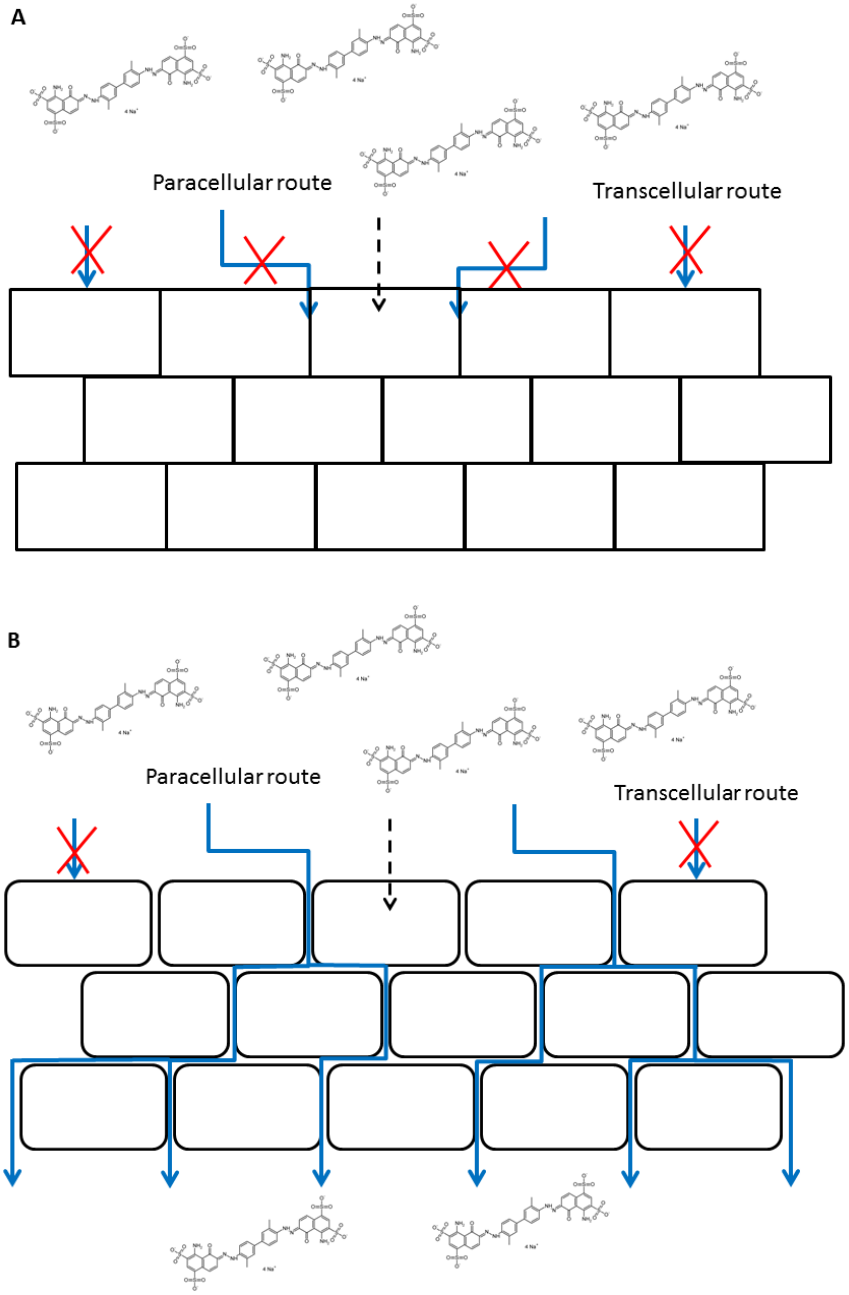

Figure 4.2: 'Defect barrier' hypothesis
(A) Normal urothelial cells are tightly linked together. EB molecules cannot pass this barrier.
(B) Tumor cells are characterized by defect cell adhesion structures, thereby enabling EB molecules to pass via the paracellular route.

We have investigated this hypothesis thoroughly in three ways. First, transmission electron microscopy (TEM) was performed to obtain a detailed ultrastructural view of cell adhesion between the cells. It was clear that in normal urothelium, cells were very tightly connected and showed a normal presence of cell junctions. Malignant urothelium was characterized by loosely attached cells with wide intercellular spaces. Also, less cell adhesion structures were present

between the tumor cells. Secondly, immunohistochemistry was performed to investigate the expression of three key constituents of TJs, AJs and desmosomes. Only desmoglein-1, component of desmosomes, was differentially expressed with a higher staining of the membranes in normal urothelium compared with malignant urothelium. Thirdly, gene expression analysis of malignant and urothelial tissue demonstrated that many genes related to components of the junctional complex were differentially expressed. Of particular interest, genes coding for proteins involved in TJ formation and regulation were differentially up- or down-regulated at a very high level. Since TJs are the structures responsible for regulating the permeability of the urothelium, this observation is in line with our observations that show an increased EB uptake. An important remark is that gene expression does not necessarily reflect protein expression. Nevertheless, this analysis on the gene level forms a good indication of the proteins that might play a role in cell-cell adhesion and might provide a guide to select the proteins that can be investigated immunohistochemically. Most importantly, also the pathway analysis supports the involvement of cell adhesion since the categories 'tight junction PW' and 'adherens junction PW' were significantly enriched.

Taken together, these experiments indicated that cell adhesion is definitely impaired between the tumor cells in our rat model, thereby confirming our hypothesis of the defect urothelial barrier and the corresponding uptake of EB. Also in the human situation, cell adhesion seems to be abnormal in bladder tumors. Most research on this subject focusses on the epithelial-to-mesenchymal (EMT) transition, an important hallmark of tumor progression and metastasis (Kalluri & Weinberg, 2009), and the related changes in cell adhesion molecules. The most important players in the EMT are three cadherins: E-cadherin, P-cadherin and N-cadherin. Simply stated, a switch from E-cadherin expression to P- and/or N-cadherin occurs during the EMT (Bryan & Tselepis, 2010). E-cadherin was not differentially expressed in our study, neither at the gene nor at the protein level. Gene expression of P-cadherin on the other hand was up-regulated in tumor tissue and might indicate the first step in cadherin switching before EMT has actually taken place. However, in our study, the role of AJs seems to be less crucial than the role of TJs. Few studies have been performed on the subject of TJs in bladder cancer. Two studies indicate that loss of TJ structure leads to invasion and eventually to metastasis of bladder cancer (Martin et al, 2011; Martin & Jiang 2009). Claudin genes are typically down-regulated in malignant tissue, except for *CLDN3*, *CLDN4* and *CLDN7,* which are found to be increased in human bladder tumor specimens (Hewitt et al, 2006). These findings are consistent with our results.

The changes observed in the expression of genes encoding TJ proteins are not only specific for bladder cancer cells, but occur in a wide variety of epithelial-derived cancers, including pancreatic, colon, lung, ovarian, thyroid, prostate, esophageal and breast cancers (Ding et al, 2013). Overexpression or down-regulation of claudins is frequently observed, although the exact functions of these claudins and the timing of up- or down-regulations remain to be elucidated. Also the expression of genes and the proteins involved in AJ formation are found to be up- or down-regulated in different kind of epithelial cancers, though the timing is variable in different kind of cancers. For example, loss of E-cadherin expression in lobular breast cancers and diffuse-type gastric cancer occurs very early in the tumorigenesis, while this decrease is only observed in late high-grade invasive tumors for prostate cancer, non-small cell lung carcinoma, colon cancer and ductal breast carcinoma (Vasioukhin, 2012). Up-regulation of P-cadherin is less studied.

Nevertheless overexpression of this protein has been observed for breast, colon, pancreatic, stomach and ovarian carcinoma (Bryan & Tselepis, 2010). Both TJ and AJ proteins seem to play an important role in the tumorigenesis of epithelial cancers. However, the interaction between those two kinds of junctions in cancer has not been extensively studied. It is known that the formation of AJs facilitates the assembly of TJs (Niessen, 2007), but more research is necessary to unravel the exact interplay between AJ and TJ proteins in cancer development.

As mentioned before (section 4.1), EB has also been shown to be tumoritropic in solid tumors after intravenous (IV) injections. The mechanisms behind this kind of accumulation are partially similar to the situation of superficial bladder cancer cells, partially not. After IV injection of EB, this compound binds firmly to the plasma protein albumin. When reaching tumor tissue, the EB-albumin complex (molecular weight of 68 kDa) is able to leak out of the blood stream into the tumor cells due to the large gaps present in the tumor vasculature. Once out of the circulatory system, EB-albumin accumulates in the interstitial space of the tumor tissue where it is retained for a long time (up to several weeks) (Maeda, 2012). This phenomenon, called the 'enhanced permeability and retention' effect in solid tumors, is not specific for EB but is also true for molecules or particles with a molecular weight larger than 40 kDa. Therefore, it has been extensively studied as a means to deliver drugs in tumor tissue (Fang et al, 2011). We can consider the situation in the bladder, where the EB solution is delivered directly in contact with the tumor cells, as similar to the situation in solid tumors once EB-albumin has leaked out of the vasculature. Also in solid tumors the cells are less adhered to each other compared to normal cells (Cooper, 2000), which enables the EB-albumin complex to penetrate in the interstitial space between the tumor cells. An important difference is the fact that in the case of accumulation in solid tumors after IV injections, EB is firmly bound to albumin, while in case of intravesical instillations, EB is administered as a solitary compound. However, in both cases it is clear that EB, whether bound to albumin or not, is only able to accumulate between the cells and not intracellularly. Due to its highly hydrophilic character, solitary EB cannot be taken up by living cells (personal observations) and is even known as a dye exclusion marker to assess cell viability in plant protoplasts (Huang et al, 1986). After incubation with an EB solution, dead/dying cells will stain blue, while healthy protoplasts remain unstained.

4.4 Translation of our findings into clinical practice

Summing up, the results of our study indicate that EB might have great potential as a diagnostic tool for bladder cancer. Before being tested in clinical trials, it would be interesting to test EB instillations in combination with WL cystoscopy in an animal model. Only few studies have ever been published on the subject of using cystoscopy in rat models (Hendricksen et al, 2007; Bolenz et al, 2007). Since a specialized mini-endoscope, connected to an imaging device is needed for this kind of experiments, cystoscopy in rats is not a technique that can be standardly used. Also, in order to interpret cystoscopy results correctly, it is necessary to have some experience in endoscopic imaging, which makes this technique unsuitable for researchers without a proper clinical background. However, performing cystoscopy in living rats would have some advantages in the light of our study. By instilling EB and monitoring the blue staining of tumor cells in living animals, there is no need to sacrifice them in order to quantify the blue staining. The accumulation of EB in different stages of tumor growth could be evaluated in the same animal

and most importantly, evaluation of EB as a means of diagnosing bladder cancer could be assessed exactly as is done in humans.

An optimal concentration and duration of EB instillations in humans will need to be found that results in a bright blue staining of tumor tissue without a non-specific blue staining of normal tissue. The best condition in our rat model was a 1 mM EB instillation for 2 hrs. Higher concentrations led to a higher non-specific blue staining. The 1 mM-2 hrs condition could be used as a starting point to optimize instillation conditions in humans. In fact, optimal instillation concentrations tested in a rat model correlated well with the optimal concentration in humans in the case of HAL. El Khatib et al (2004) investigated different concentrations of this compound in a rat tumor model. In that study, an 8 mM HAL instillation was one of the best concentrations in terms of fluorescence intensity. This result is consistent with the concentration that is nowadays applied in clinical practice for HAL instillations (BCFI, 2012). Therefore, we expect that the optimal instillation condition in our study is indicative of the right conditions in humans.

Finally, if the positive results on EB in our study can be repeated in a human setting, we expect substantial benefits by implementing the EB protocol combined with WL cystoscopy, not only concerning patient care but also in terms of economic costs. Given the widespread use of EB for different clinical applications, a future application of EB in diagnosing bladder cancer should be feasible.

4.5 Future perspectives on the use of EB for other urinary bladder diseases

In this thesis manuscript we have found some evidence of paracellular accumulation of EB in malignant urothelial tissue after intravesical instillations. This accumulation is probably due to defects in the urothelium barrier as extensively discussed in section 4.3. Hence other bladder pathologies showing similar urothelial barrier defects, e.g. interstitial cystitis/ painful bladder syndrome (IC/PBS), could potentially also be diagnosed using Evans blue WL cystoscopy. IC/PBS is a chronic and debilitating bladder disease characterized by urgency, nocturia and bladder pain. The estimated prevalence of IC ranges from 18 to over 400 cases per 100,000 individuals, with a predominance of cases found in women (Persu et al, 2010). The etiology of IC/PBS is unknown. However, it is clear that the barrier function of the bladder is at least partially impaired, exposing the suburothelial nerve endings to toxic urinary compounds that cause pain (Cervigni, 2015). Currently, there is no single diagnostic gold standard and the diagnosis is based on a review of clinical symptoms, exclusion criteria and by cystoscopy and hydrodistention of the bladder under anesthesia. Obviously, a new diagnostic tool that is minimally invasive and that does not require anesthesia, would be highly appreciated.

Possibilities to investigate EB instillations in preclinical models include the use of mice or rats in which IC/PBS is induced by administration of cyclophosphamide (Boudes et al, 2013). Another possibility is to work with a spontaneous IC/PBS model. Feline interstitial cystitis is a naturally occurring disease in cats, which reproduces many features of IC/PBS in humans diagnosed with this disorder and phenocopies much better the human disease than the available models of induced bladder injuries (Westropp & Buffington, 2002).

REFERENCES

Advanced Bladder Cancer Meta-analysis Collaboration. Neoadjuvant chemotherapy for transitional cell carcinoma of the bladder: a systematic review and meta-analysis. *Lancet* (2003) 361, 1927-34

Ahmad I, Morton JP, Singh LB, Radulescu SM, Ridgway RA, Patel S, Woodgett J, Wintorn DJ, Taketo MM, Wu XR, Leung HY, Sansom OJ. B-Catenin activation synergizes with PTEN loss to cause bladder cancer formation. *Oncogene* (2011) 13, 178-89

Alberts B, Johnson A, Lewis J, Raff M, Roberts K, Walter P. Chapter 19: Cell junctions. In: *Molecular Biology of the Cell* (2002) 4th edition, New York Garland Science

American Cancer Society. Cancer facts and figures 2015. Atlanta: American Cancer Society (2015)

Antoni D, Burckel H, Josset E, Noel G. Three-dimensional cell culture: a breakthrough in vivo. *Int J Mol Sci* (2015) 16, 5517-27

Atlay RD, Sutherst JR. Premature rupture of the fetal membranes confirmed by intra-amniotic injection of dye (Evan blue T-1824). *Am J Obstet Gynecol* (1970) 108, 993-4

Babjuk M, Burger M, Zigeuner R, Shariat S, Van Rhijn B, Compérat E, Sylvester R, Kaasinen E, Böhle A, Palou J, Rouprêt M. Guidelines on non-muscle-invasive bladder cancer (Ta, T1 and CIS). European Association of Urology, 2013.

Baris D, Karagas MR, Verrill C, Johnson A, Andrew AS, Marsit CJ, Schwenn M, Colt JS, Cherala S, Samanic C, Waddell R, Cantor KP, Schned A, Rothman N, Lubin J, Fraumeni JF Jr, Hoover RN, Kesley KT, Silverman DT. A case-control study of smoking and bladder cancer risk: emergent patterns over time. *J Natl Cancer Inst* (2009) 101, 1553-61

Belafsy PC, Blumenfeld L, LePage A, Nahrstedt K. The accuracy of the modified Evan's blue dye test in predicting aspiration. *Laryngoscope* (2003) 113, 1969-72

Belgisch Centrum voor Farmacotherapeutische Informatie (BCFI). Hoofstuk 19: Diagnostica. In: *Gecommentarieerd geneesmiddelenrepertorium* (2012) 25th edition, Maloteaux, Les Bons Villers

Bellmunt J, von der Maase H, Mead GM, Skoneczna I, De Santis M, Daugaard G, Boehle A, Chevreau C, Paz-Ares L, Laufman LR, Winquist E, Raghavan D, Marreaud S, Collette S, Sylvester R, de Wit R. Randomized phase III study comparing paclitaxel/cisplatin/gemcitabine and gemcitabine/cisplatin in patients with locally advanced or metastatic urothelial cancer without prior systemic therapy: EORTC Intergroup Study 30987. *J Clin Oncol* (2012) 30, 1107-13.

Bertram JS, Craig AW. Specific induction of bladder cancer in mice by butyl-(4-hydroxybutyl)-nitrosamine and the effects of hormonal modifications on the sex difference in response. *Eur J Cancer* (1972) 8, 587-94

Bolenz C, Wenzel M, Cao Y, Trojan L, Häcker A, Arancibia MF, Alken P, Michel MS. Newly developed mini-endoscope for diagnosis and follow-up of orthotopic bladder transitional-cell carcinoma in vivo. *J Endourol* (2007) 21, 789-94

Boudes M, Uvin P, Pinto S, Freichel M, Birnbaumer L, Voets T, De Ridder D, Vennekens R. Crucial role of TRPC1 and TRPC4 in cystitis-induced neuronal sprouting and bladder overactivity. *Plos one* (2013) 8(7): e69550

Brown T, Slack R, Rushton L. Occupational cancer in Britain. Urinary tract cancers: bladder and kidney. *Br J Cancer* (2012) 107 (S1) 1, 76-84

Bryan RT, Tselepis C. Cadherin switching and bladder cancer. *J Urol* (2010) 184, 423-31

Burger M, Catto JW, Dalbagni G, Grossman HB, Herr H, Karakiewicz P, Kassouf W, Kiemeney LA, La Vecchia C, Shariat S, Lotan Y. Epidemiology and risk factors of urothelial bladder cancer. *Eur Urol* (2013) 63, 234-41.

Burger M, Grossman HB, Droller M, Schmidbauer J, Hermann G, Dragoescu O, Ray E, Fradet Y, Karl A, Burgués JP, Witjes JA, Stenzl A, Jichlinski P, Jocham D. Photodynamic diagnosis of non-muscle-invasive bladder cancer with hexaminolevulinate cystoscopy: a meta-analysis of detection and recurrence based on raw data. *Eur Urol* (2013) 64, 846-54

Bus MTJ, de Bruin DM, de Reijke TM, de la Rosette JJMCH. Optical coherence tomography. In: *Advances in image-guided urologic surgery,* Liao JC and Su L-M (eds) (2015) Springer Science+Business Media New York

Chan E, Patel A, Heston, W, Larchian W. Mouse orthotopic models for bladder cancer research. *BJU Int* (2009) 104, 1286-91

Cervigni M. Interstitial cystitis/bladder pain syndrome and glycosaminoglycans replacement therapy. *Transl Androl Urol* (2015) 4, 638-42

Cole Cj, Pollack A, Zagars GK, Dinney CP, Swanson DA, von Eschenback AC. Local control of muscle-invasive bladder cancer: preoperative radiotherapy and cystectomy versus cystectomy alone. *Int J Radiat Oncol Biol Phys* (1995) 32, 331-40

Cooper GM. Chapter 15: Cancer. In: *The cell: A molecular approach* (2000) 2nd edition, Sunderland (MA): Sinaeur Associates

Correia da Costa JM, Vale N, Gouveia MJ, Botelho MC, Sripa B, Santos LL, Santos JH, Rinaldi G, Brindley PJ. Schistosome and liver fluke derived catechol-estrogens and helminth associated cancers. *Front Genet* (2014) 5: 444

Crawford ED, Das S, Smith JA. Preoperative radiation therapy in the treatment of bladder cancer. *Urol Clin North Am* (1987) 14, 781-87

Crooke AC, Morris CJ. The determination of plasma volume by the Evans blue method. *J Physiol* (1942) 101, 217-23

Dawson AB, Evans HM, Whipple GH. Blood volume studies: III Behavior of large series of dyes introduced into the circulating blood. *Am J Physiol* (1920) 51: 232

De Boer WI, Vermeij M, Diez de Medina SG, Bindels E, Radvanyi F, van der Kwast T, Chopin D. Functions of fibroblast and transforming growth factors in primary organoid-like cultures of normal human urothelium. *Lab Invest* (1996) 75, 147-56

DeGraff DJ, Robinson VL, Shah JB, Brandt WD, Sonpavde G, Kang Y, Liebert M, Wu XR, Taylor JA3rd, Translational Science Working Group of the Bladder Advocacy Network Think

Tank. Current preclinical models for the advancement of translational bladder cancer research. *Mol cancer Ther* (2013) 12,121-30

Dhawan D, Ramos-Vara JA, Naughton JF, Cheng L, Low PS, Rothenbuhler R, Leamon CP, Parker N, Klein PJ, Vlahov IR, Reddy JA, Koch M, Murphy L, Fourez LM, Stewart JC, Knapp DW. Targeting folate receptors to treat invasive urinary bladder cancer. *Cancer Res* (2013) 73, 875-84

Ding L, Lu Z, Lu Q, Chen YH. The claudin family of proteins in human malignance: a clinical perspective. *Cancer Manag Res* (2013) 8, 367-75

Eble JN, Sauter G, Epstein JI, Sesterhenn IA. World health organization classification of tumours. Pathology and genetics of tumours of the urinary system and male genital organs. Lyon: IARC Press, 2004

El Khatib S, Didelon J, Leroux A, Bezdetnaya L, Notter D, D'Hallewin M. Kinetics, biodistribution and therapeutic efficacy of hexylester 5-aminolevulinate induced photodynamic therapy in an orthotopic rat bladder tumor model. *J Urol* (2004) 172, 2013-17

Epstein JI, Amin MB, Reuter VR, Mostofi FK. The World health organization/international society of urological pathology consenus classification of urothelial (transitional cell) neoplasms of the urinary bladder. Bladder consensus conference committee. *Am J Surg Pathol* (1998) 22, 1435-48

European Association of Urology – Babjuk M, Böhle A, Burger M, Compérat E, Kaasinen E, Palou J, Rouprêt M, van Rhijn BWG, Shariat S, Sylvester R, Zigeuner R. Guidelines on non-muscle-invasive bladder cancer (Ta, T1 and CIS) (2015); http://www.uroweb.org/guidelines

Fajkovic H, Halpern JA, Cha EK, Bahadori A, Chromecki TF, Karakiewicz PI, Breinl E, Merseburger AS, Shariat SF. Impact of gender on bladder cancer incidence, staging and prognosis. *World J Urol* (2011) 29, 457-63

Fang J, Nakamura H, Maeda H. The EPR effect: Unique features of tumor blood vessels for drug delivery, factors involved, and limitations and augmentation of the effect. *Adv Drug Deliv Rev* (2011) 63, 136-51

Farquhar WB, Hunt BE, Taylor JA, Darling SE, Freeman R. Blood volume and its relation to peak O(2) consumption and physical activity in patients with chronic fatigue. *Am j Physiol Heart Circ Physiol* (2002) 282, H66-71

Ferlay J, Parkin DM, Steliarova-Foucher E. Estimates of cancer incidence and mortality in Europe in 2008. *Eur J Cancer* (2010) 46, 765-81

Freedman ND, Silverman DT, Hollenbeck AR, Schatzkin A, Abnet CC. Association between smoking and risk of bladder cancer among men and women. *JAMA* (2011) 306, 737-45

Fulkerson CM, Knapp DW. Management of transitional cell carcinoma of the urinary bladder in dogs: a review. *Vet J* (2015) 205, 217-25

Gabriel U, Bolenz C, Michel MS. Experimental models for therapeutic studies of transitional cell carcinoma. *Anticancer Res* (2007) 27, 3163-71

Garcia-Closas M, Malats N, Silverman D, Dosemeci M, Kogevinas M, Hein DW, Tardon A, Serra C, Carrato A, Garcia-Clasas R, Lloreta J, Castano-Vinyals G, Yeager m, Welch R, Chanock S, Chatterjee N, Wacholder S, Samanic C, Tora M, Fernandez F, Real FX, Rothman N. *NAT2* slow acetylation, *GSTM1* null genotype, and risk of bladder cancer: results from the Spanish Bladder Cancer Study and meta-analyses. *Lancet* (2005) 366, 649–59

Gibson JG, Evans WA. Clinical studies of the blood volume. I. Clinical application of a method employing the azo dye "Evans blue" and the spectrophotometer. *J Clin Invest* (1937) 16, 301-16

Gibson JG, Gregersen MI. Toxicity of two vital dyes used in plasma volume determinations. *Am J Physiol (Proc)* (1935) 113, 50.

Goh AC, Tresser NJ, Shen SS, Lerner SP. Optical coherence tomography as an adjunct to white light cystoscopy for intravesical real-time imaging and staging of bladder cancer. *Urology* (2008) 72, 133-37

Gravas S, Stenzl A. The Storz professional image enhancement system (spies) non-muscle-invasive bladder cancer study: a multicenter international randomized controlled study. *J Endourol* (2014) 28, 1254-5

Grossman HB, Natale RB, Tangen CM, Speights VO, Vogelzang NJ, Trump DL, White RW, Sarosdy MF, Wood DP, Raghavan D, Crawfor ED. Neoadjuvant chemotherapy plus cystectomy compared with cystectomy alone for locally advanced bladder cancer. *N Engl J Med* (2003) 349, 859-66

Hartsock A, Nelson WJ. Adherens and tight junctions: structure, function and connections to the actin cytoskeleton. *Biochim Biophys Acta* (2008) 1778, 660-9

He F, Mo L, Zheng XY, Hu C, Lepor H, Lee EY, Sun TT, Wu XR. Deficiency of pRb family proteins and p53 in invasive urothelial tumorigenesis. *Cancer Res* (2009) 69, 9413-21

Hendricksen K, Molkenboer-Kuenen J, Oosterwijk E, Hulsbergen-van de Kaa CA, Witjes JA. Evaluation of an orthotopic rat bladder urothelial cell carcinoma model by cystoscopy. *BJU Int* (2008) 101, 889-93

Hewitt KJ, Agarwal R, Morin PJ. The claudin gene family: expression in normal and neoplastic tissues. *BMC Cancer* (2006) 6: 186

Hoffmann D, Hoffmann I, El-Bayoumy K. The less harmful cigarette: a controversial issue: a tribute to Ernst L Wynder. *Chem Res Toxicol* (2001) 14, 767-90

Honeycutt J, Hammam O, Fu CL, Hsieh MH. Controversies and challenges in research on urogenital schistosomiasis-associated bladder cancer. *Trends Parasitol* (2014) 30, 324-32

Huang CN, Cornejo MJ, Bush DS, Jones RL. Estimating viability of plant protoplasts using double and single staining. *Protoplasma* (1986), 135, 80-87

International Collaboration of Trialists. International phase III trial assessing neoadjuvant cisplatin, methotrexate, and vinblastine chemotherapy for muscle-invasive bladder cancer: long-term results of the BA06 30894 trial. *J Clin Oncol* (2011) 29, 2171-77

Jaffer H, Adjei IM, Labhasetwar V. Optical imaging to map blood-brain barrier leakage. *Sci Rep* (2013) 3: 3117

Jefferson JJ, Leung CL, Liem RKH. Plakins: Goliaths that link cell junctions and the cytoskeleton. *Nat Rev Mol Cell Biol* (2004) 5, 542-53

Jemal A, Bray F, Center MM, Ferlay J, Ward E, Forman D. Global cancer statistics. *CA Cancer J Clin* (2011) 61, 69-90

Jones JG, Wardrop CAJ. Measurement of blood volume in surgical and intensive care practice. *BJA* (2000) 84, 226-35

Kalluri R, Weinberg RA. The basics of epithelial-mesenchymal transition. *J Clin Invest* (2009) 119, 1420-28

Kanai M, Sakurai T, Yoshinaga K, Aoyagi K, Hitsumoto T, Yoshinuma M, Uchi T, Noike H, Ohsawa H, Kawamura K, Tokuhiro K, Takahashi M, Ebihara T, Tachihara K, Uchida Y. Percutaneous dye image cardioscopy for detection of endocardial lesions. *Diagn Ther Endosc* (2000) 7, 29-33

Kaufman DS, Shipley WU, Feldman AS. Bladder cancer. *Lancet* (2009) 374, 239-49

Kaufman DS, Winter KA, Shipley WU, Heney NM, Chetner MP, Souhami L, Zlotecki RA, Sause WT, True LD. The initial results in muscle-invading bladder cancer of RTOG 95-06: phase I/II trial of transurethral surgery plus radiation therapy with concurrent cisplatin and 5-fluorouracil followed by selective bladder preservation or cystectomy depending on the initial response. *Oncologist* (2000) 5, 471-76

Kaufman DS. Challenges in the treatment of bladder cancer. *Ann Oncol* (2006) 17 Suppl 5: v106-12

Keith NM, Rowntree LG, Geraghty JT. A method for the determination of plasma and blood volume. *Arch Inter Med (Chic)* (1915) 16, 547-76

Klem B, Lappin G, Nicholson S, van de Wetering J, de Vries DE, Oosterhuis B, Garner RC. Determination of the bioavailability of [14C]-hexaminolevulinate using accelerator mass spectrometry after intravesical administration to human volunteers. *J Clin Pharmacol* (2006) 46, 456-60

Knapp DW, Ramos-Vara JA, Moore GE, Dhawan D, Bonney PL, Young KE. Urinary bladder cancer in dogs, a naturally occurring model for cancer biology and drug development. *ILAR Journal* (2014) 55, 100-118

Knowles MA, Finesilver A, Harvey AD, Berry RJ, Hicks RM. Long-term organ culture of normal human bladder. *Cancer Res* (1983) 43, 374-85

Kobayashi T, Owczarek TB, McKiernan JM, Abate-Shen C. Modelling bladder cancer in mice: opportunities and challenges. *Nat Rev Cancer* (2015) 15, 42-54

Kogevinas M, 't Mannetjes A, Cordier S, Ranft U, Gonzalez CA, Vineis P, Chang-Claude J, Lynge E, Wahrendorf J, Tzonou A, Jöckel KH, Serra C, Porru S, Hours M, Greiser E, Boffetta P. Occupation and bladder cancer among men in Western Europe. *Cancer Causes Control* (2003) 14, 907-14.

Kumar P, Nandi S, Tan TZ, Ler SG, Chia KS, Lim WY, Bütow Z, Vordos D, De la Taille A, Al-Haddawi M, Raida M, Beyer B, Ricci E, Colombel M, Chong TW, Chiong E, Soo R, Park MK,

Ha HK, Gunaratne J, Thiery JP. Highly sensitive and specific novel biomarkers for the diagnosis of transitional bladder carcinoma. *Oncotarget* (2015) [epub ahead of print].

Lazzeri M. The physiological function of the urothelium – more than a simple barrier. *Urol Int* (2006) 76, 289-95

Li K, Lin T, Fan X et al. Diagnosis of narrow-band imaging in nonmuscle-invasive bladder cancer: a systematic review and meta-analysis. *Int J Urol* (2013) 20, 602-09

Maeda H. Enhanced permeability and retention effect in relation to tumor targeting (Chapter 3), In: Kratz F, Senter P, Steinhagen (eds) *Drug Delivery in Oncology: From Basic Research to Cancer Therapy* (2012) Wiley-VCH Verlag GmbH & Co, pp 65-84

Malaowalla AM, Fong C. Toxicity of Evans blue dye in the monkey and tracing of it in the tooth pulp. *Oral Surg Oral Med Oral Pathol* (1962) 15, 1259-63

Malats N, Real FX. Epidemiology of bladder cancer. *Hematol Oncol Clin N Am* (2015) 29, 177-89

Martin TA, Jiang WG. Loss of tight junction barrier function and its role in cancer metastasis. *Biochim Biophys Acta* (2009) 1788, 872-91

Martin TA, Mason MD, Jiang WG. Tight junctions in cancer metastasis. *Front Biosci (Landmark Ed)* (2011) 16, 898-936

Miftahof RN, Nam HG. The bladder as a dynamic system (chapter 1), In: *Biomechanics of the human urinary bladder* (2013), Springer-Verlag Berlin Heidelberg, pp 1-16

Miller AT. Excretion of the blue dye, T-1824, in the bile. *Am J Physiol* (1947) 151, 229-33

Miyamoto H, Miller JS, Fajardo DA, Lee TK, Netto GJ, Epstein JI. Non-invasive papillary urothelial neoplasms: the 2004 WHO/ISUP classification system. *Pathol Int* (2010) 60, 1-8

Moore FD, Tobin LH, Aub JC. Studies with radioactive di-azo dyes. III. The distribution of radioactive dyes in tumor-bearing mice. *J Clin Invest* (1943) 22, 161-68

Müller-Graff P-K, Szelke H, Severin K, Krämer R. Pattern-based sensing of sulfated glycosaminoglycans with a dynamic mixture of iron complexes. *Org Biomol chem* (2010) 8, 2327-31

Murta-Nascimento C, Schmitz-Dräger BJ, Zeegers MP, Steineck G, Kogevinas M, Real FX, Malats N. Epidemiology of urinary bladder cancer: from tumor development to patient's death. *World J Urol* (2007) 25, 285-95

Naito S, van Rees Vellinga S, de la Rosette J. Global randomized narrow band imaging versus white light study in nonmuscle invasive bladder cancer: accession to the first milestone-enrollment of 6000 patients. *J Endourol* (2013) 27, 1-3

National Toxicology Program, Institute of Environmental Health Sciences, National Institutes of Health (NTP) – National Toxicology Program Chemical Repository Database (1992) Research Triangle Park, North Carolina

Niessen CM. Tight junctions/adherens junctions: basic structure and function. *J Invest Dermatol* (2007) 127, 2525-32

Noon AP, Catto JW. Bladder cancer in 2012: challenging current paradigms. *Nat Rev Urol* (2013) 10, 67-8

Norlén LJ, Ekelund P, Hedelin H, Johansson SL. Effects of indwelling catheters on the urethral mucosa (polypoid urethritis). *Scand J Urol Nephrol* (1988) 22, 81-6

Oyasu R. Epithelial tumours of the lower urinary tract in humans and rodents. *Food Chem Toxicol* (1995) 33, 747-55

Park JC, Citrin DE, Agarwal PK, Apolo AB. Multimodal management of muscle-invasive bladder cancer. *Curr Probl Cancer* (2014) 38, 80-108

Persu C, Cauni V, Gutue S, Blaj I, Jinga V, Geavlete P. From interstitial cystitis to chronic pelvic pain. *J Med Life* (2010) 3, 167-74

Ploeg M, Aben KKH, Kiemeney LA. The present and future burden of urinary bladder cancer in the World. *World J Urol* (2009) 27, 289-93

Rampias T, Vgenopoulou P, Avgeris M, Polyzos A, Stravodimos K, Valavanis C, Scorilas A, Klinakis A. A new tumor suppressor role for the Notch pathway in bladder cancer. *Nat Med* (2014) 20, 1199-205

Roberts WG, Palade GE. Increased microvascular permeability and endothelial fenestration induced by vascular endothelial growth factor. *J Cell Si* 1995; 108:2369-73

Rödel C, Grabenbauer GG, Kühn R, Papadopoulos T, Dunst J, Meyer M, Schrott KM, Sauer R. Combined-modelity treatment and selective organ preservation in invasive bladder cancer: long-term results. *J Clin Oncol* (2002) 20, 3061-71

Roelants M, Huygens A, Crnolatac I, Van Cleynenbreugel B, Lerut E, Van Poppel H, de Witte PA. Evans blue as a selective dye marker for white-light diagnosis of non-muscle-invasive bladder cancer: an in vitro study. *BJU Int* (2012) 109, 300-5

Scriven SD, Booth C, Thomas DF, Trejdosiewicz LK, Southgate J. Reconstitution of human urothelium from monolayer cultures. *J Urol* (1997) 158, 1147-52

Seifert HH, Meyer A, Cronauer MV, Hatina J, Müller M, Rieder H, Hoffmann MJ, Ackermann R, Schulz WA. A new and reliable culture system for superficial low-grade urothelial carcinoma of the bladder. *World J Urol* (2007) 25, 297-302

Sharma S, Ksheersagar P, Sharma P. Diagnosis and treatment of bladder cancer. *Am Fam Physician* (2009) 80, 717-23

Sievert KD, Amend B, Nagele U *et al.* Economic aspects of bladder cancer: what are the benefits and costs? *World J Urol* (2009) 27, 295-300

Smith SJ, Wilson M, Ward JH, Rahman DV, Peet AC, Macarthur DC, Rose FR, Grundy RG, Rahman R. Recapitulation of tumor heterogeneity and molecular signatures in a 3D brain cancer model with decreased sensitivity to histone deacetylase inhibition. *PLoS One* (2012) 7, e52335

Smith ZL, Guzzo TJ. Urinary markers for bladder cancer. *F1000Prime Reports* (2013) 5: 21

Sobin LH, Gospodariwicz M, Wittekind C (eds). TNM classification of malignant tumors. UICC International union against cancer 7th edn. Wiley-Blackwell, 2009 Dec, pp. 262-265.

Sorahan T, Hamilton L, Wallace DM, Bathers S, Gardiner K, Harrington JM. Occupational urothelial tumours: a regional case-control study. *Br J Urol* (1998) 82, 25-32

Stern MC, Lin J, Figueroa JD, Kelsey KT, Kiltie AE, Yuan JM, Matullo G, Fletcher T, Benhamou S, Taylor JA, Placidi D, Zhang ZF, Steineck G, Rothman N, Kogevinas M, Silverman D, Malats N, Chanock S, Wu X, Karagas MR, Andrew AS, Nelson HH, Bishop DT, Sak SC, Choudhury A, Barrett JH, Elliot F, Corral R, Joshi AD, Gago-Dominguez M, Cortessis VK, Xiang YB, Gao YT, Vineis P, Sacerdote C, Guarrera S, Polidoro S, Allione A, Gurzau E, Koppova K, Kumar R, Rudnai P, Porru S, Carta A, Campagna M, Arici C, Park SS, Garcia-Closas M. Polymorphisms in DNA repair genes, smoking, and bladder cancer risk: findings from the international consortium of bladder cancer. *Cancer Res (2009)* 69, 6857–64

Sun Y, Zeng Q, Zhang Z, Xu X, Wang Y, He J. Decreased urethral mucosal damage and delayed bacterial colonization during short-term urethral catheterization using a novel trefoil urethral catheter profile in rabbits. *J Urol* (2011) 186, 1497-501

Thun MJ, Lally CA, Flannery JT, Calle EE, Flanders WD, Heath CW Jr. Cigarette smoking and changes in the histopathology of lung cancer. *J Natl Cancer Inst* (1997) 89, 1580-86

Turco P, Houssami N, Bulgaresi P, Troni GM, Galanti L, Cariaggi MP, Cifarelli P, Crocetti E, Ciatto S. Is conventional urinary cytology still reliable for diagnosis of primary bladder carcinoma? Accuracy based on data linkage of a consecutive clinical series and cancer registry. *Acta Cytol* (2011) 55, 193-6

van Rhijn BW, Burger M, Lotan Y, Solsona E, Stief CG, Sylvester RJ, Witjes JA, Zlotta AR. Recurrence and progression of disease in non-muscle-invasive bladder cancer: from epidemiology to treatment strategy. *Eur Urol* (2009) 56, 430-42

Vandepitte J, Maes J, Van Cleynenbreugel B, Van Poppel H, Lerut E, Agostinis P, de Witte PA. An improved orthotopic rat bladder tumor model using DiI-loaded fluorescent AY-27 cells. *Cancer Biol Ther* (2010) 9, 986-93

Vandepitte J, Van Cleynenbreugel B, Hettinger K, Van Poppel H, de Witte PAM. Biodistribution of PVP-hypericin and hexaminolevulinate-induced PpIX in normal and orthotopic tumor-bearing rat urinary bladder. *Cancer Chemotherapy Pharmacol* (2011) 67, 775-81

Vasioukhin V. Adherens junctions and cancer. *Subcell Biochem* (2012) 60, 379-414

Villa L, Cloutier J, Traxer O. Chapter 11: Enhanced Imaging: NBI, PDD, SPIES. In: *Upper Urinary Tract Urothelial Carcinoma.* Eds Grasso M, Bagley DH. (2015), Springer International Publishing, p 109-120

Weijers Y, Arentsen HC, Arends TJ, Witjes JA. Management of low-risk and intermediate-risk non-muscle-invasive bladder carcinoma. *Hematol Oncol Clin N Am* (2015) 29, 219-225

Westropp JL, Buffington CA. In vivo models of interstitial cystitis. *J Urol* (2002) 167, 694–702

Williams PD, Lee JK, Theodorescu D. Molecular credentialing of rodent bladder carcinogenesis models. *Neoplasia* (2008) 10, 838-46

Winquist E, Kirchner TS, Segal R, Chin J, Lukka H, Genitourinary Cancer Disease Site Group, Cancer Care Ontario Program in Evidence-based Care Practice Guidelines Initiative. Neoadjuvant chemotherapy for transitional cell carcinoma of the bladder: a systematic review and meta-analysis. *J Urol* (2004) 171, 561-69

Wu X-R, Sun T-T, McConkey DJ, Shrader M, Papageorgiou A. Chapter 14: Animal models of bladder cancer. In: *Textbook of bladder cancer*, eds: Lerner SP, Schoenberg MP, Sternberg CN (2006), Taylor & Francis, pp 157-170

Xiao Z, McCallum TJ, Brown KM, Miller GG, Halls SB, Parney I, Moore RB. Characterization of a novel transplantable orthotopic rat bladder transitional cell tumour model. *Br J Cancer* (1999) 81, 638-46

Zagaynova EV, Streltsova OS, Gladkova ND, Snopova LB, Gelikonov GV, Feldchtein FI, Morozov A. In vivo optical coherence tomography feasibility for bladder disease. *J Urol* (2002) 167, 1492-6

Zhang ZT, Pak J, Shapiro E, Sun TT, Wu XR. Urothelium-specific expression of an oncogene in transgenic mice induced the formation of carcinoma in situ and invasive transitional cell carcinoma. *Cancer Res* (1999) 59, 3512-7

CURRICULUM VITAE

Personal data

Name:	Sanne Elsen
Date of birth:	12 March 1987
Place of birth:	Leuven, Belgium
Current position:	PhD student, Laboratory for Molecular Biodiscovery, Department of Pharmaceutical and Pharmacological Sciences, KULeuven

Education

2006-2009: Bachelor of Biology, KULeuven
Graduated magna cum laude
2009-2011: Master of Biology, KULeuven
Specialization in Integrative Physiology & Molecular Biology
Graduated magna cum laude

Positions

2011- 2016: Laboratory for Molecular Biodiscovery, Department of Pharmaceutical and Pharmacological Sciences, KU Leuven– *PhD student* (Supervisor: Peter de Witte PhD)

Evans blue as a diagnostic tool for non-musle-invasive bladder cancer: a preclinical study

Honors

2015 – Third best unmoderated poster award on the EMUC 2015 conference

Scientific publications in international peer-review journals

Waterkeyn A, Vanschoenwinkel B, **Elsen S**, Anton-Pardo M, Grillas P, Brenconck L. Unintentional dispersal of aquatic invertebrates via footwear and motor vehicles in a Mediterranean wetland area. *Aquat Conserv* (2010) 20, 580-87 IF: 2.14

Elsen S, Lerut E, Van Cleynenbreugel B, Van der Aa F, van Poppel H, de Witte PA. Biodistribution of Evans blue in an orthotopic AY-27 rat bladder urothelial cell carcinoma model: implication for the improved diagnosis of non-muscle-invasive bladder cancer (NMIBC) using dye-guided white-light cystoscopy. *BJU Int* (2015) 116, 468-77 IF: 3.53

Garg AD, **Elsen S**, Krysko DV, Vandenabeele P, de Witte P, Agostinis P. Resistance to anticancer vaccination effect is controlled by a cancer cell-autonomous phenotype that disrupts immunogenic phagocytic removal. *Oncotarget* (2015) 6, 26841-60 IF: 6.63